

CSIRO



Jet Propulsion Laboratory
California Institute of Technology

UCMERCED



**THE UNIVERSITY
OF QUEENSLAND**
AUSTRALIA



UNSW
SYDNEY

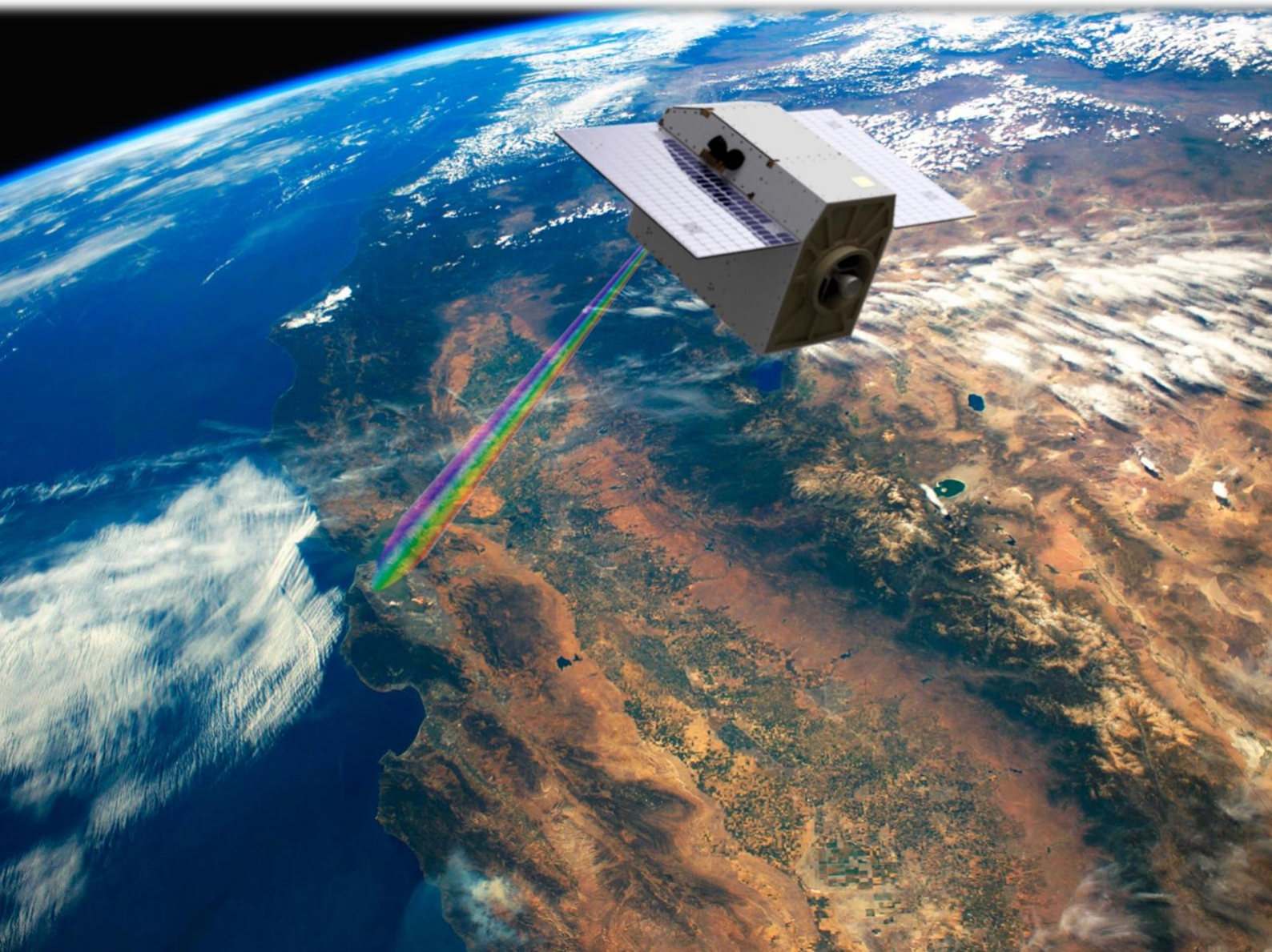
SMARTSAT
COOPERATIVE RESEARCH CENTRE



AquaSat-1 Feasibility Study Report

Toward actionable information on water quality
and aquatic ecosystems from space

August 2024



Citation

CSIRO and Jet Propulsion Laboratory/California Institute of Technology (2024) AquaSat-1 feasibility study report: Toward actionable information on water quality and aquatic ecosystems from space. CSIRO, Australia.

Copyright

© Commonwealth Scientific and Industrial Research Organisation and California Institute of Technology 2024. To the extent permitted by law, all rights are reserved, and no part of this publication covered by copyright may be reproduced or copied in any form or by any means except with the written permission of CSIRO and California Institute of Technology.

Important disclaimer

CSIRO and California Institute of Technology advise that the information contained in this publication comprises general statements based on scientific research. The reader is advised and needs to be aware that such information may be incomplete or unable to be used in any specific situation. No reliance or actions must therefore be made on that information without seeking prior expert professional, scientific and technical advice. To the extent permitted by law, CSIRO and California Institute of Technology (including their employees and consultants) excludes all liability to any person for any consequences, including but not limited to all losses, damages, costs, expenses and any other compensation, arising directly or indirectly from using this publication (in part or in whole) and any information or material contained in it.

Executive summary

The United Nations (UN) estimates that over three billion people are at risk of illness from poor water quality due partly to a lack of monitoring (UN-Water, 2021). Overall, aquatic ecosystems have significantly deteriorated in recent decades, with notable reductions in the extent of wetlands and coral reefs (Convention on Wetlands, 2021; Souter et al., 2021). Effective management and conservation of water resources requires comprehensive monitoring. However, in-situ sampling methods are costly, untimely, and limited in spatial coverage. Remote sensing can enhance monitoring by sampling at spatial and temporal scales not otherwise possible, particularly in remote areas.

For inland and coastal waters, remote sensing requires a challenging combination of high spatial, spectral, and temporal resolution, as well as high radiometric quality. This combination—referred to as ‘H4’ sensing (Muller-Karger et al., 2018)—has not yet been achieved from space, leaving information gaps in the Earth observing system for water quality and aquatic ecosystems.

Australia and the western United States (US) share similarities in their water issues and exemplify global needs for monitoring. Responding to these needs, the Commonwealth Scientific and Industrial Research Organisation’s (CSIRO’s) AquaWatch Australia program and NASA’s Western Water Applications Office (WWAO) jointly sponsored a study to **determine if a Jet Propulsion Laboratory (JPL) imaging spectrometer¹ can provide space-based observations that can be used to deliver actionable information on water quality and aquatic ecosystems for societal benefit.** This report presents the results of that study: the AquaSat-1 mission concept, which advances the capabilities of aquatic measurements from space and lays the groundwork for an operational ‘H4’ system.

To develop the mission concept, we used an applications traceability matrix (ATM) to explicitly link the sponsors’ goals with instrument and mission requirements. The study focused on three application objectives: monitoring potentially harmful algal blooms, invasive aquatic vegetation, and coral reefs. Although these are not the only possible uses of AquaSat-1, they were selected for their strong alignment with sponsor goals and their potential to drive instrument design and mission requirements. Each application objective was systematically linked to applicable physical parameters and observables, which were then used to establish key instrument and mission requirements. These requirements guided the design of an imaging spectrometer and the concept of operations. The study provides rigorous, formal traceability between physical parameters, instrument requirements, and instrument performance.

¹ We use the term imaging spectrometer to describe a true spectrometer, using the complete spectral range information, rather than specific spectral bands. These instruments are also known as hyperspectral imagers.

AquaSat-1 will image inland and coastal water target sites globally, as well as calibration sites and AquaWatch Australia pilot sites to support product validation. This study specifically focused on target sites in Australia and the western US, which are of primary interest to the study sponsors. AquaSat-1's 18 m spatial resolution allows coverage of 38% of the total river surface area and 94% of the total lake surface area within these regions. Excluding cloud coverage, the mean revisit rate for a single satellite is 4 days, while a 4-satellite constellation would achieve a revisit rate of 1 day. Cloud cover analysis indicates that a single satellite can meet the temporal requirements for each application objective, with improved temporal resolution possible with multiple satellites. AquaSat-1 will use a ground motion compensation (GMC) imaging strategy, where the satellite's pointing remains fixed over a target site, enhancing measurement sensitivity by a factor of 2-3.

The AquaSat-1 instrument considered for this application is a state-of-the-art visible to near-infrared (VNIR) imaging spectrometer, which builds on over 40 years of imaging spectroscopy heritage at JPL. It features a fast F/1.8 optical system comprised of a three-mirror telescope and Dyson-type spectrometer, a wide Teledyne CHROMA-D detector, and a concave grating optimised for aquatic imaging. The instrument covers a spectral range of 350-1050 nm, has a spectral response function of 5.6 nm, and a swath width of 54 km. The study demonstrated that a tailored small satellite platform can effectively support the AquaSat-1 concept of operations and instrument without necessitating significant development activities. The proposed satellite concept has an estimated wet mass of approximately 330 kg and a volume of 2 m³.

AquaSat-1 complements the Surface Biology and Geochemistry (SBG), Geostationary Littoral Imaging and Monitoring Radiometer (GLIMR), and Plankton, Aerosol, Cloud, Ocean Ecosystem (PACE) missions by filling a critical gap in high spatial and temporal resolution data for priority water bodies to support NASA's Earth Science to Action needs. The AquaSat-1 mission concept addresses the unallocated targeted observable on aquatic-coastal biogeochemistry identified in the most recent Decadal Survey for Earth Science and Applications from Space (ESAS 2018) (National Academies of Sciences, 2018). The application objectives also support the United Nations Sustainable Development Goals 6 (Clean Water and Sanitation), 14 (Life Below Water), and 15 (Life Below Land), as well as several targets of the Kunming-Montreal Global Biodiversity Framework.

The AquaSat-1 mission concept offers a feasible approach to providing space-based observations that can be used to deliver actionable information for water quality and aquatic ecosystems. By leveraging international collaboration and cutting-edge technology, AquaSat-1 establishes a next-generation capability for aquatic remote sensing to meet local, regional, and global needs.

Acknowledgments

This feasibility study was funded by the CSIRO and SmartSat CRC's AquaWatch Australia Mission and NASA's Western Water Applications Office. The JPL team wishes to acknowledge the support of the Earth Sciences Directorate, as well as the Science and Engineering divisions. The study was partially carried out at the Jet Propulsion Laboratory, California Institute of Technology, under a contract with the National Aeronautics and Space Administration (80NM0018D0004).

CSIRO and JPL wish to acknowledge the Traditional Owners of the lands on which this report was written. JPL is situated on the lands of the Tongva peoples, specifically the Hahamog'na band. These lands, known as Tovaangar or the Los Angeles basin, continue to be the homelands of the Kizh Gabrieleño Band of Mission Indians and other Indigenous peoples of the region. CSIRO acknowledges the Traditional Owners of all its sites in Australia, including the Ngunnawal (Canberra), Kurna (Adelaide), Wallumattagal (Sydney), Whadjuk (Perth), and Turrbal, Jagera, and Yuggera (Brisbane) peoples. Both organisations recognise their continuing connection to the lands, seas, skies, and waters. With this acknowledgment, we affirm and honour Indigenous sovereignty, and pay our respects to all our relations—past, present, and future. We recognise our history and commit to fostering a future where Indigenous voices are celebrated.

If you are reading this from outside CSIRO or JPL, we encourage you to take a moment to learn about or reflect on the Indigenous lands you are on.

Related publications

The following publications are outputs of this feasibility study (oldest to newest):

- Bright C, et al. (2023) The AquaSat-1 mission concept: Actionable information on water quality and aquatic ecosystems for Australia and Western USA, IGARSS 2023 - 2023 IEEE International Geoscience and Remote Sensing Symposium, Pasadena, CA, USA, pp. 4590-4593, DOI: 10.1109/IGARSS52108.2023.10282912.
- Ardila DR, et al. (2023) GC54A-01 Advancing management of water quality and aquatic ecosystems from space: the AquaSat-1 mission concept, presented at 2023 AGU Fall Meeting, 10-15 Dec.
- Frasson RPM, et al. (2024) The impact of spatial resolution on the characterization of rivers and lakes from space, Environmental Research Communications, in press.
- UNSW Canberra Space (2024) Australian National Concurrent Design Facility report: AquaSat-1 platform evaluation, available at: www.unsw.edu.au/canberra/our-research/our-facilities/australian-national-concurrent-design-facility.
- Malthus T, et al. (2024) Radiometric sensitivity requirements for monitoring live coral cover and associated benthic types from space, in preparation.
- Voss S, et al. (2024) Evaluating cloud cover impact on revisit times for coastal and inland water body monitoring from space, in preparation.
- Ardila DR, et al. (2025) An imaging spectrometer tailored to water quality and aquatic ecosystem monitoring from space: the AquaSat-1 concept, IEEE Aerospace Conference, in preparation.

Study team

This study included team members across Australia and the US from several organisations, including CSIRO, NASA Jet Propulsion Laboratory (JPL), University of California Merced (UC Merced), University of Queensland, and University of New South Wales (UNSW). The complete study team is as follows:

Project leadership

David Ardila (JPL): Task lead (US)

Courtney Bright (CSIRO): Task lead (Australia)

System/mission

Nick Carter (CSIRO): Systems engineering

Eleonor Logan-Cole (CSIRO): Constellation & cloud cover

Joshua Pease (CSIRO): Target sites

Renato Prata de Moraes Frasson (JPL): Target sites

Sander Voss (CSIRO): Constellation & cloud cover

Applications/science

Hannelie Botha (CSIRO): Water quality subject matter expert (SME)

Dylan Cowley (University of Queensland): Coral SME

Arnold Dekker (CSIRO): Aquatic ecosystems remote sensing SME

Erin Hestir (UC Merced): Water quality and aquatic vegetation SME

Klaus Joehnk (CSIRO): Water quality SME

Jeremy Kravitz (NASA ARC): Water quality SME

Leo Lymburner (CSIRO): EO data analytics SME

Mitchell Lyons (UNSW): Coral SME

Tim Malthus (CSIRO): Water quality and coral SME

Mark Matthews (CyanoLakes): Harmful algal blooms SME

Meredith Roe (University of Queensland): Coral SME

Chris Roelfsema (University of Queensland): Coral SME

Bozena Wojtasiewicz (CSIRO): Water quality SME

Instrument

Christine Bradley (JPL): Optics

Steven Davis (JPL): Mechanics

Robert Green (JPL): Project scientist

Pantazis Mouroulis (JPL): Optics

Bryant Mueller (JPL): Thermal

Peter Sullivan (JPL): Electronics/detector

David R. Thompson (JPL): Instrument scientist and algorithms

Satellite platform (under contract to CSIRO)

Tarik Errabih (UNSW): Systems engineering

Miriam Lim (UNSW): Electrical and computer systems engineering

Ryan Jeffreson (UNSW): Operations and orbit analysis

Michael McKinnell (UNSW): Mission design and system operations

Cameron Seidel (UNSW): Communications and radio frequency engineering

Alex Smith (UNSW): Software and ground system engineering

Paul van Staden (UNSW): Mission assurance

Jai Vennik (UNSW): Structures and mechanism design

Reviewers

Three reviews took place during the study. We thank the following individuals for their robust participation in this process:

Roger Franzen (Review Board Chair, Earthspace, Australia)
Alex Held (Review Board Member, CSIRO, Australia)
Indrani Graczyk (Review Board Member, NASA WWAO, US)
Janet Anstee (CSIRO, Australia)
Simon Barraclough (Australian Space Agency, Australia)
Tim Bolton (CSIRO, Australia)
David Brodrick (Australian National University, Australia)
Nagur Cherukuru (CSIRO, Australia)
Mark Cheung (CSIRO, Australia)
Michael L. Eastwood (JPL, US)
Isabelle Fratter (Centre national d'études spatiales (CNES), France)
Michelle Gierach (JPL, US)
Stephanie Granger (NASA WWAO, US)
Craig Ingram (CSIRO, Australia)
Andrew Lambert (University of New South Wales, Australia)
Christine Lee (JPL, US)
Leo Lymburner (Geoscience Australia, Australia)²
Harish M Manohara (JPL, US)
James P Mcguire (JPL, US)
Denis Naughton (Geoscience Australia, Australia)
Stuart Phinn (University of Queensland, Australia)
Ellen Preece (California Department of Water Resources, US)
Arvind Ramana (Australian Space Agency, Australia)
Chris Roelfsema (University of Queensland, Australia)²
Blake Schaeffer (Environmental Protection Agency, US)
Carl Seubert (SmartSat CRC, Australia)
Daniel Wilson (JPL, US)

² Became a team member after the project requirements review.

Contents

| | |
|---|------------|
| Executive summary | i |
| Acknowledgments | iii |
| Related publications | iv |
| Study team | v |
| Reviewers | vii |
| Acronyms and abbreviations | x |
| 1 Introduction | 1 |
| 2 Study approach | 4 |
| 2.1 Scope | 4 |
| 2.2 Programmatic elements..... | 5 |
| 2.3 Applications traceability matrix | 6 |
| 3 Application objectives and traceability | 10 |
| 3.1 Application objective 1: Potentially harmful algal blooms | 13 |
| 3.2 Application objective 2: Invasive aquatic vegetation | 18 |
| 3.3 Application objective 3: Coral reefs | 21 |
| 3.4 Observables..... | 25 |
| 3.5 Instrument requirements..... | 26 |
| 3.6 Mission requirements | 30 |
| 4 Mission description | 32 |
| 4.1 Concept of operations..... | 32 |
| 4.2 Target site prioritisation strategy | 34 |
| 4.3 Revisit analysis and crossing time | 40 |
| 4.4 Spatial resolution | 47 |
| 4.5 Mission trades | 50 |
| 5 Instrument description | 51 |
| 5.1 JPL imaging spectroscopy heritage | 51 |
| 5.2 Instrument model | 53 |
| 5.3 Instrument calibration | 54 |
| 5.4 Instrument implementation..... | 56 |
| 5.5 Instrument accommodation requirements | 63 |
| 5.6 Instrument trades | 64 |
| 6 Satellite platform description | 65 |
| 6.1 Platform requirements..... | 66 |
| 6.2 Platform concept design | 66 |
| 6.3 Platform trades | 78 |
| 7 Technology readiness level and technical risks | 81 |
| 8 Relationship between AquaSat-1 and other missions | 83 |
| 9 Conclusions | 86 |
| 10 References | 87 |

| | | |
|-------------------|--|-----------|
| Appendix A | Recommendations for future work | 98 |
| Appendix B | Additional revisit and cloud cover analysis | 99 |

Acronyms and abbreviations

| | |
|--------|---|
| AIS | Airborne Imaging Spectrometer |
| AO | application objective |
| AOCS | attitude and orbit control system |
| AR | Anti-reflection |
| ARF | along-track response function |
| ATM | applications traceability matrix |
| AVIRIS | Airborne Visible-Infrared Imaging Spectrometer |
| CBE | current best estimate |
| CCA | crustose coralline algae |
| CDOM | coloured dissolved organic matter |
| ConOps | concept of operations |
| COTS | commercial off-the-shelf |
| CPM | Carbon Plume Mapper |
| CRISM | Compact Reconnaissance Imaging Spectrometer for Mars |
| CRF | cross-track response function |
| CSIRO | Commonwealth Scientific and Industrial Research Organisation |
| CTIA | capacitive transimpedance amplifier |
| CyAN | Cyanobacteria Assessment Network |
| CWIS | Compact Wide-Swath Imaging Spectrometer |
| DION | Dark Water Inland Observatory Network |
| ECCOE | EROS Cal/Val Centre of Excellence |
| ECMWF | European Centre for Medium-Range Weather Forecasts |
| EMI | electromagnetic interference |
| EMIT | Earth Surface Mineral Dust Source Investigation |
| EnMAP | Environmental Mapping and Analysis Program |
| EPA | Environmental Protection Agency |
| EPS | electrical power system |
| ERA5 | European Centre for Medium-Range Weather Forecasts Reanalysis Version 5 |
| FoR | field of regard |

| | |
|-----------|--|
| FoV | field of view |
| FPA | focal plane array |
| FPGA | field programmable gate array |
| FWHM | full width at half maximum |
| GEOSS | Group on Earth Observations System of Systems |
| GLIMR | Geostationary Littoral Imaging and Monitoring Radiometer |
| GMC | ground motion compensation |
| GSD | ground sample distance |
| HAB | harmful algal bloom |
| HICO | Hyperspectral Imager for the Coastal Ocean |
| IWG | Interagency Working Group |
| IAV | invasive aquatic vegetation |
| IMOS | Integrated Marine Observing System |
| IOPs | inherent optical properties |
| JPL | Jet Propulsion Laboratory |
| LTAN | local time of ascending node |
| LTDN | local time of descending node |
| MCR | mission concept review |
| MEL | master equipment list |
| MEV | maximum expected value |
| NASA | National Aeronautics and Space Administration |
| NOAA | National Oceanic and Atmospheric Administration |
| NSW | New South Wales |
| OBC | on-board computer |
| OCI | Ocean Color Instrument |
| PACE | Plankton, Aerosol, Cloud, ocean Ecosystem |
| PEL | power equipment list |
| PID | proportional-integrative-derivative controller |
| PFT | phytoplankton functional type |
| RadCalNet | Radiometric Calibration Network |
| ROIC | readout integrated circuit |
| R_{rs} | remote sensing reflectance |
| SBG | Surface Biology and Geology |

| | |
|-----------|--|
| SBG-VSWIR | Surface Biology and Geology visible to shortwave infrared |
| SIOPs | mass specific inherent optical properties |
| SME | subject matter expert |
| SNR | signal-to-noise ratio |
| SRF | spectral response unction |
| SWORD | Surface Water and Ocean Topography River Database |
| TMA | three-mirror anastigmat |
| TOA | top-of-atmosphere |
| TOBA | telescope optical bench assembly |
| TRL | technology readiness level |
| TSU | thermal storage unit |
| UC Merced | University of California Merced |
| UN | United Nations |
| UNESCO | United Nations Educational, Scientific and Cultural Organization |
| UNSW | University of New South Wales |
| US | United States |
| UTC | Coordinated Universal Time |
| UQ | University of Queensland |
| VNIR | visible to near infrared |
| WHO | World Health Organization |
| WWAO | Western Water Applications Office |

1 Introduction³

The United Nations (UN) estimates that over three billion people are at risk of illness from poor water quality due partly to a lack of monitoring (UN, 2023). Additionally, aquatic ecosystems are rapidly degrading, with 35% of wetlands and 14% of coral lost globally since 1970 (Convention on Wetlands, 2021) and 2009 (Souter et al., 2021), respectively. Comprehensive monitoring of inland and coastal waters is essential for effective management, conservation, and environmental accounting, but in-situ sampling methods are often costly, not timely, and limited in spatial coverage.

Remote sensing can enhance traditional in-situ monitoring by sampling at spatial and temporal scales not otherwise possible, particularly in remote regions. However, inland and coastal water monitoring presents a challenge in the mission design trade-space because targets are typically small with low signal levels. Satellite instruments designed primarily for ocean imaging lack the spatial resolution needed to effectively capture many inland and coastal waters. Conversely, instruments designed for land imaging generally do not offer the combined spectral resolution and radiometric sensitivity to discern key indicators of water quality and aquatic ecosystem structure (CEOS, 2018). Muller-Karger et al. (2018) have highlighted the need for a 'H4' imaging capability that meets the competing requirements of high spatial, spectral, and temporal resolution, as well as high radiometric quality.

Australia and the western United States (US) face similar water issues, highlighting global needs for effective monitoring. Both regions experience prolonged droughts that place significant strain on their water resources. These droughts are often interrupted by extreme flooding events, creating a 'climate whiplash' effect that negatively impacts water quality—a critical aspect of water security. During droughts, reduced water flow and low water levels can lead to higher contaminant concentrations, increased algal blooms, and the spread of invasive species, all of which undermine the health and function of aquatic ecosystems. Floods can increase runoff and sedimentation, facilitate invasive species dispersal, and cause wastewater overflows and infrastructure damage, further degrading water quality, especially in already stressed systems. Additionally, bushfires (wildfires) contribute to excess sediment and nutrients in rivers and lakes. Timely and accurate information is essential to support management strategies that address both extremes and protect water quality.

Imaging spectroscopy has been recognised as a powerful tool for the quantitative monitoring of water quality and aquatic ecosystems. CSIRO previously led a feasibility study that evaluated the benefits and technological challenges of a satellite system dedicated to the biogeochemistry of inland and coastal waters (CEOS, 2018). This assessment responded to recommendation C.10 from the Group on Earth Observations System of Systems (GEOSS) water strategy report (GEOS, 2014). It called for a visible to near-infrared (VNIR) imaging

³ Throughout this report we use Australian orthographic and spelling conventions.

spectrometer with a spatial resolution between 17 and 33 m, as well as the highest achievable radiometric quality and temporal resolution within technical and financial constraints.

In response to shared water challenges and as a logical next step to previous studies (CEOS, 2018; SmartSat, 2021), CSIRO's AquaWatch Australia program (AquaWatch) and NASA's Western Water Applications Office (WWAO) jointly sponsored the present study to **determine if a JPL imaging spectrometer⁴ can provide space-based observations that can be used to deliver actionable information on water quality and aquatic ecosystems for societal benefit.** For this study, we define 'actionable information' as data that can be used to inform management decisions. The focus was on evaluating the space segment, specifically assessing whether the necessary data for water managers could be 1) detected from space using a JPL imaging spectrometer, and 2) supported by a feasible mission concept and satellite platform. While data processing and downstream analysis are essential for delivering actionable information, they were beyond the scope of this study and will be addressed in future work.

The study was led by the Jet Propulsion Laboratory (JPL) and the CSIRO, with significant contributions from the University of California Merced (UC Merced), the University of Queensland and the University of New South Wales (UNSW). The outcome of the study is the AquaSat-1 mission concept, outlined in this report and related publications, which lays the groundwork for an operational 'H4' system (as described earlier). The study developed application objectives in three areas: potentially harmful algal blooms, invasive aquatic vegetation, and coral reefs. Although these are not the only possible uses of AquaSat-1, they were selected for their strong alignment with sponsor goals and their potential to drive instrument design and mission requirements.

NASA's WWAO mission is to improve how water is managed in the arid western US by getting NASA science, data and technology into the hands of water managers and decision makers. WWAO harnesses NASA's power of perspective while working to identify some of the most pressing water issues in the US West. The office works with water stakeholders at local and national levels to find ways to solve water problems that touch on water availability, water use, water quality, disasters and extreme events, and watershed health.

AquaWatch is a CSIRO initiative that aims establish an integrated ground-to-space national water quality monitoring system to support water management with accurate data and predictive forecasting (see Figure 1-1) (CSIRO, 2024). The space segment of AquaWatch is envisaged as a 'virtual constellation' of existing and planned Earth observing satellites, supplemented by bespoke satellites (such as AquaSat-1) to fill information gaps for inland and coastal water quality monitoring. AquaWatch Australia imagery and data products will be freely and openly available to enhance public good and support sustainable development goals.

⁴ We use the term imaging spectrometer to describe a true spectrometer, using the complete spectral range information, rather than specific spectral bands. These instruments are also known as hyperspectral imagers.

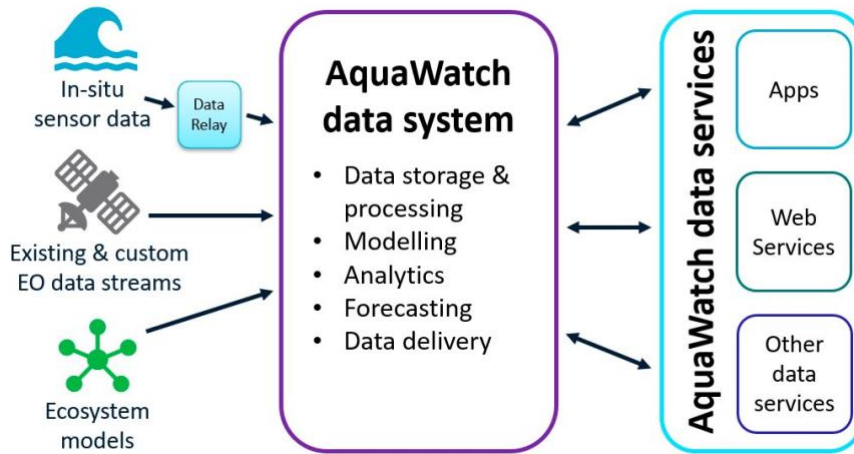


Figure 1-1: Components of CSIRO's AquaWatch system—an in-development ground-to-space water quality monitoring system with global applicability. AquaSat-1 is proposed as a new satellite under 'custom EO data streams' to fill critical information gaps in the Earth observing system for inland and coastal water quality and aquatic ecosystems. Image source: CSIRO (2023).

2 Study approach

2.1 Scope

NASA defines the purpose of Pre-Phase A concept studies as:

'...to produce a broad spectrum of ideas and alternatives for missions from which new programs and projects can be selected. Determine feasibility of desired system; develop mission concepts; draft system-level requirements; assess performance, cost, and schedule feasibility; identify potential technology needs and scope.' (NASA, 2023).

Generally, the goal of a concept study is to generate the products necessary for a successful Mission Concept Review (MCR) (NASA Goddard Space Flight Centre, 2023).

For this study, we tailored the Pre-Phase A activities described in the above references to address the needs of the study sponsors. Table 2-1 compares the activities performed in this study to the NASA success criteria for Pre-Phase A concept studies. Further development of the AquaSat-1 concept will need to be aligned with specific sponsor requirements and flight opportunities.

The study team developed preliminary instrument and spacecraft architectures, as well as a concept of operations (ConOps) aimed at delivering data necessary for the application objectives outlined in the applications traceability matrix (ATM). Additionally, we commissioned a satellite platform evaluation to identify a platform that can support the AquaSat-1 instrument and ConOps (UNSW Canberra Space, 2024). This focus on the space segment ensures that AquaSat-1 can generate data to support meaningful decision-making in water management.

This phase of the study did not extend to the downstream analysis of how the data will be processed, analysed, and utilised by end-users. Addressing these aspects is essential for fully demonstrating AquaSat-1's capability to provide actionable information. Future work will address data processing workflows, user interfaces, and integration with decision-support systems to ensure the data is effectively used by water managers and other stakeholders.

Table 2-1: NASA success criteria for Pre-Phase A concept studies as applied to the AquaSat-1 feasibility study.

| Pre-Phase A concept study activities | Performed? |
|---|---|
| Review/identify any initial customer requirements or scope of work (mission, science, top-level system). | Yes. The ATM application objectives and physical parameters (Section 3) can be used as Level 1 requirements. Key instrument (Section 3.5) and mission requirements (Section 3.6) are also identified. |
| Identify and involve users and other stakeholders. | Yes: Identified stakeholders and relied on previous documentation for user-needs assessments. |
| Develop and baseline the ConOps. | Yes. |
| Identify risk classification. | No: Risk is program and agency dependent. Out of scope of study. |
| Identify initial technical risks | Yes (Section 7). |
| Identify the roles and responsibilities in performing mission objectives (i.e., technical team, flight, and ground crew) including training. | No: out of scope. |
| Develop plans (develop preliminary Systems Engineering Management Plan; develop and baseline Technology Development Plan; define preliminary verification and validation approach). | No technology development needed. Others: out of scope. |
| Prepare program/project proposals. | No: out of scope. Programmatic analysis (cost, schedule) was not performed. |
| Satisfy MCR entrance/success criteria from NPR 7123.1. | Partially, as indicated above. |

2.2 Programmatic elements

The study was managed by one task lead from JPL and one from CSIRO. The task leads assembled a science and technical team from the participating institutions, consulting with specific subject matter experts as needed. Over 20 months, starting November 2022, the team met remotely at least once per week. In addition, members of the JPL and CSIRO teams met in-person three times throughout the study.

In the context of this study, CSIRO and JPL organised an aquatic remote sensing workshop in Brisbane, Australia in April 2023. Over three days, an international group of stakeholders, scientists, and engineers discussed topics related to remote sensing of water quality and aquatic ecosystems. The results of this workshop informed the direction and scope of this study and led to the expansion of the science team.



Figure 2-1: A subset of the team with external collaborators during the April 2023 aquatic remote sensing workshop, on an educational field trip to Moreton Bay, Queensland, Australia. First row, left to right: Courtney Bright, Erin Hestir, Robert Green, Glenn Campbell. Second Row: David Ardila, David Blondeau-Patissier. Third Row: Joshua Pease, Mark Matthews, Arnold Dekker. Fourth Row: Tarun Saunders. Stuart Phinn, Neil Sims. Fifth row: David Brewer, Tim Malthus, Nagur Cherukuru.

The team drew heavily on previous end-user consultations carried out by CSIRO and WWAO, as well as on agency policy documents and the published literature. Three hybrid independent reviews were conducted during the study: a requirements review (April 2023), an instrument review (June 2023), and a full study review (April 2024). The reviews were used to determine compliance of the study to the activities indicated in Table 2-1, and the reviewers are listed in the frontmatter of this report.

2.3 Applications traceability matrix

The development of the applications and their flow-down to instrument and mission requirements was accomplished via an applications traceability matrix (ATM). The ATM is the core of the study, defining the success criteria: the mission will be deemed successful if the application objectives (AOs) are achieved, with the physical parameters measured at the specified precision or better. The ATM developed for this study is presented in Tables 2-2 and 2-3, split across two tables for readability.

The application goals column of the ATM lists the sponsors goals that AquaSat-1 is responsive to. These are high-level goals that reflect agency or societal priorities and provide institutional traceability to the AquaSat-1 activities.

The application objectives column details a flow-down of these goals, based on input from subject matter experts in the study team and literature sources. The justification for the application objectives is provided in Section 3. These are not intended to provide an extensive list of potential applications but to identify the driving objectives for the mission.

The measurement requirements for the mission are captured in the next two columns: physical parameters and observables. The physical parameters are quantitative statements of the application objectives, but with emphasis on the physical quantity of interest. These list one-sigma (1σ) precision values on the quantities of interest, derived as specified in Sections 3.1, 3.2, and 3.3. When combined with the physical parameters, the application objectives are used to generate the Level 1 requirements.

The next two columns in the ATM correspond to the instrument requirements and instrument performance. The difference between the columns reflects the engineering margin in the system fabrication. Finally, key mission requirements are defined in the last column of the ATM, as derived from the previous columns (Section 3.1).

Table 2-2: Applications traceability matrix (ATM) part 1 – Application goals, application objectives, and measurement requirements.

| Application goals | Application objectives | Measurement requirements | |
|---|---|--|--|
| | | Physical parameters (within a ≤ 20 m by ≤ 20 m area) | Observables (with 23.4° solar angle and nadir observations) |
| 1: Potentially harmful algal blooms (HABs) | | | |
| <p>NASA's WWAO Columbia River Basin Needs Assessment Workshop Report (NASA WWAO, 2020): Scaled-down version of CyAN (Cyanobacteria Assessment Network) to cover smaller bodies of water and develop an early warning system for drinking water systems managers.</p> <p>CSIRO AquaWatch End-User Consultation Report (Dekker and MacLeod, 2021), Processes of interest: Inland processes: Sediment and nutrient load from e.g., catchment run-off, erosion, bushfires; nutrient bound in sediments; influence of agricultural and other catchment activities; linkage with catchment processes; blackwater events; inland algal blooms. Coastal processes: Coastal algal blooms; shallow water and benthic system, monitoring over time; sediments impact on seagrass; impact of dissolved organic carbon (DOC)/blackwater events on marine life.</p> <p>ESAS 2018 (National Academies of Sciences, 2018): Application objective E-3a: Quantify the flows of energy, carbon, water, nutrients, and so on sustaining the life cycle of terrestrial and marine ecosystems and partitioning into functional types (Most Important). H-3a: Develop methods and systems for monitoring water quality for human health and ecosystem services (Important).</p> | <p>For inland and coastal waters in Australia and the western US, inform management of potentially HABs by detecting pigments across phytoplankton functional types, including pigments that may indicate the presence of toxins or nutrient pollution.</p> | <p>Phytoplankton functional type fraction to $1\sigma \leq 10\%$ absolute fraction, for chlorophyll-a concentrations $\geq 3 \mu\text{g/L}$ (1).</p> | <p>TOA radiance $\leq 7 \mu\text{W/nm/cm}^2/\text{sr}$ at 400 nm, $\leq 0.05 \mu\text{W/nm/cm}^2/\text{sr}$ at 1020 nm with FWHM≤ 10 nm (2).</p> |
| 2: Invasive aquatic vegetation (IAV) | | | |
| <p>WWAO 2016 Rapid Needs Assessment (WWAO, 2016): Assessment of Ecosystem health; water quality in reservoirs</p> <p>ESAS 2018 (National Academies of Sciences, 2018): Application objective E-1e: Support targeted species detection and analysis (e.g., foundation species, invasive species, indicator species, etc.) (Important). E-3a: Quantify the flows of energy, carbon, water, nutrients, and so on sustaining the life cycle of terrestrial and marine ecosystems and partitioning into functional types (Most Important).</p> | <p>For inland waters in Australia and the western US, inform management of IAV in rivers, lakes, reservoirs, and wetlands by measuring the fractional cover of floating and emergent vegetation by functional type.</p> | <p>For floating and emergent vegetation of functional types of interest, fractional area cover to $1\sigma \leq 10\%$ absolute coverage fraction.</p> | <p>TOA radiance $\leq 16 \mu\text{W/nm/cm}^2/\text{sr}$ at 782 nm, $\leq 9 \mu\text{W/nm/cm}^2/\text{sr}$ at 1020 nm with FWHM≤ 10 nm (3).</p> |
| 3: Coral reefs | | | |
| <p>CSIRO AquaWatch End-User Consultation Report (Dekker and MacLeod, 2021), Processes of interest: Coastal - Shallow water and benthic system, monitoring over time</p> <p>ESAS 2018 (National Academies of Sciences, 2018): Application objective E-1a: Quantify the global distribution of the functional traits, functional types, and composition of vegetation and marine biomass, spatially and over time (Very Important). E-1e: Support targeted species detection and analysis (e.g., foundation species, invasive species, indicator species, etc.) (Important). E-3a: Quantify the flows of energy, carbon, water, nutrients, and so on sustaining the life cycle of terrestrial and marine ecosystems and partitioning into functional types (Most Important).</p> | <p>For coastal waters in Australia and the western US, inform management of coral reef ecosystem condition by measuring the habitat benthic cover for coral reefs.</p> | <p>Coral fractional area cover to $1\sigma \leq 10\%$ absolute coverage fraction, under ≤ 10 m of relatively clear water.</p> | <p>TOA radiance $\leq 7 \mu\text{W/nm/cm}^2/\text{sr}$ at 400 nm, $\leq 0.04 \mu\text{W/nm/cm}^2/\text{sr}$ at 1020 nm with FWHM≤ 10 nm (4).</p> |

(1) Assuming median inland inherent optical properties (IOPs) in Australian waters (Drayson et al., 2022).

(2) Scene: Change in cyanobacteria (*Microcystis aeruginosa*) for a water mixture with 50% cyanobacteria (*Microcystis aeruginosa*), 12.5% dinoflagellates, 12.5% cryptophytes, 12.5% chlorophytes (green algae), 12.5% diatoms. Median IOPs in Australian waters, normalised reflectances.

(3) Scene: Change in water hyacinth for a scene with 40% water hyacinth, 15% water primrose, 15% floating-leaved plants, 15% helophytes, 15% submerged aquatic vegetation.

(4) Scene: Change in coral fraction, 10m depth, average water conditions of Heron Island, Great Barrier Reef in Australia; 40% Coral, 40% Turf, 10% Macro-algae, 10% Crustose Coralline Algae.

Table 2-3: Applications traceability matrix (ATM) part 2 – Instrument requirements, instrument performance, and mission requirements.

| Instrument requirements | | Instrument performance | Mission requirements |
|--|---|---|--|
| Spectral range Driven by atmospheric correction and AO2. | 400 - 1020 nm | 350-1050 nm | <p>Targets: Estuaries, rivers (≥ 60 m wide) and lakes/reservoirs (≥ 60 m wide) in Australia and the western US Coral reefs ≤ 10m depth.</p> <p>ConOps: Mission lifetime: ≥ 1 year. Orbit: Sun-synchronous 12 pm orbit, 400 km \pm 40 km (equivalent to ± 2 m ground sample distance (GSD)). Latency: ≤ 2 days. When averaging over a year, obtain a useable image: Monthly or better for HABs and IAV targets; quarterly or better for coral targets.</p> <p>Pointing: 3-axis stabilization with nadir pointing. Field of regard (FoR): 60 deg cross-track (for improved revisit). Ground motion compensation (GMC): ≤ 10x dwell per target (see Section 4.1). Slew rate: ≥ 3 deg/sec based on preliminary reference mission. Accuracy: ≤ 2.6 deg (1/3 swath). Drift: $\leq \pm 4$ arcsec per 225 arcsec travel. (0.5 pix/25 pix). Jitter: ≤ 0.9 arcsec per 25 ms integration (0.1 pix/integration). Knowledge: ≤ 4 arcsec (0.5 pix). Science data rate: > 2.4 Gbps at 6.4 nm sampling in 350-1050 nm. Science data volume: 114 GB/day (assumes 50 images, 50 km x 50 km, 2x compression).</p> |
| Spectral sampling (1) | ≤ 8 nm | 3.2 nm sampling coadded to 6.4 nm | |
| Spectral response function (SRF) | ≤ 10 nm | 5.3 nm | |
| Swath width | ≥ 50 km (2) | 54 km | |
| Ground sample distance (GSD) | ≤ 20 m | 18 m | |
| Radiometric calibration absolute uncertainty at top of atmosphere (TOA) | $\leq 5\%$ | 3% | |
| Radiometric range (maximum reflectance) | 0.7 Lambertian reflectance with illumination at 0 degrees zenith angle. | 0.87 Lambertian | |
| TOA radiance signal to noise ratio (4), 23.4 deg solar-zenith Driven by AO3. | Wavelength nm, SNR points; 400 nm: ≥ 287 ; 500 nm: ≥ 324 ; 600 nm: ≥ 216 ; 700 nm: ≥ 145 ; 800 nm: ≥ 85 ; 900 nm: ≥ 40 ; 1000 nm: ≥ 12 ; 1020 nm: ≥ 8.0 . | With 10x GMC at 10 nm SRF (3), wavelength nm, SNR points; 400 nm: 584, 500 nm: 657; 600 nm: 446; 700 nm: 310; 800 nm: 195; 900 nm: 105; 1000 nm: 40; 1020 nm: 27. | |

(1) See Feasibility Study for an Aquatic Ecosystem Earth Observing System (CEOS, 2018).

(2) Enough to cover narrowest dimension of all lakes/reservoirs/ivers in the area of interest.

(3) Includes only instrument and scene shot noise errors. Does not include calibration or algorithmic errors.

(4) See note (4), Table 2-2.

3 Application objectives and traceability

The design of AquaSat-1 was driven by practical applications. While the imaging spectroscopy data will greatly benefit scientific research, the mission's primary goal is to provide water managers and policymakers with data to support informed decision-making. This approach aligns with NASA's Earth Science to Action strategy (NASA, 2024a).

We identified three application objectives that drive the system design, leverage the capabilities of imaging spectroscopy, and address unmet needs of both the study sponsors and the Earth observation community:

- 1) **Potentially harmful algal blooms:** For inland and coastal waters in Australia and the western US, inform management of potentially harmful algal blooms by detecting pigments across phytoplankton functional types (PFTs)⁵, including pigments that may indicate the presence of toxins or nutrient pollution.
- 2) **Invasive aquatic vegetation:** For inland waters in Australia and the western US, inform management of floating and emergent invasive aquatic vegetation (IAV) in lakes, reservoirs, and wetlands by measuring the fractional cover of aquatic plants by functional type.
- 3) **Coral reefs:** For coastal waters in Australia and the western US (including Hawai'i), inform management of coral reef ecosystem condition by measuring coral reef habitat benthic cover.

These objectives are traceable to goals of CSIRO's AquaWatch program, NASA's WWAO, and the following US National Academies Decadal Survey for Earth Sciences and Applications from Space (ESAS 2018) (National Academies of Sciences, 2018) objectives:

- E-1a: Quantify the global distribution of the functional traits, functional types, and composition of vegetation and marine biomass, spatially and over time (Very Important).
- E-1e: Support targeted species detection and analysis (e.g., foundation species, invasive species, indicator species, etc.) (Important).
- E-3a: Quantify the flows of energy, carbon, water, nutrients, and so on sustaining the life cycle of terrestrial and marine ecosystems and partitioning into functional types (Most Important).
- H-3a: Develop methods and systems for monitoring water quality for human health and ecosystem services (Important).

⁵ A functional type represents an aggregation of organisms according to some well-defined property that sets a role or 'function' for them in a system (IOCCG, 2014). For this study, we define 'function' as whether phytoplankton may produce toxins that are hazardous to humans and animals.

Additionally, ESAS 2018 identified aquatic-coastal biogeochemistry as an unallocated⁶ targeted observable, focusing on 'distribution, composition, and functioning of rapidly changing coastal and inland water ecosystems and associated biogeochemical impacts' (ESAS 2018, pg. 148). The absence of a dedicated program leaves a gap in inland and near-coastal measurements within the Surface Biology and Geology Targeted Observable. AquaSat-1 aims to address this gap by providing essential measurements where no current flight programs exist.

Although not explicitly outlined as sponsors goals, AquaSat-1 data will also support the following international goals and targets:

- UN Sustainable Development Goals (SDGs):
 - Goal 6 seeking to ensure availability and sustainable management of water and sanitation for all.
 - Goal 14 to conserve and sustainably use the oceans, seas, and marine resources for sustainable development.
 - Goal 15 to protect, restore, and promote sustainable use of terrestrial ecosystems - including wetlands - and halt biodiversity loss (UN Department of Economic and Social Affairs, 2024).
- Kunming-Montreal Global Biodiversity Framework:
 - Target 1 to plan and manage all areas to reduce biodiversity loss.
 - Target 2 to restore 30% of all degraded ecosystems.
 - Target 3 to conserve 30% of land, water, and seas.
 - Target 6 to reduce the introduction of invasive alien species by 50% and minimise their impact.
 - Target 7 to reduce pollution to levels that are not harmful to biodiversity.
 - Target 8 to minimise impacts of climate change on biodiversity and build resilience.
 - Target 11 to restore, maintain, and enhance nature's contributions to people.
 - Target 14 to integrate biodiversity in decision-making at every level (UN Environment Programme, 2024).

Imaging spectroscopy is a versatile tool with broad applications. Beyond the three application objectives that drive the system design, AquaSat-1 has the potential to support additional applications, including (but not limited to):

- Monitoring other water quality parameters of interest, such as turbidity, coloured dissolved organic matter (CDOM), suspended sediments, vertical light attenuation, and Secchi disk transparency.
- Assessing kelp forests.

⁶ Within the context considered by ESAS 2018, unallocated targeted observables are those for which there are no planned flight programs that would address them.

- Assessing wetlands, including mangrove habitats.
- Supporting oil spill detection and response efforts.

The following subsections provide detailed descriptions of each application objective and their traceability to mission and instrument requirements.

3.1 Application objective 1: Potentially harmful algal blooms

Application objective 1:

For inland and coastal waters in Australia and the western US, inform management of potentially harmful algal blooms by detecting pigments across phytoplankton functional types, including pigments that may indicate the presence of toxins or nutrient pollution.

Physical parameter: phytoplankton functional type fraction to a precision (1σ) \leq 10% absolute fraction, for chlorophyll-a concentrations \geq 3 $\mu\text{g/L}$ (assuming median inland inherent optical properties in Australian waters).

This application is traceable the following sponsor and community goals:

- NASA's WWAO Columbia River Basin Needs Assessment Workshop Report (NASA WWAO, 2020): Scaled-down version of CyAN (Cyanobacteria Assessment Network) to cover smaller bodies of water and develop an early warning system for drinking water systems makers.
- CSIRO AquaWatch End-User Consultation Report (Dekker and MacLeod, 2021), Processes of interest:
 - Inland processes: Sediment and nutrient load from e.g., catchment run-off, erosion, bushfires; nutrient bound in sediments; influence of agricultural and other catchment activities; linkage with catchment processes; blackwater events; inland algal blooms.
 - Coastal processes: Coastal algal blooms; shallow water and benthic system, monitoring over time; sediments impact on seagrass; impact of dissolved organic carbon (DOC)/blackwater events on marine life.
- ESAS 2018 (National Academies of Sciences, 2018):
 - Objective E-3a: Quantify the flows of energy, carbon, water, nutrients, and so on sustaining the life cycle of terrestrial and marine ecosystems and partitioning into functional types (Most Important).
 - Obj. H-3a: Develop methods and systems for monitoring water quality for human health and ecosystem services (Important).

Freshwater and marine microalgae (phytoplankton) are essential components of aquatic ecosystems. They form the base of aquatic food chains, convert dissolved carbon dioxide to organic compounds, and release oxygen during photosynthesis. However, excessive nutrient inputs and other environmental factors can lead to phytoplankton overgrowth, resulting in algal blooms, which are often visible to the naked eye and through remote sensing (see Figure 3-1). These algal blooms can significantly disrupt ecosystem function, for example, by restricting light penetration and by depleting dissolved oxygen when they decompose. Certain types of algae also produce toxins that can cause illness or death in fish, mammals,

birds, and humans. These harmful algal blooms (HABs) present a serious public health risk, affecting recreational water use, drinking water quality, agriculture, and aquaculture.



Figure 3-1: Satellite image (Sentinel-2) showing a blue-green algal bloom and an incoming bushfire-generated ash plume in Lake Hume at the NSW/Victoria border in Australia. Lake Hume is a major reservoir located at the origin of the River Murray, providing irrigation, urban water supplies, and recreational benefits to an economically significant region of Southeastern Australia (Murray–Darling Basin Authority, 2023). It is also an AquaWatch Australia pilot site.

In the United States, the Environmental Protection Agency (EPA) and the National Oceanic and Atmospheric Administration (NOAA) are responsible for monitoring, compiling, summarising and facilitating access to data related to HABs in freshwater and marine environments, respectively. Their primary goals are to protect human health, safeguard the environment, and advance research to enhance understanding of HABs. The Harmful Algal Bloom and Hypoxia Research and Control Act of 1998, reauthorised in 2004, 2014, and 2019, establishes the role of the Interagency Working Group, which includes 13 federal agencies collaborating to maintain a national program for controlling and mitigating HAB events. The Harmful Algal Blooms and Hypoxia Comprehensive Research Plan and Action Strategy (IWG-HABHRCA, 2017) outlines recommendations to enhance scientific understanding of HABs, integrate and strengthen monitoring programs, improve predictive capabilities, and expand stakeholder communications and collaborations. This strategy specifically highlights satellite remote sensing as a crucial tool in achieving these objectives.

In partnership with the Australian states and territories, the Australian and New Zealand governments have developed guidelines for water quality management (ANZECC, 2000)

providing water managers with tools and guidance to assess, manage, and monitor water quality. Revised guidelines (Australian Government, 2024b) include an expanded water quality management framework and new principles and processes to enhance and protect indigenous cultural and spiritual values related to water. These guidelines are part of the National Water Quality Management Strategy (Australian Government, 2024a), which aims to protect Australia's water resources by improving water quality. It includes guidance on HAB monitoring actions, alert systems, and treatment options.

In Australia, algal blooms are best managed locally or regionally due to the highly variable conditions across the continent. Local councils and state water authorities are ideally positioned to investigate outbreaks, inform the public, and take mitigation actions. For example, in the state of New South Wales, the Regional Algal Co-ordination Committees, as part of the state water agency (WaterNSW), are responsible for local management of algal blooms. To improve stakeholder communication and early warning of algal blooms, the Regional Algal Co-ordination Committees have adopted satellite-derived information for susceptible cases in their weekly reports. This approach has become increasingly important in light of recent extreme events, such as cyanobacteria blooms stretching thousands of river kilometres along the Murray River and mass fish kills in the Baaka-Darling River, which were exacerbated by large cyanobacteria blooms (Murray–Darling Basin Authority (MDBA), 2019).

Toxin-producing phytoplankton include the relatively well-known cyanobacteria ('blue-green algae', found in both freshwater and marine environments), dinoflagellates (marine), and diatoms (marine), along with potential sub-types. Other toxin producing phytoplankton, such as haptophytes (e.g., the 'golden algae', found in brackish and marine waters) or euglenoids (*Euglenia sanguinea*, found in freshwater), have been associated with mass fish kills. The names of these algae hint at their pigment content. The ability to distinguish between these toxin-producing phytoplankton and non-toxin producing phytoplankton (e.g., chlorophytes and cryptophytes) is crucial for early warning of potential toxin exposure risks. This capability could trigger earlier public health alerts and further investigation by water managers, including targeted sampling and laboratory analysis, which can take up to two weeks.

As shown in Figure 3-2, PFTs can be optically similar but can be distinguished with sufficiently high spectral resolution (10 nm or less) (Dierssen et al., 2015; Hunter et al., 2008; IOCCG, 2014; Kudela et al., 2015). High signal-to-noise ratio (SNR) is crucial for identifying PFTs during the early stages of an algal bloom, when the biomass is relatively low and a single species not yet dominant. While some satellite instruments, such as PACE OCI, MODIS, and Sentinel-3 OLCI, are capable of PFT discrimination, their pixel sizes exceed 300 m, which limits their effectiveness for inland and coastal waters.

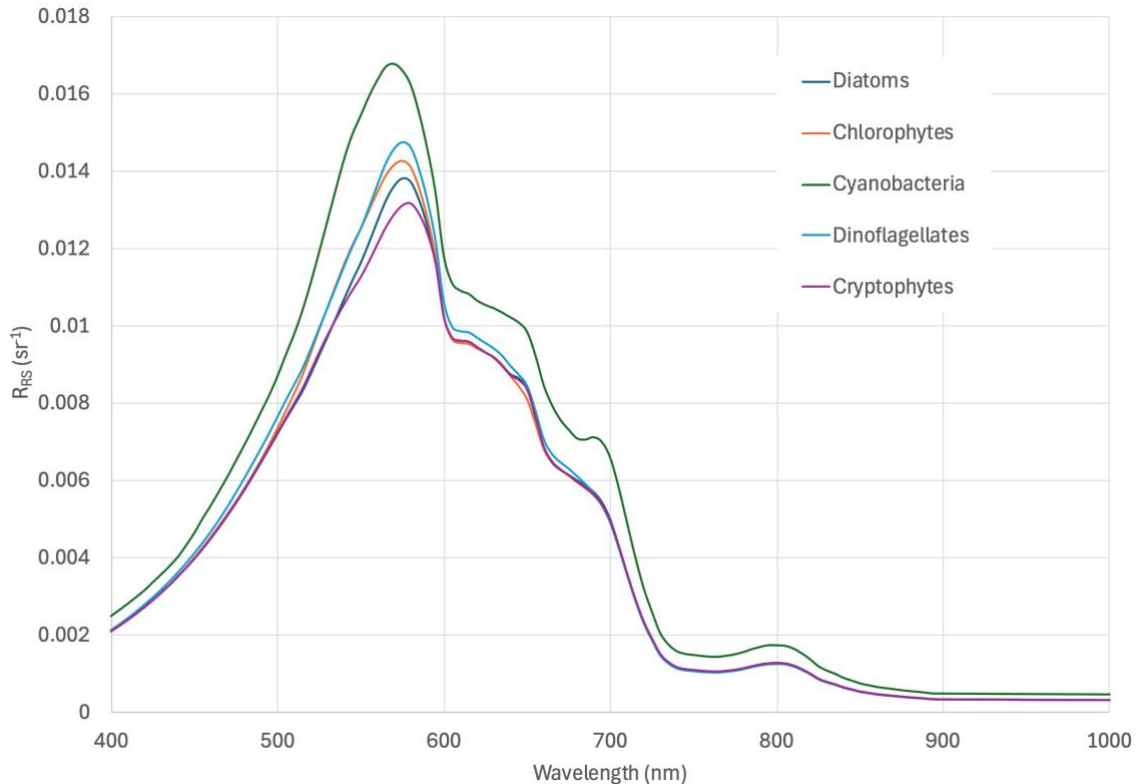


Figure 3-2: Remote sensing reflectance (R_{rs}) resulting from HydroLight (Sequoia Scientific, 2024) radiative transfer simulations of water containing pure samples of key groups of phytoplankton that may be part of PFTs. Cyanobacteria, dinoflagellates, and diatoms can produce toxins harmful to human and animal health, whereas chlorophytes and cryptophytes are not known to produce toxins. Discriminating between these spectral shapes and associated PFTs will enable early warning to water managers of potential toxin exposure. Mass specific inherent optical properties (SIOPs) from Kravitz et al. (2021); Lain et al. (2023); Matthews and Bernard (2013).

To derive requirements for this application objective, we considered national (US and Australia) and international water quality guideline values for microcystin, a toxin produced by a range of cyanobacteria. These guideline values exist for a variety of uses, such as drinking water, recreation, and agriculture. We used the stringent drinking water guideline values to derive AquaSat-1 performance requirements. The applicable guideline values for microcystins in drinking water sources are:

- Australian Drinking Water Guidelines health-based guideline value of 1.3 $\mu\text{g/L}$ for lifetime consumption (NHMRC and NRMCC, 2011).
- US EPA 10-day health advisory value of 0.3 $\mu\text{g/L}$ for bottle-fed infants and young children of pre-school age, or 1.6 $\mu\text{g/L}$ for school-age children through adults (US EPA, 2015).
- World Health Organization (WHO) health-based guideline value 1 $\mu\text{g/L}$ for lifetime consumption (WHO, 2022).

For this study, we parametrise the microcystin concentration by the chlorophyll-a concentration. Typical values range from 0.1 to 0.5 $\mu\text{g/L}$ microcystin per 1 $\mu\text{g/L}$ chlorophyll-a (WHO, 2021a). We used a conservative conversion factor of 1 $\mu\text{g/L}$ microcystin per 1 $\mu\text{g/L}$ chlorophyll-a, which results in a higher sensitivity requirement.

A realistic scenario for the presentation of cyanobacteria in a potential HAB is a mixture where cyanobacteria constitute 50% of the chlorophyll-a. As detailed in Section 3.4, to determine the physical parameter of interest and the associated observables, we adopted a water mixture with various PFTs totalling 3 µg /L of chlorophyll-a, of which 1.5 µg/L is contributed *Microcystis aeruginosa*. This concentration aligns with both Australian and US-EPA guidelines for drinking water.

Table 3-1 summarises the factors influencing temporal resolution requirements for algal bloom observations. End-user needs for temporal resolution generally favour the highest possible frequency that is technologically and financially feasible (CEOS, 2018). In practice, different management objectives require different temporal resolutions. Currently, algal bloom monitoring is conducted weekly for select water bodies, typically after a bloom has been reported (Dekker and MacLeod, 2021; Hardy et al., 2016; WHO, 2021b). For AquaSat-1, we aim to monitor algal bloom dynamics and responses to management interventions. Thus, we have set the temporal resolution requirement to monthly or better useable imagery when averaging the revisit times over a year. Here ‘useable’ is defined as having 10% or less cloud cover over the target site. Our analysis indicates that the temporal resolution for HAB target sites ranges from 1 to 3 weeks, depending on cloud coverage, with higher temporal resolution achievable using a constellation of multiple satellites (see Section 4.3).

This application objective also drives the mission's latency requirement, defined as the time between data acquisition and the availability of high-level products to end users. The high-level data products will include the PFT fraction within the ground sample distance (GSD), as well as chlorophyll-a concentration and other water quality metrics, such as CDOM and turbidity. For this study, we set the latency requirement to be 2 days or less, representing a significant improvement over current practices (Table 3-1) and aligning with the results of end-user surveys (Dekker and MacLeod, 2021).

Table 3-1: Temporal resolution drivers for algal bloom observations, with the AquaSat-1 requirement set to ‘monthly or better’ usable imagery for HABs target sites. The revisit and cloud cover analysis in Section 4.3 shows that AquaSat-1 meets this requirement.

| Temporal resolution | Enabled observations |
|--|---|
| Daily or better | Warning when HABs approaching drinking water intakes or recreational areas. Interaction of HAB development with internal lake dynamics. |
| Weekly or better Current practice, but event-driven and with high latency (up to 2 weeks). | Spatiotemporal development of blooms (transport). Monitoring short term impacts of intense blooms (low dissolved oxygen and fish kills). Early warning of poor water quality for drinking/recreation. |
| Monthly or better AquaSat-1 requirement | Monitoring to trigger immediate responses and spatial changes in HAB population due to management interventions, dynamics, and meteorological and hydrological conditions. |
| Quarterly or better | Monitor hotspots of HAB development. Monitoring of growth and decay cycles (population dynamics). Monitoring the impact of catchment processes and management on bloom formation and trophic status. |
| Annual or better | Long term reporting; link with human health impacts. |

3.2 Application objective 2: Invasive aquatic vegetation

Application objective 2:

For inland waters in Australia and the western US, inform management of floating and emergent invasive aquatic vegetation (IAV) in lakes, reservoirs, and wetlands.

Physical parameter: fractional area cover to $1\sigma \leq 10\%$ absolute coverage fraction for floating and emergent vegetation functional types of interest.

This application is traceable the following sponsor and community goals:

- WWAO 2016 Rapid Needs Assessment (WWAO, 2016): Assessment of Ecosystem health; water quality in reservoirs.
- ESAS 2018 (National Academies of Sciences, 2018):
 - Obj. E-1e: Support targeted species detection and analysis (e.g., foundation species, invasive species, indicator species, etc.) (Important).
 - Obj. E-3a: Quantify the flows of energy, carbon, water, nutrients, and so on sustaining the life cycle of terrestrial and marine ecosystems and partitioning into functional types (Most Important).

In aquatic habitats, invasive vegetation is increasing globally (Havel et al., 2015), negatively impacting biodiversity, human livelihoods and well-being, and water resources infrastructure (Pimentel et al., 2000; Reid et al., 2019). Recent estimates indicate that invasive aquatic vegetation (IAV) has led to global economic losses of approximately USD\$32 billion between 1975 and 2020, with costs now exceeding USD\$700 million annually. However, this figure likely underestimates the true impact, as data on the distribution and effects of these invasive species remain limited in many countries and ecosystems (Macêdo et al., 2024).

IAV can obstruct commercial vessel travel, recreation, and essential processes like hydropower, irrigation, and water management (Keller et al., 2018; Villamagna and Murphy, 2010). It also disrupts ecological processes, affecting water quality, carbon and nutrient cycling, and species and communities (Emery-Butcher et al., 2020; Guy-Haim et al., 2018; Hestir et al., 2016). For example, Figure 3-3 illustrates how invasive water hyacinth impedes irrigation channels and water delivery to farms in California's San Joaquin Valley. Although herbicides are commonly used to manage IAV, recent studies suggest their effectiveness is limited (Khanna et al., 2023; Rasmussen et al., 2022) and raise concerns about potential herbicide resistance (Peterson et al., 2018; Richardson, 2008).

There is growing recognition that water management and restoration efforts significantly influence IAV dynamics, presenting water managers with complex decisions. Effective decision-making requires information on IAV distribution and potential spread, and must account for biodiversity targets, restoration projects, water flow management, and herbicide treatment permits.



Figure 3-3: Water hyacinth impedes irrigation channels, impeding water delivery to farms in California’s San Joaquin Valley. Image credit: Timothy Ukena.

High spectral resolution data is essential for discriminating plant functional types, genera, and species (Bolch et al., 2021; Bolch et al., 2020; Dierssen et al., 2021; Hestir et al., 2008; Santos et al., 2016; Underwood et al., 2003; Yang and Everitt, 2010). Although this application objective does not drive the system’s SNR requirements (see Section 3.4), it does impact the spectral requirements. When paired with a spectral range of at least 700 nm to 1040 nm, a spectral resolution of 10 nm or less is sufficient to discriminate the fine spectral features that distinguish similar vegetation types (see Figure 3-4). This allows for the detection of subtle reflectance differences that indicate biochemical, physiological, and structural variations among plant functional types. Note that species-level mapping relies on there being greater intra-species variation than inter-species variation, and often this level of differentiation is not accomplished with only a single snapshot of data (Fernandes et al., 2013; Wolf et al., 2013).

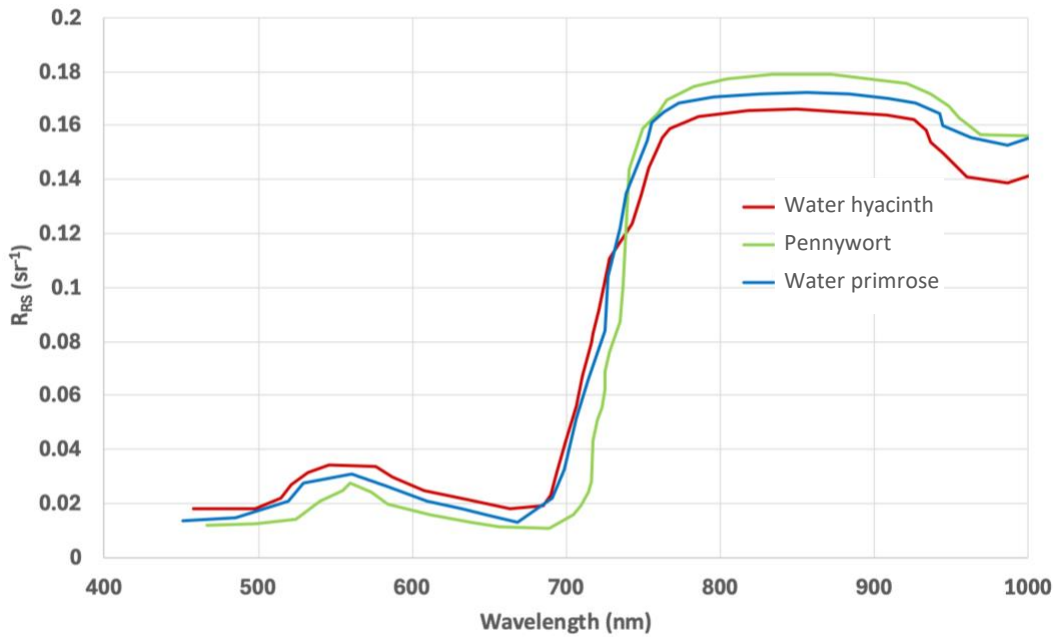


Figure 3-4: Remote sensing reflectance (R_{rs}) of two globally highly invasive aquatic plants, water primrose and water hyacinth, and a native species (pennywort) (Hestir and Dronova, 2023). High spectral resolution data are needed to distinguish these to functional-type and genera-level to enable informed decision making and management.

Table 3-2 summarises the temporal resolution drivers for aquatic vegetation observations, indicating that monthly or more frequent imagery is necessary to assess growth dynamics, impact of flow decisions, and the effectiveness of mitigation measures (Hestir et al., 2023, unpublished data, under NASA contract #80NSSC23K1563). High temporal resolution data (better than the annual current practice) is crucial for capturing plant phenological states for improved detection (Bolch et al., 2020), especially when spectroscopic differences alone are insufficient to distinguish plant phenotypes. As in application objective 1, the requirement refers to the annual average cloud-free revisit time.

Table 3-2: Temporal resolution drivers for aquatic vegetation observations, with the AquaSat-1 requirement set to ‘monthly or better’ usable imagery for IAV target sites. The revisit and cloud cover analysis in Section 4.3 shows that AquaSat-1 meets this requirement.

| Temporal resolution | Enabled observations |
|---|---|
| Daily or better | Pump operations. |
| Weekly or better | Enhanced warning of floating mat transport for pump fouling; improved phenology metrics for target herbicide application. |
| Monthly or better AquaSat-1 requirement | Dynamics of growth and impact of flow decisions and mitigation measures. |
| Quarterly or better | Management of growth and decay cycles. |
| Annual or better Current practice. | Ecosystem assessment; long term reporting. |

3.3 Application objective 3: Coral reefs

Application objective 3:

For coastal waters in Australia and the western US (including Hawai'i), inform management of coral reef ecosystem condition by measuring the habitat benthic cover for coral reefs.

Physical parameter: coral fractional area cover to $1\sigma \leq 10\%$ absolute coverage fraction, within ≤ 10 m depth of relatively clear water (defined as average water conditions of Heron Island, in the Great Barrier Reef in Australia).

This application is traceable the following sponsor and community goals:

- CSIRO AquaWatch End-User Consultation Report (Dekker and MacLeod, 2021), Processes of interest: Coastal - Shallow water and benthic system, monitoring over time.
- ESAS 2018 (National Academies of Sciences, 2018):
 - Obj. E-1a. Quantify the global distribution of the functional traits, functional types, and composition of vegetation and marine biomass, spatially and over time (Very Important).
 - Obj. E-1e. Support targeted species detection and analysis (e.g., foundation species, invasive species, indicator species, etc.) (Important).
 - Obj. E-3a. Quantify the flows of energy, carbon, water, nutrients, and so on sustaining the life cycle of terrestrial and marine ecosystems and partitioning into functional types (Most Important).

Coral reefs, though occupying less than one percent of the global ocean surface, harbor nearly a quarter of marine life and support the livelihoods of nearly a billion people (Morrison et al., 2019; Souter et al., 2021). The goods and services they provide are vital for the health of interconnected ecosystems and directly impact the well-being of local communities (Moberg and Folke, 1999). Management and conservation efforts for coral reef ecosystems, often conducted at regional to national scales, heavily rely on spatial information systems and assessments of economic and environmental value (Beck et al., 2018). Recent advancements in reef mapping—particularly through remote sensing-based approaches—have significantly improved our understanding of coral reefs across various spatial scales, from local to global levels, thereby aiding informed decision-making and conservation strategies (Lyons et al., 2024). The 2024 mass bleaching event on the Great Barrier Reef (see Figure 3-5) and other global occurrences have intensified the urgency for developing methods for monitoring changes in coral cover over time.



Figure 3-5: Heron reef (part of the Great Barrier Reef) in March 2024 during a bleaching event. If this bleached coral doesn't recover, it will be rapidly overgrown with algae, which is indistinguishable from live coral using existing satellite imagery. AquaSat-1 will be able to differentiate these cover types. Image credit: Meredith Roe.

Increased precision in remote sensing of coral reefs is imperative for effective monitoring and management, particularly due to the complex and dynamic nature of these ecosystems. Current limitations, such as the inability to accurately distinguish between optically similar benthic cover types under various environmental conditions (Hedley et al., 2012) or to detect the abundance of those types within a pixel, detract from the usefulness of satellites for routine monitoring of biodiversity and condition (Asner et al., 2020; Lyons et al., 2024). For example, following a bleaching event, corals may either recover or die, with dead corals often being overgrown by turf algae within a period ranging from weeks to several months. AquaSat-1 is designed to distinguish between these two outcomes, which is not possible with current multispectral satellite data.

There are two key enhancements where increased precision of imaging spectroscopy offers significant advantages compared to existing multispectral data: 1) separation of benthic types and detection of dominant benthic types in mixed substrate pixels, and 2) detection of the absolute or relative change in fractional cover of target benthic types within mixed substrate pixels. High spectral resolution enhances the ability to differentiate between various benthic types and detect subtle changes in their composition or cover, which are the key biophysical variables required for reef status and condition assessments (Obura et al., 2019).

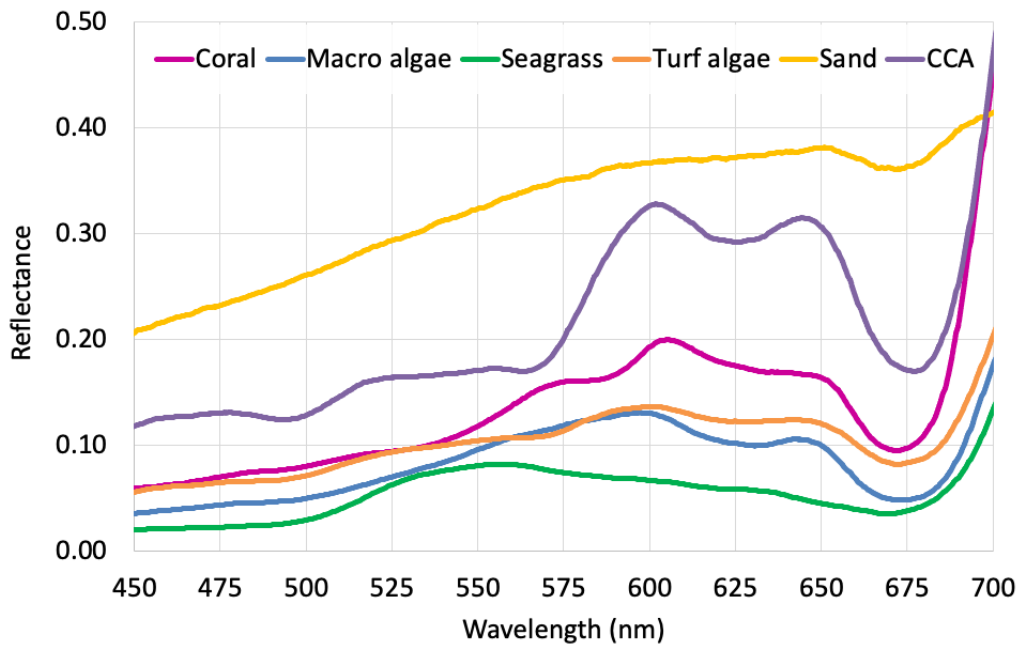


Figure 3-6: Representative radiance reflectance of six key coral reef habitat benthic cover types: coral, macro algae, seagrass, turf algae, sand (light sand), and crustose coralline algae (CCA). Reflectance was calculated by averaging corresponding in-situ underwater measurements of each benthic cover type, with endmembers obtained from Roelfsema and Phinn (2017). The wavelength axis is limited to 700 nm because light at longer wavelengths is strongly absorbed by the water column, resulting in minimal signal beyond this range.

Temporal drivers operate from near-annual down to near-daily time scales (Table 3-3). State-of-the-reef reporting typically occurs on an annual basis; however, these assessments are often based on extrapolations from a limited number of small-scale surveys conducted across different reefs (Souter et al., 2021). Quarterly space-based observations of coral coverage would permit large-scale seasonal monitoring (CEOS, 2018). This approach would enable comprehensive pre- and post-bleaching assessments, support seasonal state-of-the-reef reporting, and provide earlier indications of the impacts of management actions. As in application objectives 1 and 2, the requirement refers to the annual average cloud-free revisit time.

Table 3-3: Temporal resolution drivers for coral coverage observations, with the AquaSat-1 requirement set to ‘quarterly or better’ usable imagery for coral target sites. The revisit and cloud cover analysis in Section 4.3 shows that AquaSat-1 meets this requirement.

| Temporal resolution | Enabled observations |
|---|--|
| Daily or better | Bleaching dynamics research (note 1-2 weeks’ worth of daily imagery during a bleaching event is sufficient). |
| Weekly or better | Monitoring short-term impacts from extreme weather events, bleaching, crown of thorns starfish, ship grounding, pollution events, etc. |
| Monthly or better | Monitoring changes from poor water quality, warming, acidification, etc. |
| Quarterly or better AquaSat-1 requirement | Monitoring seasonality of macro algae and long-term system changes resulting from poor water quality, warming, acidification, etc. |
| Annual or better Current practice. | Annual state of the reef reporting and assessing impact of management strategies. |

Maps with increased precision and detail, along with downstream products, would enable significant advancements for end-users in monitoring and managing coral reef habitats. With the ability to reliably separate coral and algae cover types, as well as coral and seagrass habitats, within low error margins, resource managers and scientists would gain new capacity for monitoring habitat distribution and dynamics. The capability to accurately account for the total area of coral and to estimate the changes in coral percentage cover would enhance the precision of ecosystem assessments and facilitate more informed decision-making processes. This level of accuracy and reliability would be particularly valuable for assessing the effectiveness of conservation measures, identifying areas of concern for targeted intervention such as recolonisation efforts, and monitoring long-term trends in coral reef and seagrass health for both local and global scale case studies. The following is a preliminary assessment of the expected coral coverage benchmarks for end-users, summarised from the journal paper in preparation (Malthus, 2024):

- Separate coral from algae in pixels with common mixtures of reef substrates.
- Detect coral fractional cover to within 10%.

For many tropical coral reef areas around the world, seagrass is a major ecosystem component and has similar spectral characteristics to other coral reef benthic cover types (Figure 3-6) (Hedley et al., 2012). Seagrass was therefore included in this study (Malthus, 2024), and the following is a preliminary assessment of the expected benchmarks for end-users:

- Separate pixels dominated by seagrass from other common mixtures of biotic and non-biotic benthic substrates (e.g., coral, sand, mud, macro algae).
- Detect seagrass fractional cover to within 10%.

Light penetration in the water column decreases exponentially with depth. This effect is wavelength dependent, with blue and red-near-infrared wavelengths attenuated faster than other wavelengths. With increasing depth, the penetrating light becomes increasingly restricted to the green-yellow region, where there is less vertical attenuation. A satellite sensor with broad spectral band coverage, high spectral resolution, and high radiometric sensitivity will be able to discriminate relevant habitat classes at deeper depths. In high and moderate transparency water, typical of coral and seagrass habitats, the ability to reliably map high coral cover density rapidly degrades in water deeper than approximately 10 m. This is why mapping solutions at spatial resolutions greater than 3-5 m pixel resolution are generally limited to 10 m water depth (Lyons et al., 2024). Therefore, we set an additional requirement to discriminate submerged cover types at 10 m or less. A space-borne imaging spectrometer meeting these benchmarks would empower end-users with practical data sources needed to implement proactive management, accounting, and conservation strategies that multispectral instruments are currently unable to provide.

3.4 Observables

The observables for AquaSat-1 are the top-of-atmosphere (TOA) radiances. Defining the TOA observable requires the specification of a scene and an observation scenario.

For application objective 1, phytoplankton content was modelled using different mass-specific inherent optical property (SIOP) sets to simulate mixed populations. Remote sensing reflectance (R_{rs}) values were generated for dominant blooms of five phytoplankton types: cyanobacteria (*Microcystis aeruginosa*), dinoflagellates, diatoms, green algae (chlorophytes), and cryptophytes (Dierssen et al., 2015). The dominant blooms were assumed to be 50% cyanobacteria by volume, with the remaining 50% consisting of a mixture of the other types. Specifically, a chlorophyll-a concentration of 3 $\mu\text{g/L}$ corresponds to 1.5 $\mu\text{g/L}$ of *Microcystis aeruginosa* and 1.5 $\mu\text{g/L}$ of the other functional types combined. To simulate median Australian waters (Drayson et al., 2022), the background SIOPs for phytoplankton, non-algal particles, and CDOM were randomly varied within the 50% percentile. A total of 100 simulation sets were produced for each measurement goal to account for this variability.

For application objective 2, the remote sensing reflectance was derived for a scene where a given pixel consists of 40% water hyacinth, 15% water primrose, 15% floating-leaved plants, 15% helophytes, and 15% submerged aquatic vegetation. The primary quantity of interest is the coverage of water hyacinth. In the performance analysis described below, the choice of the dominant species is not a significant factor; the performance remains similar regardless of which species is predominant.

For application objective 3, the remote sensing reflectance used in the performance simulations corresponds to the average water conditions at Heron Island in the Great Barrier Reef, Australia. In this case, we are interested in measuring the change in coral fraction for a pixel with a benthic cover consisting of 40% coral, 40% turf algae, 10% macroalgae, and 10% crustose coralline algae.

In each of these scenarios, the remote sensing reflectances were converted to TOA radiances, assuming nadir observations with a solar angle of 23.4° . The atmosphere was considered to have negligible aerosol loading and a water vapor column concentration of 1.5 g cm^{-2} . As discussed in Section 4.3.5, the instrument performance is only weakly dependent on the solar angle. In all cases, the requirement is to detect noise-equivalent changes in the quantity of interest with a precision of $1\sigma \leq 10\%$.

3.5 Instrument requirements

The AquaSat-1 instrument is described in Section 5.

In the instrument requirements columns of the ATM, the spectral range is specified as 400 to 1020 nm. This range is the minimum required to meet all application objectives. The spectral sampling (≤ 8 nm) and spectral response function (SRF) (≤ 10 nm) are derived from requirements for ocean color sensors (CEOS, 2018). The swath width (≥ 50 km) is determined based on the narrowest dimension of the water bodies of interest. As discussed in Section 4.4, the ground sample distance (GSD) of ≤ 20 m provides access to more than 90% of all lake and reservoir areas in the regions of interest, nearly doubling the observable number of these features compared to missions with a 30 m GSD, such as Landsat-8, Carbon Plume Mapper (CPM), EnMAP, Prisma, or the planned Surface Biology and Geology (SBG). The absolute uncertainty is set to $\leq 5\%$, which is half of the precision error specified for the physical parameters. The radiometric range 0.7 Lambertian enables imaging of bright terrains, such as those covered with fresh vegetation (application objective 2).

The instrument's signal-to-noise ratio (SNR) requirements and performance are assessed as follows: For a single defined observation scenario—considering the water surface, observing geometry, and atmospheric conditions—the instrument's noise performance is translated into errors in downstream products. The error propagation procedure, outlined by Rodgers (2000) and others, linearizes the retrieval algorithm around a reference value for the quantity of interest. For small perturbations in radiance, this retrieval can be optimised by accounting for instrument noise, yielding a linear operator known as a matched filter (Manolakis et al., 2000). Propagating instrument noise through this linear transformation provides the noise-equivalent change in the quantity of interest, allowing for a quantitative assessment of noise impact on performance.

The results of this process for the instrument described in Section 5 are shown in Figure 3-7, Figure 3-8, and Figure 3-9. The analysis considers both standard pushbroom acquisitions and ground motion compensation (GMC), where the satellite's pointing remains fixed over a target site, increasing exposure time by a factor of 10 (see Section 3.2.2). As shown in the figures, the system can achieve the physical parameters with the specified ATM precision in all cases.

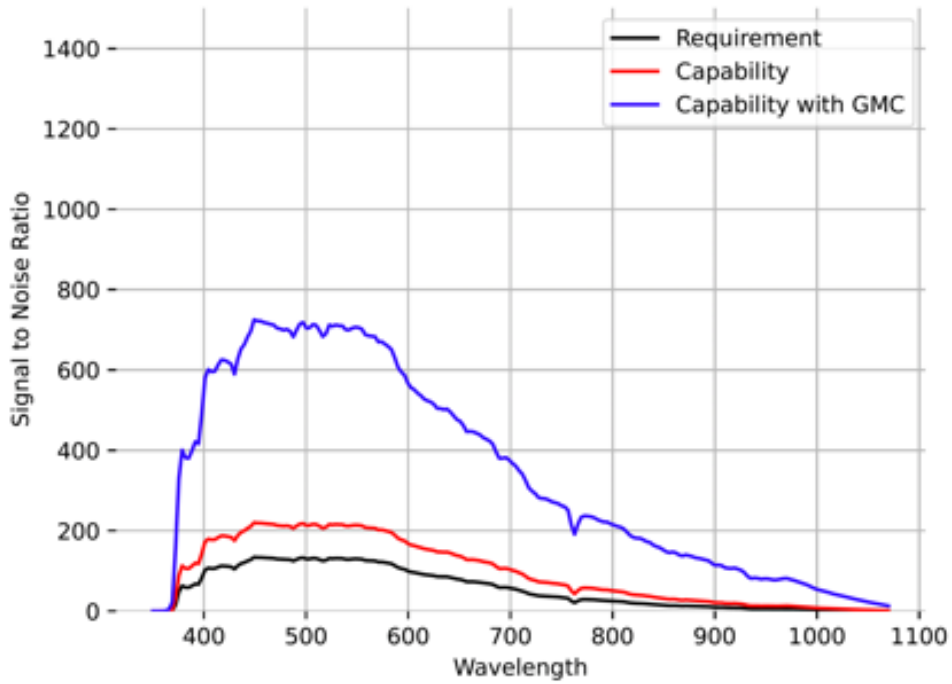


Figure 3-7: Radiometric requirements and performance for the physical parameter corresponding to application objective 1: measure 50% cyanobacteria population with 10% absolute error (i.e., when cyanobacteria changes from 50% to 40% or 50% to 60%) in a PFT mixture with 3 $\mu\text{g/L}$ chlorophyll-a. The black trace corresponds to the requirement, the red trace to the system performance assuming pushbroom operations, and the blue trace to the performance assuming GMC operations.

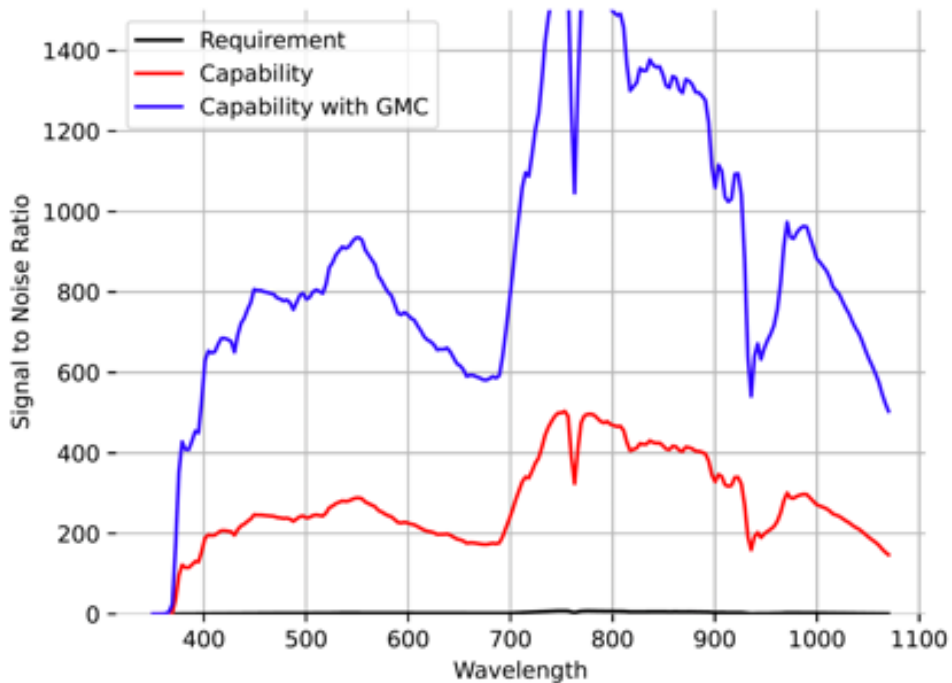


Figure 3-8: As per Figure 3-7 but for application objective 2: Measure 40% coverage of Water Hyacinth with 10% absolute error.

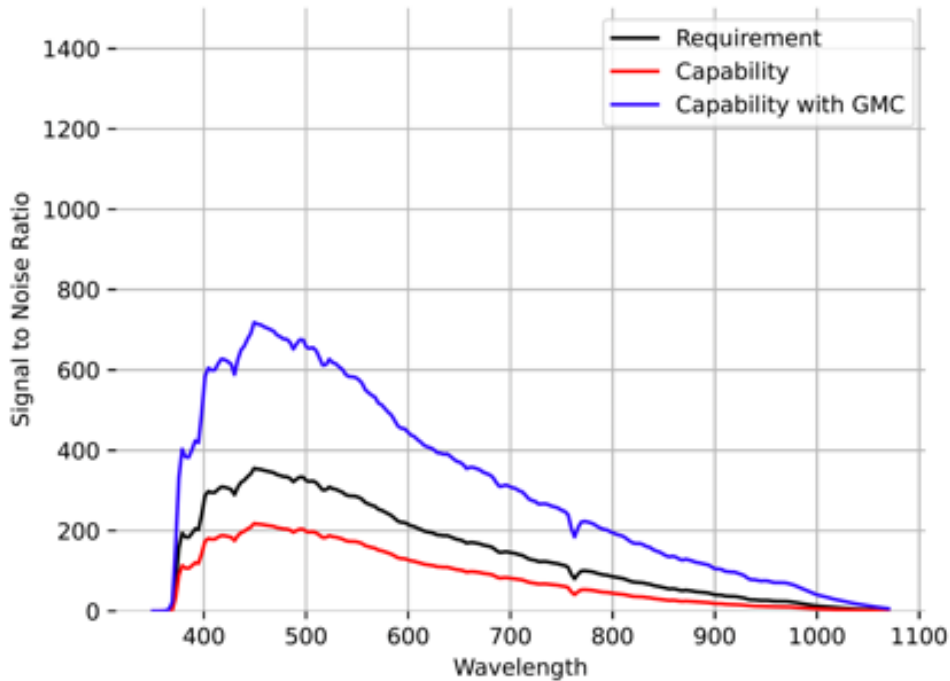


Figure 3-9: As per Figure 3-7 but for application objective 3: Measure 40% benthic coverage of coral with 10% absolute error under 10 m of relatively clear waters. This objective drives the need for GMC operations, as the SNR cannot be reached only with pushbroom mode.

For all application objectives, the GMC performance shows substantial SNR margins beyond the requirements. These margins are necessary at this early stage of the design. For application objectives 1 and 2, factors such as glint, trees, canyons, etc., may degrade the SNR in real-world scenarios. Additionally, low water transparency will decrease our ability to retrieve the parameters of interest. The large SNR margins help mitigate these risks, ensuring that the physical parameters can be measured with the required precision even under challenging conditions.

These substantial margins also offer additional capability. For example, for application objective 1, the SNR requirement is based on a mixture of PFTs. However, when observing a water mixture consisting solely of *Microcystis aeruginosa*, AquaSat-1 can detect chlorophyll-a concentrations $0.3 \pm 10\%$ $\mu\text{g/L}$ in GMC mode. Using the conservative conversion outlined in Section 3.1, this corresponds to the US-EPA 10-day Health Advisory for total microcystins for bottle-fed infants and young children of pre-school age (US EPA, 2015). Although not specified in the objectives, AquaSat-1 can also measure changes in CDOM and attenuation with a precision of $1\sigma=10\%$ for the typical waters considered.

As shown in Figure 3-9, the requirement to detect coral coverage under 10 m of water drives the need for GMC. The system's performance degrades rapidly with water column depth (see Figure 3-11). At 25 m, the 1σ uncertainty in coral coverage reaches 100%.

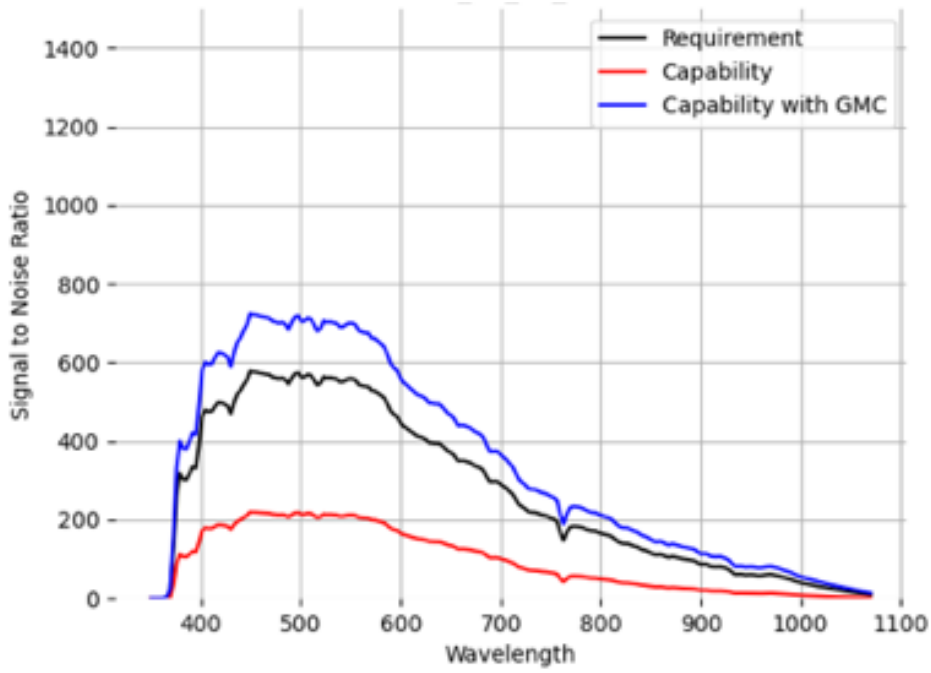


Figure 3-10: Performance simulations indicate that AquaSat-1 can detect $0.3 \pm 10\%$ $\mu\text{g/L}$ of chlorophyll-a when using GMC.

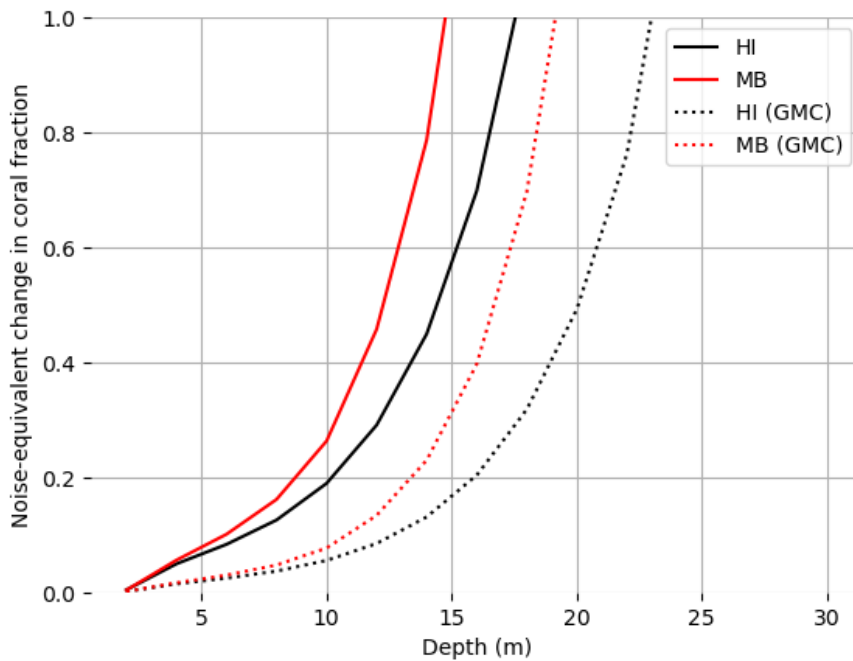


Figure 3-11: 1σ uncertainty in the determination of coral coverage for different water models. The plot shows the performance with pushbroom observations (solid lines) and with GMC (dotted). MB: Moreton Bay, HI: Heron Island.

3.6 Mission requirements

Key mission requirements are listed in the last column of the ATM (Tables 2-2 and 2-3). Table 3-4 lists the complete mission requirements and rationale for the system, expressed as ‘shall’ statements for formal requirements flow-down.

Table 3-4: AquaSat-1 mission requirements.

| ID | Requirement | Rationale |
|------------|--|--|
| AS1-MIS-1 | The mission shall comprise a space segment, ground operations segment, and a science data processing segment. | Driven by sponsor and study scope (see Section 2.1). |
| AS1-MIS-2 | The space segment shall consist of one satellite comprising the JPL-developed VNIR imaging spectrometer instrument payload and the satellite platform. | Driven by sponsor and study scope (see Section 2.1). |
| AS1-MIS-3 | The ground operations segment shall include all facilities required to plan, schedule, execute, monitor, and maintain the health and safety of the satellite during operations. | Driven by sponsor and study scope (see Section 2.1). |
| AS1-MIS-4 | The science data processing segment shall provide the equipment, resources and facilities to receive, process, archive and distribute the science data products to the investigators. | Driven by sponsor and study scope (see Section 2.1). |
| AS1-MIS-5 | AquaSat-1 shall orbit about Earth in a Sun-synchronous orbit with a local time of descending node of 12:00 (noon) \pm 15 minutes. | Chosen as baseline. However, both in terms of SNR and cloud coverage, all times between 10:00 and 14:00 are equivalent (see Section 4.3.5). |
| AS1-MIS-6 | AquaSat-1 shall achieve at least 12 months of science operations. | Minimum lifetime to detect seasonal changes and appropriate for a pathfinder mission. |
| AS1-MIS-7 | AquaSat-1 on-board consumables (including degradation) shall permit 3 years of on-orbit operations. | To support possible mission extension. |
| AS1-MIS-8 | AquaSat-1 shall de-orbit within five years of completing its operational mission. | To meet Inter-Agency Space Debris Coordination Committee (IDAC) guidelines. |
| AS1-MIS-9 | The mission shall achieve a latency of \leq 2 days between image acquisition and generation of high-level science data products. | Driven by end-user needs for application objective 1 (see Section 3.1). |
| AS1-MIS-10 | AquaSat-1 shall be capable of imaging estuaries, rivers (\geq 60 m wide), lakes/reservoirs (\geq 60 m wide), and wetlands (\geq 60 m wide) in Australia and the US West, and coral reefs (\leq 10 m depth). | Minimum linear dimension of target site is 3x the spatial resolution to ensure at least one unmixed water pixel. Permits coverage of 38% of the total river surface area and 93% of the total lake surface area within the study region (see Section 4.4). |
| AS1-MIS-11 | AquaSat-1 shall be capable of imaging applicable radiometric calibration sites and AquaWatch Australia pilot sites. | To permit on-orbit instrument calibration (see Section 5.3). |
| AS1-MIS-12 | When averaged over a year, AquaSat-1 shall obtain a useable image: monthly or better for harmful algal bloom (HAB) targets; monthly or better for invasive aquatic vegetation (IAV) targets; seasonal or better for coral targets. | Driven by end-user needs for each application objective (see Section 3). |

| ID | Requirement | Rationale |
|------------|--|---|
| AS1-MIS-13 | AquaSat-1 shall be capable of pushbroom imaging. | To permit possible descope of ground motion compensation (GMC) imaging (see Section 4.1) and operational flexibility in image strategy. |
| AS1-MIS-14 | AquaSat-1 shall be capable of 'ground motion compensation' (GMC) imaging, where the effective ground track velocity is slowed by up to 10x using the attitude control system. | Driven by application objective 3 signal-to-noise ratio requirements (see Section 3.5). |
| AS1-MIS-15 | AquaSat-1 shall have a 60° full-cone field of regard centred on nadir. | As large as practical for increased revisit frequency and observation opportunities (see Section 4.1), while still permitting a passive thermal control system (see Section 5.4.3) and reliable atmospheric correction. |
| AS1-MIS-16 | AquaSat-1 shall maintain a spatial resolution of 18 m ± 10% when the instrument is pointed nadir. | Driven by end-user needs for each application objective (see Section 3) and need to maintain spatial resolution over mission lifetime. Permits coverage of 38% of the total river surface area and 94% of the total lake surface area within the study region (see Section 4.4). |
| AS1-MIS-17 | AquaSat-1 shall be designed to withstand and operate through all environmental conditions encountered throughout its lifecycle. | To ensure mission lifetime requirement is met. |
| AS1-MIS-18 | AquaSat-1 shall be 3-axis stabilized, with the following attitude determination and control capability for the instrument's boresight (3σ): pointing error ≤ 2.6° (1/3 swath); knowledge error ≤ 4 arcsec (0.5 pixel); drift ≤ ± 4 arcsec per 225 arcsec travel (0.5 pixel per 25 pixels travel); jitter ≤ 0.9 arcsec per 25 ms integration (0.1 pixel per integration); slew rate > 3°/s. | Slew rate based on a preliminary design reference mission using standard attitude actuators for SmallSat missions (see Section 6.2.1). Further analysis is needed to confirm this value. Other pointing requirements derived from heritage with previous JPL missions, in particular airborne efforts such as AVIRIS (JPL, 2024a). Pointing requirements are relatively benign because ground registration permits reconstruction of pointing after image acquisition. As this implementation relies on ground knowledge, it may limit the mission's ability to observe over the open ocean and may impose a limit on the coral reefs that can be observed, if no land is available for georeferencing. Further work required to explore this in detail. |
| AS1-MIS-19 | AquaSat-1 shall support a science data volume > 80 GB/day. | Based on science data rate of instrument described in Section 5 and a preliminary design reference mission that assumed 30 images per day. Further analysis is needed to confirm this value. |

4 Mission description

4.1 Concept of operations

The AquaSat-1 baseline orbit is Sun-synchronous, with a 400 km altitude and 12:00 (noon) local time of descending node (LTDN). During its one-year long pathfinder mission, AquaSat-1 will image inland and coastal water target sites globally, as well as calibration sites and AquaWatch Australia pilot sites to support product validation. This study focusses specifically on target sites in Australia and the western US, which are of primary interest to the study sponsors. Figure 4-1 displays a representative, non-exhaustive map of the proposed target sites.

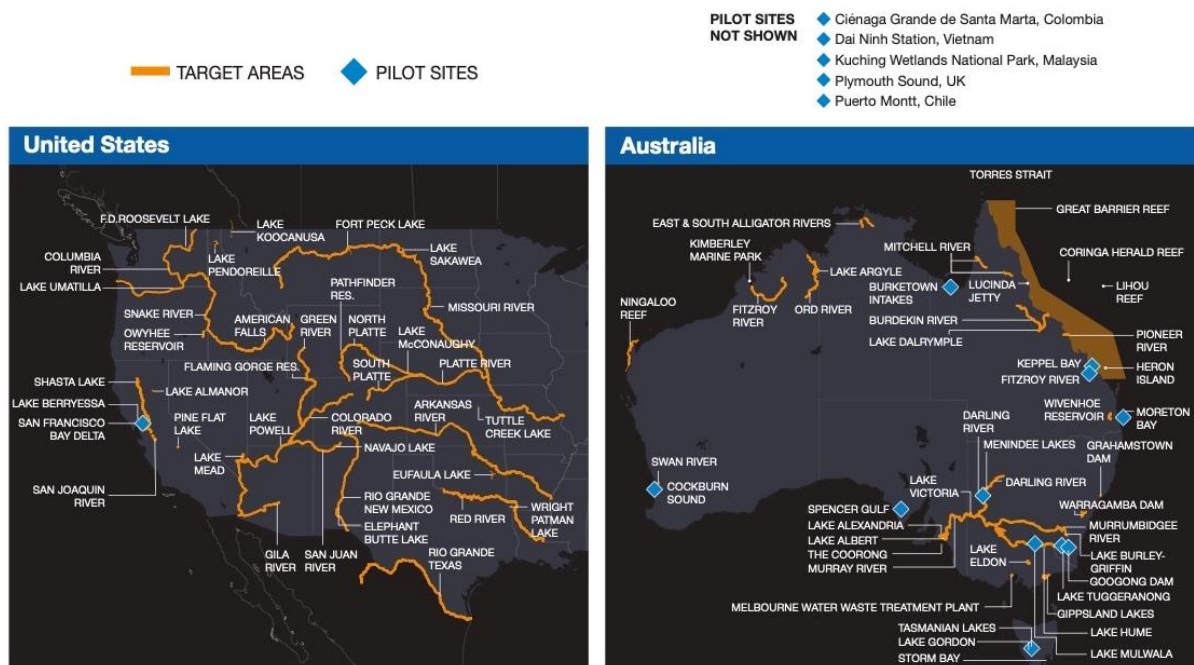


Figure 4-1: Representative target sites for AquaSat-1. Calibration sites, international AquaWatch pilot sites, some reservoirs, and coral reefs in the Caribbean and Hawai'i have been omitted for clarity.

AquaSat-1 will slew up to $\pm 30^\circ$ to achieve a global revisit rate of 5 days at the equator and 3.5 days at 45° latitude, not accounting for factors such as cloud cover, sunglint, or target site conflicts. Since multiple target sites may be within the instrument's field-of-regard during an overpass, a strategy is needed to prioritise these sites (see Section 4.2).

AquaSat-1 will support both pushbroom and ground motion compensation (GMC) imaging. In GMC mode (illustrated in Figure 4-2), the satellite's pointing remains fixed over a target site to increase the effective integration time by up to 10 times. This strategy enhances the measurement signal-to-noise ratio (SNR) by factors of 2 to 3, providing significant sensitivity benefits for detecting water-leaving reflectance signatures.

GMC has been successfully utilised by the Mars-orbiting Compact Reconnaissance Imaging Spectrometer for Mars (CRISM) mission, which employed a scan mirror (Murchie et al., 2004; Seelos et al., 2024). The Tanager-1 mission, featuring a Carbon Plume Mapper (CPM) instrument, will soon demonstrate this technique in Earth orbit (Zandbergen et al., 2022). AquaSat-1 will be the first demonstration of GMC for wide-swath imaging of Earth.

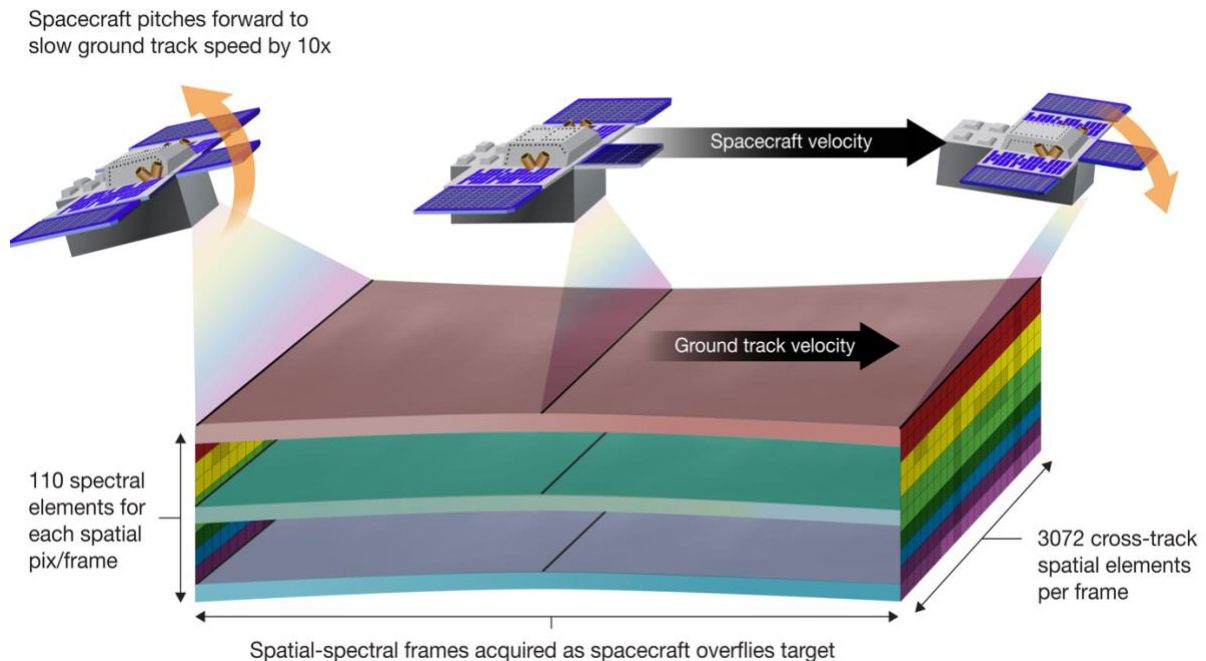


Figure 4-2: Illustration of the GMC imaging strategy. This increases the integration time by a factor of 10 for a 3-fold increase in SNR, at the expense of ground coverage.

GMC is a key enabling technology for inland and coastal aquatic observations from space, where the combination of high spatial resolution and subtle surface signals present challenges. Historically, photon-gathering limitations have constrained orbital spectroscopic water quality observations to coarse spectral resolution (e.g., Sentinel-2), or coarse spatial resolution (e.g., the PACE mission). GMC offers the potential for high-spatial, high-spectral resolution observations—a step change in capability of orbital water quality monitoring.

Appropriate handling of GMC data in downstream processing is essential. In GMC mode, the sensor maintains a fixed exposure time, requiring frames to be co-adding in post-processing either on-board or on-ground. Additionally, the effective size of the pixel projected on Earth changes due to variations in viewing geometry during acquisition, resulting in a 'bowtie' effect in the reconstructed data cube. These variable view angles must be accounted for during atmospheric correction, a functionality that is already available in at least one contemporary open-source software package, e.g., ISOFIT (Thompson et al., 2018).

4.2 Target site prioritisation strategy

Target sites are categorised into three key groups, arranged by priority, as described in the following sections.

4.2.1 Category 1: Calibration sites

The AquaSat-1 instrument will not include on-board radiometric calibration devices. Instead, post-launch calibration will be achieved by regularly observing vicarious calibration sites. For further details on pre- and post-launch calibration, see Section 5.3.

The primary candidate for radiometric calibration is the Radiometric Calibration Network (RadCalNet) (Bouvet et al., 2019). RadCalNet provides SI-traceable TOA reflectance for a nadir view at 30-minute intervals. This open-access data includes associated uncertainties at a 10 nm spectral sampling interval over a spectral range of 400 nm to 1000 nm, with some sites supporting calibration up to 2500 nm. The TOA reflectance is defined over an area of at least 45 m x 45 m for all sites, making it observable by AquaSat-1.

Table 4-1: Proposed AquaSat-1 radiometric calibration sites.

| Site | Country | Coordinates |
|-----------------------|-----------|--------------------|
| La Crau | France | 43.5588, 4.8644 |
| Railroad Valley Playa | US | 38.497, -115.690 |
| Baotou | China | 40.8514, 109.6291 |
| Gobabeb | Namibia | -23.6002, 15.1195 |
| Pinnacles Desert * | Australia | -30.5895, 115.1563 |

*Established by CSIRO; an application for acceptance into the RadCalNet is under preparation.

It is worth noting that additional radiometric calibration sites have been identified and catalogued by the EROS Cal/Val Centre of Excellence (ECCOE) (USGS, 2023) due to their spatial and radiometric invariance. These sites may also be considered for this target site category. Additionally, specific inland and coastal aquatic sites that serve as reference points for comparing the measured remote sensing reflectance. Examples are provided in Table 4-2.

Table 4-2: Proposed AquaSat-1 aquatic reference sites.

| Site | Country | Coordinates | Description |
|---------------|-----------|--------------------|--|
| Lucinda Jetty | Australia | -18.5202, 146.3862 | Located in the coastal waters of the Great Barrier Reef World Heritage Area this site provides above water radiance measurements from 350 to 800 nm. |
| Googong Dam | Australia | -35.4222, 149.2672 | The first site established as part of the Dark water Inland Observatory Network (DION). It provides remote sensing reflectance measurements from 350 to 800 nm every 15 minutes. |

4.2.2 Category 2: Application objective test sites

Throughout the mission, AquaSat-1 will regularly image a set of inland and coastal aquatic targets chosen to demonstrate the application objectives. Sites proposed for this category will be evaluated based on the criteria below. These guidelines are not rigid rules, and a site does not need to meet all criteria to be considered.

Guideline 1: The site exhibits aquatic processes and phenomena aligned with an application objective.

AquaSat-1 is designed to meet three key application objectives (see Section 3), which are measurable and directly linked to end-user requirements. Therefore, sites that are suitable for testing these objectives should be prioritised for selection.

Guideline 2: The site geometry demonstrates the unique capabilities of AquaSat-1.

As the only mission designed primarily for inland and coastal waters, AquaSat-1's 18 m spatial resolution is one-to-two orders of magnitude higher than current or planned ocean imagers. This high spatial resolution enables on-orbit spectroscopic measurements for aquatic sites that were previously inaccessible. Sites that can demonstrate this unique capability should be given preferential consideration, provided the site is at least 54 m wide for inland waterbodies to be observable. Table 4-3 and Table 4-4 propose a set of example sites that are strong candidates for category 2 targets in Australia and the US, respectively.

Guideline 3: The site is well-characterised through in-situ instrumentation and on-going field campaigns.

Ground-based measurements at aquatic sites provide localised data on specific phenomena and, when collected over extended periods, can enhance our understanding of long-term ecosystem trends. Historical and current ground samples are invaluable for validating data products from AquaSat-1. Notable candidates for such measurements include Australia's Integrated Marine Observing System (IMOS) and AquaWatch pilot sites. These pilot sites, currently being established in Australia, the US, and internationally, monitor water quality using in-situ instrumentation and above-water radiometers.



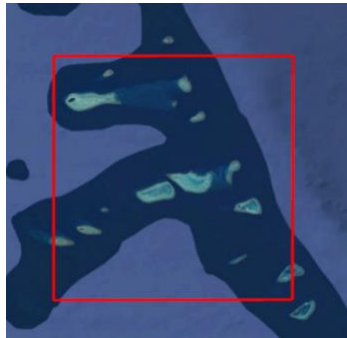

Guideline 4: The site is important to project partners and stakeholders.

Demonstrating AquaSat-1's capability to support decision-making is a crucial milestone for mission success. This requires close collaboration with project partners and stakeholders, including CSIRO's AquaWatch Australia and NASA's WWAO. Preference will be given to sites in Australia and the western US, although other global sites can also be considered.

Guideline 5: The site has significant ecological or human health importance.

This criterion emphasises the site's value in terms of its ecological significance or its impact on human health. Examples include sites listed under the Ramsar convention (Ramsar, 2023) and UNESCO World Heritage Sites (UNESCO World Heritage Convention, 2024), which hold significant ecological, economic, and societal importance. Critical aquatic infrastructure sites, such as drinking reservoirs, should also be given preferential consideration.

Table 4-3: Example sites in Australia that are strong candidates for category 2 targets.

| | |
|---|---|
| <p>BURDEKIN DELTA, QUEENSLAND, AUSTRALIA</p> <p>Centroid coordinate: -19.636067, 147.397429</p> <p>Applicable application objective: IAV</p> <p>Merit: The Burdekin River floodplain hosts a large concentration of wetlands that are recognised under the Ramsar Convention and sink significant nutrients for the northern Great Barrier Reef. Since the mid-twentieth century the region has undergone significant hydrological changes to support local agriculture, which has encouraged the growth of invasive aquatic vegetation such as water hyacinth and para grass (Perna et al., 2012). This vegetation poses a significant threat to the biodiversity within the region and is commonly observed at the Burdekin River Delta. Both biological and chemical control measures have proved to be ineffective in this region (Julien et al., 2001), and thus expensive physical removal is commonly required. Further, reports published by the Great Barrier Reef Marine Park Authority (GBRMPA, 2013) highlight the importance of managing invasive weeds for the protection of the surrounding reef.</p> |  |
| <p>FITZROY RIVER & KEPPEL BAY, QUEENSLAND, AUSTRALIA</p> <p>Centroid coordinate: -23.436876, 150.883427</p> <p>Applicable application objective: HABs</p> <p>Merit: The Fitzroy River is a major agricultural catchment which delivers significant loads of sediments and nutrients into Fitzroy estuary and the southern end of the Great Barrier Reef. As such, this site is the focus of studies by institutes including CSIRO, the Australian Institute of Marine Science, and many universities. It is instrumented with two AquaWatch above-water radiometers in the river and bay, respectively. The site also has significant spatial variability, making it a valuable candidate for demonstrating the high spatial resolution capabilities of AquaSat-1.</p> |  |
| <p>HERON REEF, CAPRICORN BUNKER GROUP QUEENSLAND, AUSTRALIA</p> <p>Centroid coordinate: -23.442397, 151.914772</p> <p>Applicable application objective: Coral</p> <p>Merit: Heron Reef (28 km²) is located at the southern end of the UNESCO World Heritage listed Great Barrier Reef. The composition and coverage of the surrounding benthic habitat are well characterised through decades of field campaigns (Roelfsema et al., 2021; Tanner and Connell, 2022), and it is representative of an offshore reef. This site is of high importance due to its use in various Earth observation research projects, with over 1400 publications. It is also highly accessible through the University of Queensland (UQ) Heron Island Research station. Furthermore, the UQ Remote Sensing Research Centre has used the site for ongoing calibration and validation exercises since 1999, in collaboration with both national and international partners.</p> |  |
| <p>KAKADU NATIONAL PARK, NORTHERN TERRITORY, AUSTRALIA</p> <p>Centroid coordinate: -12.400019, 132.847996</p> <p>Applicable application objective: IAV</p> <p>Merit: Kakadu National Park is Australia's largest national park and is one of the few World Heritage sites listed for both its natural and cultural significance. The invasive aquatic species <i>para grass</i> was first observed in the park's floodplains in the 1950s (Salau, 1995) and has continued to spread across the region. Since 1986, the growth of <i>para grass</i> on the Magela Creek floodplain has been extensively studied through airborne mapping (Boyden et al., 2019) to better support conservation efforts in the area. Additionally, the narrow reaches of the floodplains make it an excellent candidate for demonstrating the high-spatial resolution capabilities of AquaSat-1.</p> |  |

LAKE HUME, VICTORIA, AUSTRALIA

Centroid coordinate: -36.092802, 147.169947

Applicable application objective: HABs

Merit: A major lake located at the origin of the River Murray, Lake Hume provides irrigation, urban water supplies, and recreational benefits to an economically significant region of South-Eastern Australia (Cruse and Gillespie, 2008). A comprehensive series of historical Earth observation and in-situ data has been compiled by scientists at CSIRO to better understand water-quality issues within the lake, which has supported advanced water quality modelling capabilities. This site is also a PrimeWater Horizon2020 project site, and the AquaWatch mission has strong engagement with local end-users and water managers.

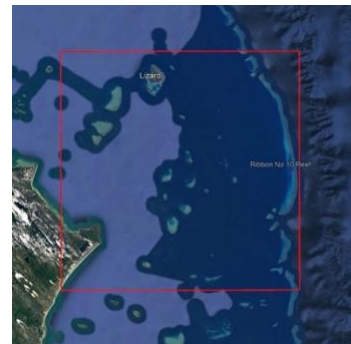


LIZARD ISLAND, QUEENSLAND, AUSTRALIA

Centroid coordinate: -14.853933, 145.503883

Applicable application objective: Coral

Merit: Lizard Island is located at the northern end of the UNESCO World Heritage listed Great Barrier Reef. It has been extensively studied by various researchers, including University of Queensland partners. This site has a history of frequent coral disturbances due to bleaching events and tropical cyclones (Madin et al., 2018). Following severe tropical cyclones in 2017, the site has been well characterised through a series of ongoing field campaigns focussed on examining the recovery of the reef (Tebbett et al., 2022). The island also hosts a research station capable of supporting further field campaigns. Its proximity to the mainland makes it particularly valuable for studying the impact of terrestrial influences on the reef



SPENCER GULF, SOUTH AUSTRALIA, AUSTRALIA

Centroid coordinate: -34.714764, 136.085657

Applicable application objective: HABs

Merit: The Spencer Gulf is a key aquaculture bay for South Australia, generating over half of the state's total seafood production (Tanner et al., 2019). This site is affected by water column eutrophication and benthic habitat disturbances associated with aquaculture, which can lead to harmful algal blooms. The AquaWatch mission has established instrumentation at this site and collaborates closely with local industry and research associations

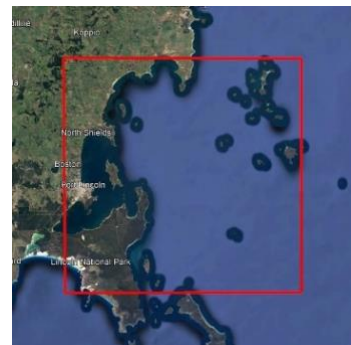


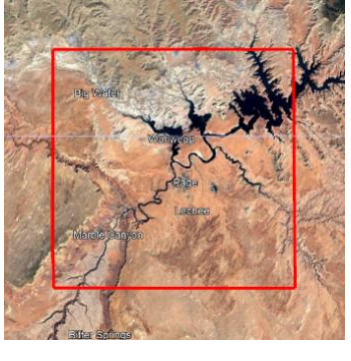
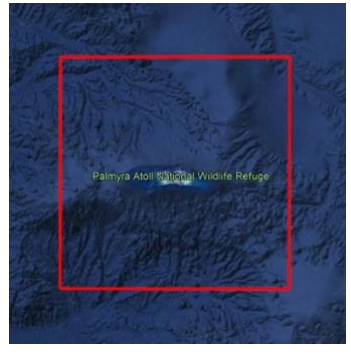


Table 4-4: Example sites in the US that are strong candidates for category 2 targets.

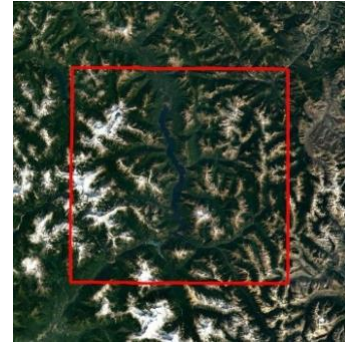
| | |
|---|---|
| <p>ELEPHANT BUTTE LAKE, NEW MEXICO, USA Centroid coordinate: 33.243841, -107.169249 Applicable application objective: HABs Merit: Located on the southern end of the Rio Grande, this reservoir is the largest in the state of New Mexico. It provides irrigation and drinking water to New Mexico and western Texas and serves as a major recreational waterbody within the region. Wastewater treatment plants upstream from the reservoir have been identified as a major source of nitrogen (Hogan, 2013), and this influx is believed to contribute to the documented instances of harmful algal blooms at this location.</p> |  |
| <p>LAKE MEAD, NEVADA & ARIZONA, USA Centroid coordinate: 36.144365, -114.476630 Applicable application objective: HABs, IAV Merit: Lake Mead was formed by the Hoover Dam on the Colorado River system. As the largest reservoir in the US, it supplies water to approximately 25 million people across Nevada, Arizona, and California for drinking and agricultural purposes (Edalat and Stephen, 2019). The lake is experiencing significant water stress due to drought and increased population growth. Consequently, considerable efforts have been made to study the archived water quality measurements still recorded by the state’s water authority (Adjovu et al., 2023; Hannoun and Tietjen, 2023).</p> |  |
| <p>LAKE POWELL, UTAH & ARIZONA, USA Centroid coordinate: 36.936111, -111.484167 Applicable application objective: HABs, IAV Merit: Lake Powell is the second largest lake along the Colorado River and is upstream from Lake Mead. It functions as a water storage facility for the upper basin states of the Colorado River Compact (Colorado, Utah, Wyoming, and New Mexico). This lake receives significant sediment loads from the canyons surrounding the upstream Colorado River and its tributaries (Wildman et al., 2011), which exacerbates water quality issues, particularly during periods of drought.</p> |  |
| <p>PALMYRA ATOLL, USA Centroid coordinate: 5.881717, -162.080452 Applicable application objective: Coral Merit: Palmyra Atoll is a US National Wildlife Refuge situated approximately halfway between Hawaii and American Samoa. The atoll’s coral habitat has largely escaped the anthropogenic stresses commonly observed in less isolated ecosystems, resulting in a region with substantial biomass and coral cover (Koweek et al., 2015). Despite being well-studied (Sandin et al., 2008; Smith et al., 2016), the remote location poses challenges for conducting field trials, making the region well-suited to remote sensing. Additionally, the atoll’s high variability in coral depth makes it an excellent candidate for demonstrating the capabilities of the AquaSat-1 instrument for monitoring coral coverage.</p> |  |

ROSS LAKE, WASHINGTON, USA

Centroid coordinate: 48.848956, -121.030727

Applicable application objective: IAV

Merit: This reservoir is a major recreational waterbody within the North Cascades National Park. Due to high recreational use, harsh climatic conditions, and the physical characteristics of the basin, the lakes within this park are prone to poor water-quality (Lawlor, 2019). Additionally, the lake is surrounded by narrow, vegetated canyons, making it an excellent candidate for demonstrating the capabilities and limitations of GMC.

**SACRAMENTO DELTA, CALIFORNIA, USA**

Centroid coordinate: 38.1231, -122.0497

Applicable application objective: HABS, IAV

Merit: The Sacramento Delta serves as a vital source of drinking water and agricultural irrigation for California, while also providing vital habitats for waterfowl and endangered fish species. However, the region is susceptible to many invasive species, including aquatic weeds like water hyacinth (Pitcairn et al., 2021), which adversely impact water quality, ecosystem health, and recreational activities within the Delta (Jackson et al., 2006). Consequently, the area is the focus of large-scale ecosystem restoration programs and scientific studies, often led by project partners at the University of California Merced (Laćan and Resh, 2016; Lee et al., 2021), who have also contributed to establishing an AquaWatch above-water radiometer at the site.



4.2.3 Category 3: Opportunistic sites

Sites that do not meet the criteria for inclusion in categories 1 and 2 will be imaged opportunistically during the mission. These sites will be assessed using a merit-based system, with each proposed site assigned a qualitative priority ranking (low, medium, high). While the criteria for category 2 will be considered, the priority ranking will also be based on the following criteria adapted from the EnMAP operations plan (Guanter et al., 2015):

- Cloud cover probability, based upon either historical or forecasted data.
- Satellite tasking allocation, taking into account higher-priority acquisitions, available on-board storage, required orbital manoeuvres, and non-imaging operational modes.
- Sun-glint avoidance, where the proposed viewing geometry preferentially avoids sun-glint.

4.3 Revisit analysis and crossing time

This section investigates the impact of constellation size and cloud cover on revisit frequency. Additionally, we discuss how the orbit's equatorial crossing time affects SNR and access to cloud-free observations. The results presented are a summary of a paper currently under preparation. Further details are provided in Appendix B.

4.3.1 Orbit design

The orbit requirements are specified in AS1-MIS-05, AS1-MIS-07, AS1-MIS-08, AS1-MIS-12 and AS1-MIS-16, which specify the orbit type, local time of descending node (LTDN), spatial resolution, and orbit maintenance. The orbit was further refined in the AquaSat-1 Platform Evaluation (UNSW Canberra Space, 2024), which focused on orbits suitable for Earth observation missions by using a predictable repeating ground-track. This approach aids in long-term observation planning, target revisits, and overall mission analysis to support operations. The parameters for the reference AquaSat-1 orbit are presented in Table 4-5.

Table 4-5: AquaSat-1 reference orbit parameters.

| Parameter | Value |
|------------------|---------------------------|
| Orbit type | Repeating Sun-synchronous |
| Repeat cycle | 13 days / 202 orbits |
| Nominal altitude | 399.5 km |
| Inclination | 97.05 degrees |
| Eccentricity | 0.0 |
| Mean LTDN | 12:00 (noon) |

4.3.2 Single satellite revisit analysis

The AquaSat-1 orbit was modelled using SaVoir (Taitus Software, 2024) based on the parameters detailed in Table 4-5. We modeled the entire field of regard, using a pushbroom sensor and allowing the satellite pitch and roll capabilities of up to ± 30 degrees (AS1-MIS-15). Ground motion compensation (GMC) and potential planning conflicts were considered out of scope of this analysis, as the primary goal was to identify the overall imaging capability. Planning conflicts and prioritisation involve multiple stakeholders, weather forecasts, and water quality needs and conditions at the time of planning.

We used a subset of the proposed category 2 target sites (see Section 4.2.2) for this analysis, with four sites selected from Australia and four from the US. This selection provides a balanced representation of the geographical and climatic variability across the site list. This balance is crucial as geographical location significantly influences orbit revisit results and cloud cover impact.

A 25% minimum area coverage threshold value was applied to the output orbit results. The area coverage refers to the percentage of the bounding box (defined by the area coordinates

for each target site in Section 4.2.2) imaged during an AquaSat-1 pass. Passes with less than 25% area coverage are excluded from the presentation.

The SaVoir results indicated that each target site has 3 or 4 imaging opportunities within one 13-day repeat cycle (see Figure 4-3), with a mean revisit time of 3.7 days across all target sites. The number of imaging opportunities per site within one 13-day cycle depends on the proximity of the satellite’s ground track to the target site. This varies with the orbit and launch epoch, influencing how the ground trace shifts. Figure 4-4 illustrates this variation, showing either 3 or 4 imaging opportunities based on the proximity of the ground tracks to the target site.

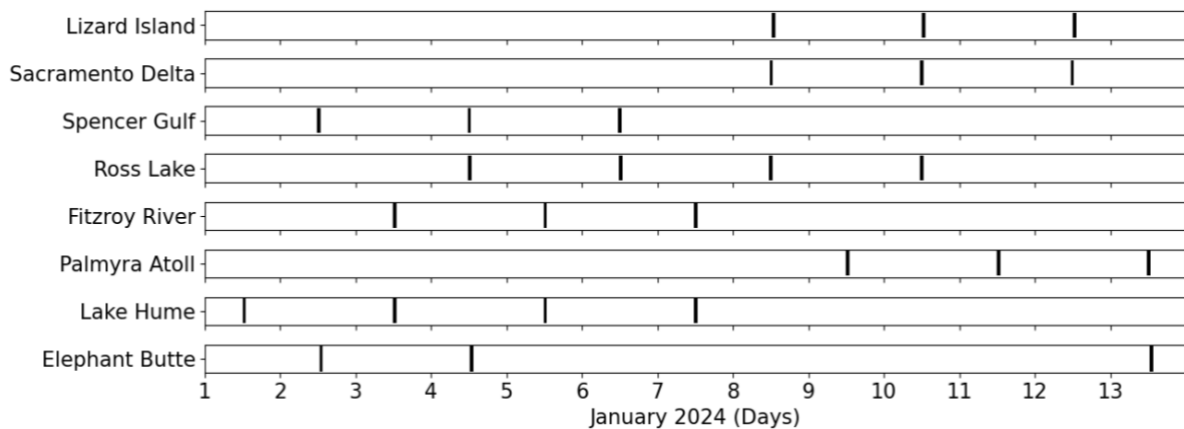


Figure 4-3: Satellite imaging opportunities for all target sites. Imaging opportunities for one satellite over a 13-day repeat cycle (assuming 2024-Jan-01 11:54:40 epoch), with minimum area coverage threshold of 25%. Imaging opportunities shown for each target site in local time.



Figure 4-4: Illustration of variance in number of imaging opportunities depending on target location relative to the ground tracks. All passes shown in red correspond to an imaging opportunity for orbit epoch 2024-Jan-01 11:54:40. Left: Lizard Island gives 3 imaging opportunities. Right: Lake Hume gives 4 imaging opportunities.

It should be noted that there is significant variation in revisit time across the repeat cycle. The 3 or 4 imaging opportunities for each target site occur consecutively with a 2-day separation between them, followed by a substantial gap of up to 9 days before the next set of imaging opportunities. For each target site, the timing of these imaging opportunities varies at

different stages of the repeat cycle, as illustrated in Figure 4-3. This distribution is examined further in Appendix B.

4.3.3 Constellation revisit analysis

If the orbital plane is fixed to maintain a 12:00 (noon) LTDN, increasing the number of satellites in the constellation reduces the revisit time until daily revisits of target sites are achieved. For instance, in the case of Lizard Island, the constellation size was varied from 1 satellite to 5 satellites and optimised for equally spaced imaging opportunities (see Figure Figure 4-5). The results, shown in Figure 4-6, indicate that a 5-satellite constellation achieves daily imaging opportunities for Lizard Island.

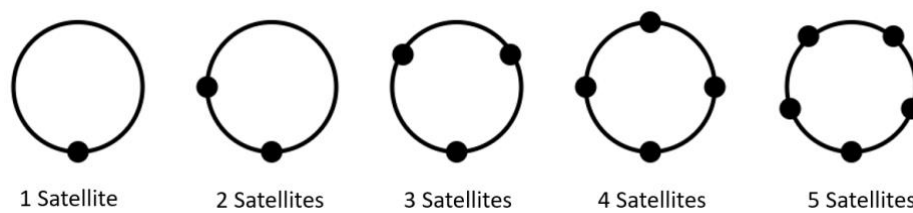


Figure 4-5: The location (true anomaly) of the satellites in orbit for a 1 to 5 satellite constellation.

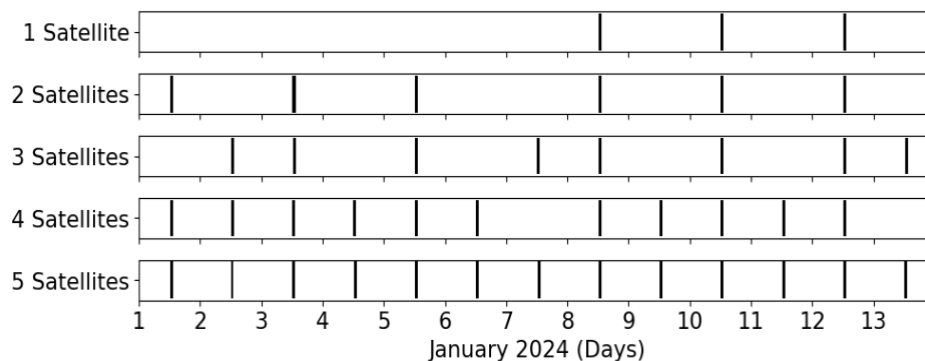


Figure 4-6: Lizard Island imaging opportunities for constellations with 1 to 5 satellites over one 13-day repeat cycle (assuming 2024-Jan-01 11:54:40 epoch). The analysis is based on a minimum area coverage threshold of 25%. Imaging opportunities are displayed according to local time.

Table 4-6 shows the mean revisit time for various constellation sizes, ranging from 1 to 5 satellites. The mean revisit time decreases from 3.7 days with a single satellite to less than 1 day with a 5-satellite constellation. The less than 1-day mean revisit results from multiple passes occurring in quick succession, which are not visible in Figure 4-6. Notably, the variance in revisit time is significantly reduced with larger constellations. Further details are available in Appendix B.

Table 4-6: Number of days between clear imaging opportunities for 1 to 5 satellite constellations, with minimum area coverage threshold of 25%. This is an average across all eight target sites.

| Constellation size | 1 satellite | 2 satellites | 3 satellites | 4 satellites | 5 satellites |
|--------------------|-----------------|----------------|----------------|----------------|-----------------|
| Mean revisit | 3 days 17 hours | 2 days 2 hours | 1 day 8 hours | 1 day 1 hour | 0 days 20 hours |
| Maximum revisit | 9 days 0 hours | 4 days 0 hours | 2 days 0 hours | 2 days 0 hours | 1 day 0 hours |

4.3.4 Cloud cover impact

The European Centre for Medium-Range Weather Forecasts (ECMWF) provides hourly data on cloud cover through a globally comprehensive dataset that combines model data with observations from around the world (European Commission, 2023). The ERA5 database, utilised in this analysis, represents the fifth generation of ECMWF reanalysis data, offering climate and weather information for the past eight decades for any location on Earth.

For this analysis, the data variable extracted from the ERA5 dataset is ‘total cloud cover’. This data is provided as gridded data with a resolution of $0.25^\circ \times 0.25^\circ$. For each target site, the centroid coordinates are used to identify the nearest ERA5 grid coordinate and its corresponding data. The output is expressed as a cloud fraction ranging from 0 to 1, where 0 signifies 0% cloud cover and 1 signifies 100% cloud cover. It is important to note that the precise location of the cloud cover within the $0.25^\circ \times 0.25^\circ$ grid is not specified (see Figure 4-7 and Figure 4-8).

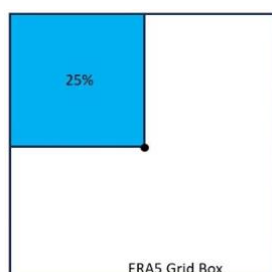


Figure 4-7: ERA5 cloud cover example within grid box. This would return a value of 0.25, indicating that 25% of the grid box is covered by cloud.

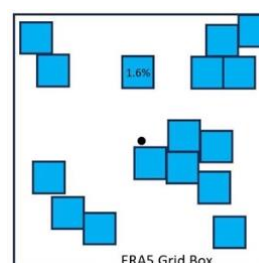


Figure 4-8: ERA5 cloud cover example within grid box. This would also return a value of 0.25, indicating that 25% of the grid box is covered by cloud.

We collected daily data from 2013 to 2023 for each priority target site at the local pass time of AquaSat-1. To determine clear imaging opportunities, we adopted a similar approach to Hestir and Dronova (2023), defining clear imaging opportunities as those with 10% or less cloud cover, meaning the area was at least 90% cloud-free. Thus, passes with 10% or less total cloud cover were considered suitable for clear imaging.

The average number of clear imaging opportunities in one year was calculated from the 2013-2023 dataset, as summarised in Table 4-7. To account for variations in potential launch dates, the pass dates were shifted by up to 13 days in the analysis. The results, shown in Table 4-7,

reveal significant variability depending on the site, with diverse geographical locations exhibiting markedly different weather patterns.

Table 4-7: Average number of clear imaging opportunities per year for each priority target site. The average is calculated from data spanning 2013-2023, using a threshold of $\leq 10\%$ cloud cover for defining clear conditions. The simulation considers the specific days when the satellite would have passed over each target site.

| Target site | Sacramento Delta | Elephant Butte | Fitzroy River / Keppel Bay | Lake Hume | Spencer Gulf | Ross Lake | Lizard Island | Palmyra Atoll |
|---------------------|------------------|----------------|----------------------------|-----------|--------------|-----------|---------------|---------------|
| Clear days per year | 179 | 159 | 102 | 90 | 71 | 57 | 21 | 7 |

Figure 4-9 shows the average number of days between clear imaging opportunities for each priority target site in each quarter of the year. For one satellite, the mean number of days between satellite passes across all target sites is 3.7 days (see Section 4.3.2). The figure illustrates the significant impact of cloud cover on all target sites. The smallest mean interval between clear imaging opportunities is 6 days (Sacramento Delta), while the largest is 100 days (Palmyra Atoll), despite satellite passes occurring every 3.7 days. With a single satellite, the revisit requirement is generally met for all sites throughout the year, except for Spencer Gulf during June to August. Averaged over the entire year, the mean revisit interval meets the requirement for all sites. Further details on the actual distribution of visits are provided in Appendix B.

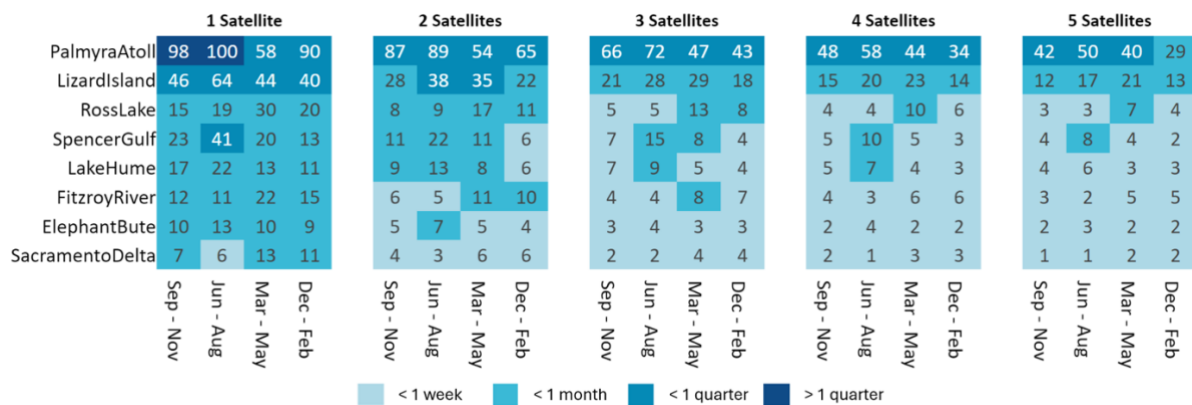


Figure 4-9: The mean number of days between clear imaging opportunities for each priority target site for satellite constellations consisting of 1-5 satellites. This is presented for each quarter of the year. **HABs sites:** Ross Lake, Spencer Gulf, Lake Hume, Fitzroy River, Elephant Butte, Sacramento Delta. **IAV sites:** Ross Lake, Lake Hume, Elephant Butte, Sacramento Delta. **Coral sites:** Palmyra Atoll, Lizard Island.

Key conclusions from this section are:

- **Cloud cover impact:** The influence of cloud cover on imaging opportunities differs significantly based on target site location and time of year.

- **Single satellite revisit requirement:** The revisit requirement outlined in AS1-MIS-12 is met for all sites with a single satellite, when considering the annual mean revisit and the effect of cloud cover.
 - **HAB sites:** Seasonal mean revisit times range from 6 days (Sacramento Delta, June-August) to 30 days (Ross Lake, March-May). The annual average is less than 30 the monthly requirement for all sites.
 - **IAV sites:** Seasonal mean revisit times vary from 6 days (Sacramento Delta, June-August) to 41 days (Spencer Gulf, June-August), with an annual average for Spencer Gulf of 24 days, which is less than monthly requirement.
 - **Coral sites:** Mean revisit times span from 40 days (Lizard Island, December-February) to 100 days (Palmyra Atoll, June-August). The annual average for Palmyra Atoll is 87 days, which is less than the seasonal requirement.
- **Multi-satellite constellations:** The mean revisit time improves significantly with multiple satellites. For a 5-satellite constellation:
 - **HABs and IAV sites:** Mean revisit times range from 1 day to 8 days, depending on season.
 - **Coral sites:** Mean revisit times range from 12 to 50 days, depending on season.

4.3.5 Equatorial crossing time trade

The cloud cover analysis was conducted using a sun-synchronous orbit with a 12:00 LTDN, as specified in AS1-MIS-5 (see Section 3.6). To further understand how LTDN affects SNR and cloud cover, we performed a trade study comparing various LTDN values. We found that orbits with LTDN values between 10:00 and 14:00 offer comparable performance regarding both cloud coverage (Figure 4-10) and SNR (Figure 4-11).

Figure 4-10 illustrates the impact of a 10:00 versus a 14:00 LTDN on cloud coverage over the course of a year. The results show that the benefit of choosing either an earlier or later LTDN is not uniform across all target sites. Some sites may benefit from an earlier LTDN, while others might see improvements with a later LTDN. Palmyra Atoll and Sacramento Delta do not show significant benefits from either LTDN shift.

Figure 4-11 presents the simulated instrument performance for application objective 3 (coral reefs) at 10:00 and 12:00 LTDN. The plot shows that radiometric performance is only minimally affected by the equatorial crossing time. Although the lower solar angle at 10:00 LTDN reduces the photons returned to the sensor, leading to a slightly higher SNR requirement and decreased capability compared to the 12:00 LTDN, the difference is minor relative to the instrument's performance margins. Options for 10:00, 12:00, and 14:00 LTDN all meet the requirements with sufficient margin, suggesting that the 12:00 LTDN requirement specified in Section 3.6 could be relaxed without significantly compromising instrument performance. Note that the 14:00 LTDN performance is identical to the 10:00 and is therefore omitted from the plot.

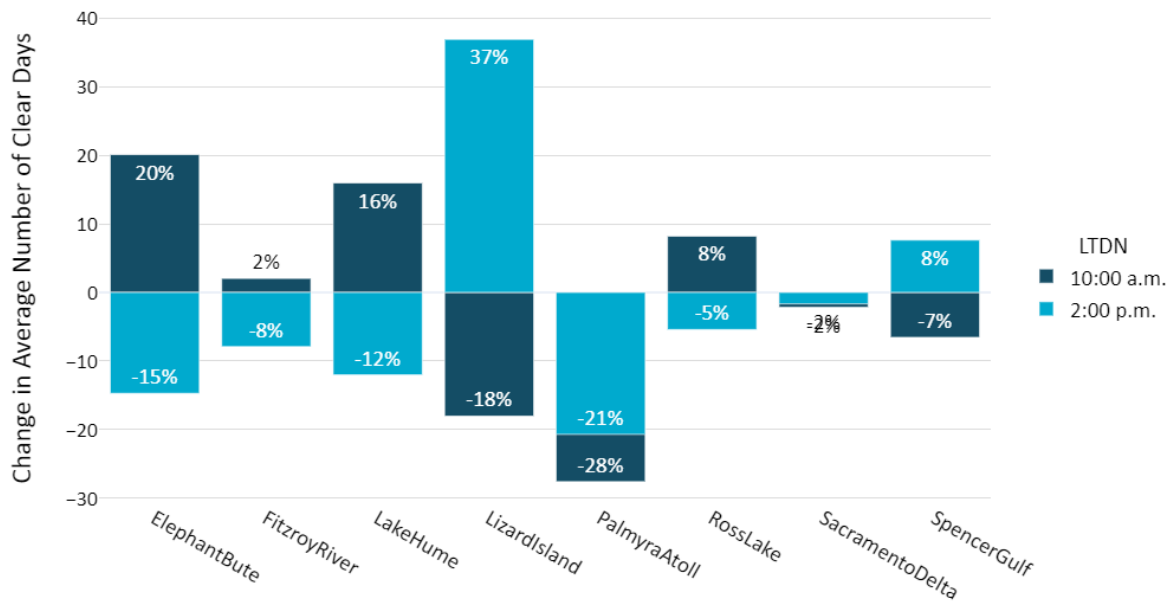


Figure 4-10: The change in number of clear days between the 12:00 baseline LTN, and an LTN of 10:00 or 14:00 for priority target sites. Results suggest that LDTN has minimal net impact on cloud cover when a geographically varied set of sites are considered.

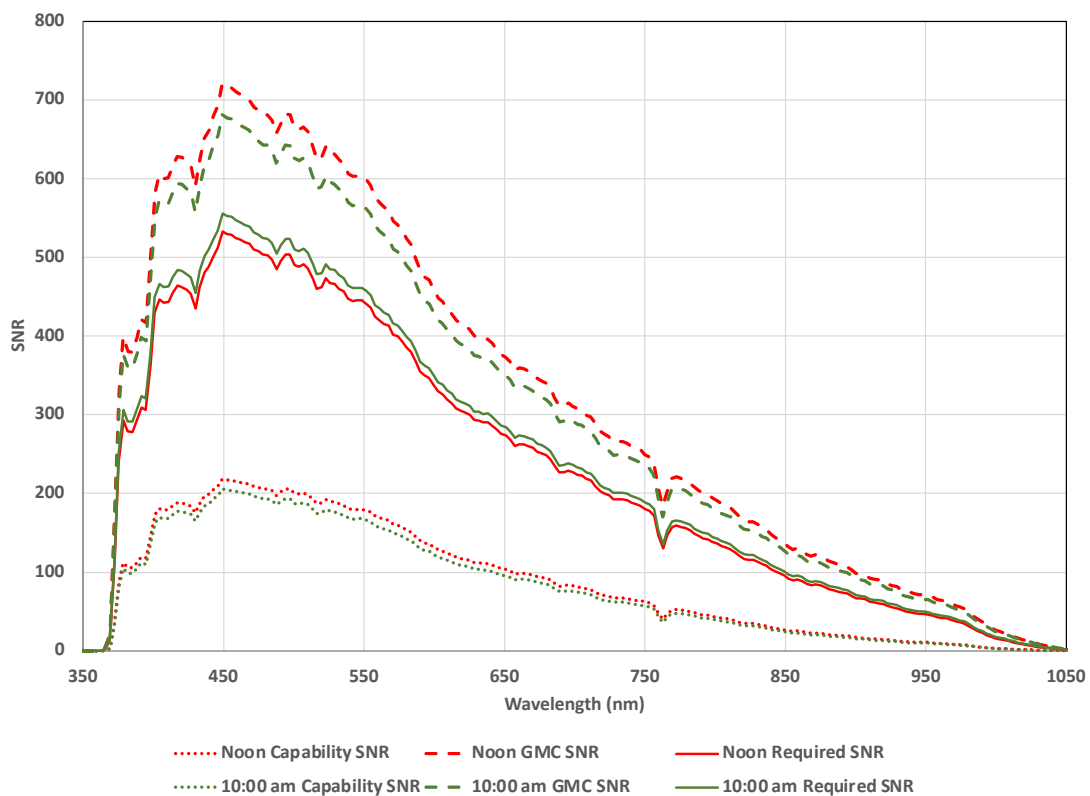


Figure 4-11: Radiometric requirements and performance for the physical parameter corresponding to application objective 3 (coral coverage) for orbits with a 10:00 LTN (green) and 12:00 LTN (red). The solid line represents the requirement, the dotted line represents the capability with pushbroom imaging, and the dashed line represents the capability with GMC imaging. Results indicate that the 12:00 LTN requirement could be relaxed without significantly compromising instrument performance.

4.4 Spatial resolution

In this section, we examine the impact of spatial resolution on the ability to detect inland water targets, such as rivers, lakes, and reservoirs, within the study areas of Australia and the western US. Coastal targets, such as coral reefs, are not included in this analysis as they do not drive the spatial resolution requirements. We recommend that future studies explore how spatial resolution affects the detection of coral and seagrass coverage.

This section summarises findings from the corresponding journal article by Frasson et al. (2024). Throughout this study, spatial resolution is described using the ground sample distance (GSD), a standard practice in the field. However, for water quality applications, signals from small water features can be mixed with signals from adjacent terrain. Therefore, in line with common practice (e.g., Schaeffer and Myer (2020)), we assume that the smallest feature that can be effectively analysed from space is approximately three times the size of the GSD.

4.4.1 Extension of lakes and river databases

We use the HydroLAKES database (Messenger et al., 2016) to quantify the fraction of lakes observable in the study area. HydroLAKES provides detailed information on the geometry and location of 1.43 million lakes worldwide with a surface area greater than 100,000 m². Although this database is extensive, its threshold of 100,000 m² may exclude smaller lakes, potentially offering an overly optimistic assessment of the GSD required to characterise lakes from space.

To address this, we extended the database to include lakes as small as 25 m² using a regression, which yielded an r^2 value of 0.97 for lakes within the study area. To compute the minimum shore-to-shore distance, which is not explicitly included in the HydroLAKES database, we computed a characteristic length based upon the lake perimeter, area, and shape factor, and extended this to lakes down to 25 m².

Rivers within the study areas were extracted from the Surface Water and Ocean Topography River Database (SWORD) (Altenau et al., 2021). This database contains river centerlines, broken into segments of 200 m in length, where the average river width in each segment is provided down to a resolution of 30 m. To evaluate finer resolutions, we took advantage of the scaling property observed between river width and occurrence (Allen and Pavelsky, 2018) ($r^2=0.86$ for the combined areas of interest) to estimate the length and frequency of occurrence of rivers narrower than those contained in SWORD, down to a width of 5 m.

4.4.2 Impact of spatial resolution on observable lakes and rivers

We assessed river coverage using two metrics: the total length of rivers that can be effectively monitored with the proposed GSDs, normalised by the total river length in the study area, and the river surface area. Narrow rivers, although more numerous, are often challenging to sample accurately due to their size, whereas wider rivers are typically more significant for

water flow and are frequently associated with power laws relating width to discharge (Feng et al., 2021; Feng et al., 2019; Frasson et al., 2019; Gleason and Smith, 2014; Gleason et al., 2014; Hagemann et al., 2017). Wider rivers play a crucial role in transporting sediment, carbon, and pollutants through the river network and into lakes and reservoirs. Consequently, the river surface area metric gives more weight to wider rivers.

For lakes, we evaluated the fraction of the total lake surface area and the number of lakes within the study area that can be monitored at various GSD values. This approach is beneficial as larger lakes typically store more water, making them more critical for water supply, recreational use, and other purposes. Figure 4-12 shows the results of this analysis for the lakes and rivers within the study area.

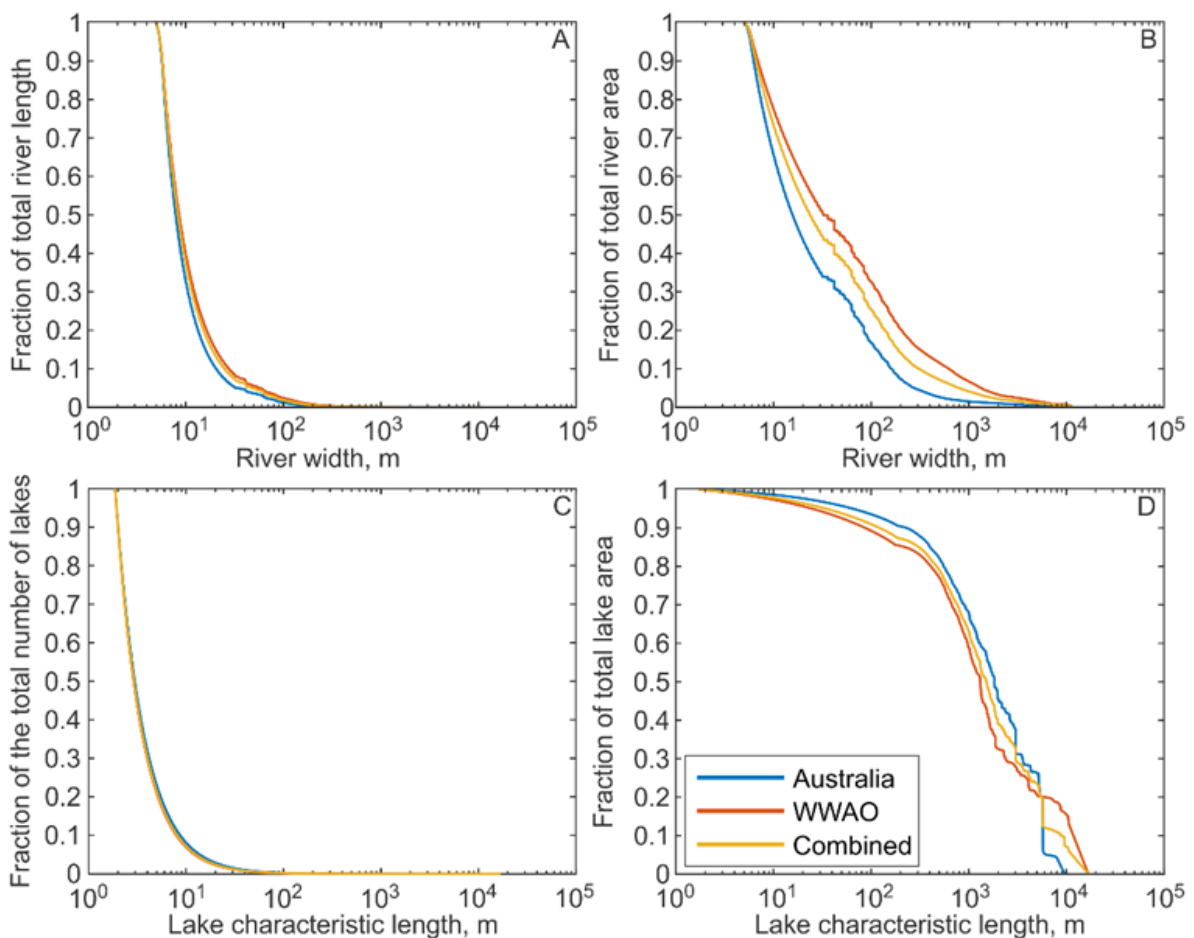


Figure 4-12: Panel A: Fraction of the total river length larger than a certain width vs. river widths. B: Fraction of the total river surface area larger than a certain width vs. river widths. C: Fraction of the total number of lakes with a minimum shore-to-shore distance (characteristic length) larger than a certain characteristic length vs. characteristic length. D: Fraction of the total surface area of lakes larger than a certain characteristic length vs. characteristic length.

We compare the proposed GSD of AquaSat-1 with other satellites in Table 4-8. The key observations are:

- **Coverage:** AquaSat-1’s proposed 18 m GSD would enable coverage of 38% of the total river surface area and 93.8% of the total lake surface area within the study region.
- **Comparison with other missions:** AquaSat-1 offers approximately twice the fractional river length coverage and total number of lakes compared to Landsat-8 and SBG.
- **Lake dimension and GSD:** The cumulative distribution of the narrowest lake dimension reveals a ‘knee’ around 400 m. This indicates that the increase in lake coverage for a GSD smaller than approximately 130 m is modest. Conversely, the fractional coverage for rivers increases steeply with smaller GSD sizes.
- **Cost considerations:** There are significant costs associated with smaller GSDs. They reduce both the instrument swath and SNR per pixel, requiring a larger instrument to maintain performance, which in turn increases the overall mission costs.

Table 4-8: Comparison between the GSD of existing and proposed missions with potential water quality monitoring capabilities and the metrics computed for our area of interest. Here we assume that the GSD must be smaller than three times the river width or the lake characteristic length for a waterbody to be observable. HICO is the Hyperspectral Imager for the Coastal Ocean. EMIT is the Earth Surface Mineral Dust Source Investigation sensor. CPM is the Carbon Plume Mapper instrument. Sentinel 2’s GSD is different for different spectral bands and the selection of relevant bands depends on the intended use. The estimated number of lakes in the region interest with an area of at least 25 m² is 22,544,952.

| GSD (m) | Example satellites | Observable river length fraction | Observable river area fraction | Observable number of lakes | Observable lake area fraction |
|---------|---------------------|----------------------------------|--------------------------------|----------------------------|-------------------------------|
| 10 | Sentinel-2 | 0.08 | 0.45 | 288,013 | 0.95 |
| 18 | AquaSat-1 | 0.04 | 0.38 | 112,620 | 0.94 |
| 20 | Sentinel-2 | 0.04 | 0.36 | 96,561 | 0.93 |
| 30 | Landsat-8, SBG, CPM | 0.02 | 0.27 | 50,740 | 0.91 |
| 60 | Sentinel-2, EMIT | 0.006 | 0.15 | 16,155 | 0.88 |
| 100 | HICO | 0.002 | 0.10 | 9,229 | 0.85 |
| 300 | Sentinel-3, GLIMR | 0.0004 | 0.04 | 1,125 | 0.66 |
| 1000 | PACE | 0.00004 | 0.01 | 56 | 0.32 |

4.5 Mission trades

Table 4-9 summarises the mission trades considered during this feasibility study and refers to detailed analysis elsewhere in this report where applicable. Instrument-level trades are discussed in Section 5.6.

Table 4-9: Mission trades considered in this feasibility study.

| Topic | Options (selected option in bold) | Key considerations | Rationale |
|--------------------------|--|--|---|
| Equatorial crossing time | Noon , 10:00 am, 2:00 pm | SNR, cloud cover, cross-calibration, sunglint | Varying LTDN between 10:00 and 2:00 pm has minimal impact on net cloud cover across target sites, and on SNR. Cloud cover and SNR do not drive choice of LTDN. See Section 4.3.5. Recommend sunglint analysis for future work. |
| Altitude | 400 km , 600 km | Fuel cost, mission lifetime, revisit time | 600 km is feasible but with ~70% increase in satellite wet and dry mass. Reduced agility offset by increased target site visibility. See Section 6.3.1. |
| Observing strategy | Pushbroom, GMC (10x) | SNR, surface coverage | GMC is needed to meet SNR requirements for coral cover application objective. GMC (10x) has increased retrieval performance and decreased data rate (by 10x), at expense of imaging coverage. Consider configurable GMC implementation. See Section 6.3.2. |
| Image strip length | Variable , 50 km | Number of target sites, revisit | To maximise imaging opportunity and revisit. |
| Field of regard | +/-15 deg, +/-30 deg , +/-45 deg | Revisit, SNR, atmospheric correction | Demonstrated on other missions (e.g., EnMAP) and permits 5-day average revisit at the equator. |
| Propulsion type | Electric, chemical | Mass and cost | Solar array and radiator considerably larger for electric propulsion solution, decreasing agility and increasing complexity, respectively. See Section 6.3. |
| Atmospheric correction | 350 to 1050 nm , separate radiometer, extended spectral range | Cost, ease of calibration, scenes to be observed | Terrestrial information content sufficient for atmospheric correction. |

5 Instrument description

The proposed AquaSat-1 instrument⁷ is a state-of-the-art 350-1050 nm imaging spectrometer, with ≤ 10 nm full width at half maximum (FWHM) spectral response function. It builds on the heritage of JPL's Earth Surface Mineral Dust Source Investigation (EMIT) and CPM. The instrument utilises a fast F/1.8 optical system comprised of a three-mirror telescope coupled with a Dyson-type spectrometer. We selected a Dyson imaging spectrometer design for advantages in compactness, high photon throughput, and ease of alignment. The detector is a 3072×512-pixel Teledyne CHROMA-D with 18 μm pixels. The concave grating is optimised for blue spectral response and designed to be fabricated by the JPL Microdevices Laboratory via E-beam grayscale lithography, like those from EMIT and CPM. Limiting the spectral range to the VNIR removes the need for active cooling, greatly simplifying the design.

5.1 JPL imaging spectroscopy heritage

JPL has a long history of designing, fabricating, and operating imaging spectrometers (Mouroulis and Green, 2018). In the late 1970s, technological advancements in detectors, optics, and computers made it possible to create instruments that could capture a spectrum for each point in an image. JPL started developing the Airborne Imaging Spectrometer (AIS) in 1979, and it first flew in 1982. Building on the success of AIS, JPL developed the Airborne Visible-Infrared Imaging Spectrometer (AVIRIS) for NASA's Earth science missions. AVIRIS covers the visible to short-wavelength infrared (VSWIR) spectral range from 380 to 2510 nm and first flew in 1986 (JPL, 2022).

Since these early experiences, JPL's imaging spectrometers have been used for a broad range of scientific studies on Earth, the Moon and other planets and satellites in the solar system (JPL, 2022). For AquaSat-1, the most relevant instruments are EMIT, CPM, and CRISM.

EMIT launched in 2022 and is currently operating from the International Space Station (JPL, 2024b). It is a Dyson spectrometer, similar to the one proposed for AquaSat-1, but with a two-mirror telescope, a spectral range of 380 nm to 2,500 nm, and a GSD of 60 m. Its primary mission is to accurately map the composition of regions that produce mineral dust to advance Earth system models. Although there are differences in implementation, EMIT's datasets are similar to what AquaSat-1 will produce, providing valuable expertise in data transfer, processing, algorithm development, and data analysis.

EMIT also demonstrates the power of imaging spectroscopy in various fields, including greenhouse gas monitoring and water quality analysis. However, EMIT cannot perform GMC,

⁷ We use the terms payload and instrument interchangeably.

which limits its sensitivity, and its large GSD value makes it unsuitable for the applications proposed by AquaSat-1.

CPM is a close analogue to AquaSat-1 (Zandbergen et al., 2022). It is a Dyson imaging spectrometer with a three-mirror telescope, 30 m GSD, and spectral range of 400 nm to 2,500 nm. The complete payload was fabricated and tested by JPL. A copy of the CPM payload was launched in August 2024 onboard the Tanager-1 satellite, which will measure methane and carbon dioxide point-source emissions. While CPM provides direct engineering heritage to AquaSat-1, its larger GSD limits its ability to perform water quality measurements in small bodies of water. Its sensitivity in the blue region of the spectrum will also be lower than AquaSat-1's. In addition, the revisit requirements of AquaSat-1 are likely incompatible with Tanager-1's mission, and aside from the greenhouse gas products, the data from Tanager-1 are not free and openly available.

CRISM was operational around Mars from 2006 to 2023 and demonstrated the GMC mode for the first time, with a GSD of 100 to 200 m (JPL and John Hopkins Applied Physics Laboratory, 2018). Figure 5-1 shows a CRISM image of the Mars surface, with the characteristic bowtie shape resulting from GMC observations.



Figure 5-1: Example CRISM image of the Mars surface, showing the characteristic bowtie shape resulting from GMC observations (JPL, 2006).

The JPL heritage of successful missions provides an important risk reduction base to AquaSat-1.

5.2 Instrument model

We model the AquaSat-1 instrument performance using techniques developed over decades of spectrometer development at JPL. The basic radiometric model is a component-wise description of performance for all the components along the optical path. For the Dyson design, our optical path includes telescope mirror silver coatings, the Dyson lens anti-reflection (AR) coating, an order sorting filter to reject higher order diffractions from the long wavelengths. It includes diffraction loss at the slit, the grating and the detector quantum efficiency. Figure 5-2 shows these terms for the AquaSat-1 instrument point design.

The instrument benefits from several technological advances to reduce noise. First, a digital readout focal plane array (FPA) isolates the electronics from thermal instability and minimises electromagnetic interference (EMI). Second, the instrument layout and component selection promote high optical throughput to minimise photon shot noise. Next, coaddition of adjacent spectral channels further increases signal—our base design samples natively at 3.2 nm, but bins these to a 6.4 nm product for improved signal levels. Finally, GMC operations allow longer integration times by pitching the spacecraft platform to reduce the effective down-track advance of the pushbroom field of view. This allows reductions in noise without sacrificing spatial resolution. Figure 5-3 shows different noise sources for a typical aquatic spectrum, demonstrating that the measurement is photon noise limited despite viewing an (ostensibly) dark target.

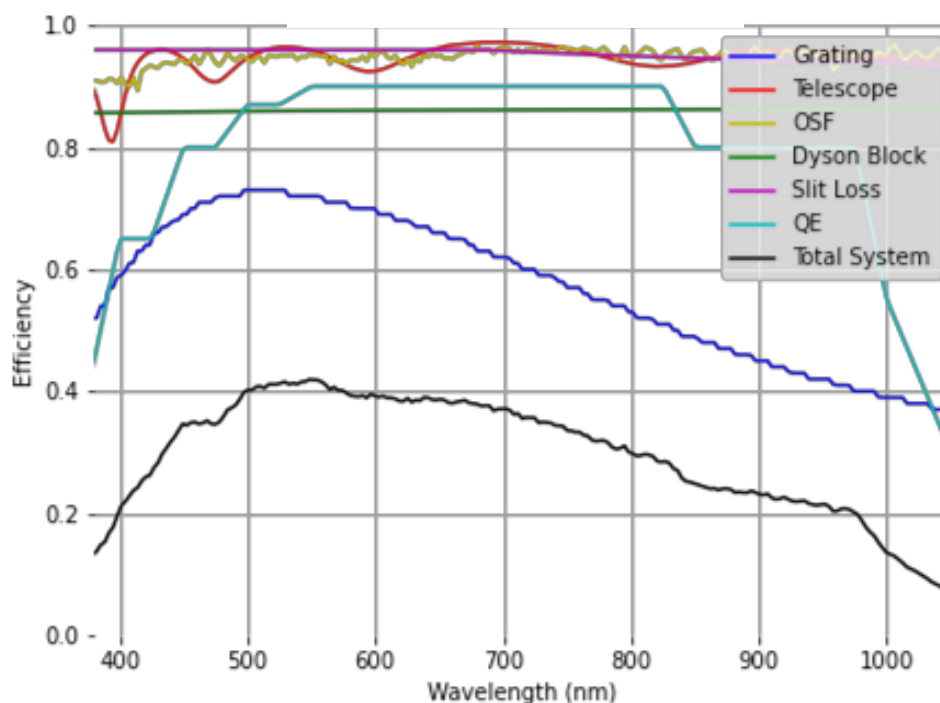


Figure 5-2: Instrument optical efficiency terms. The grating response is optimised in the blue.

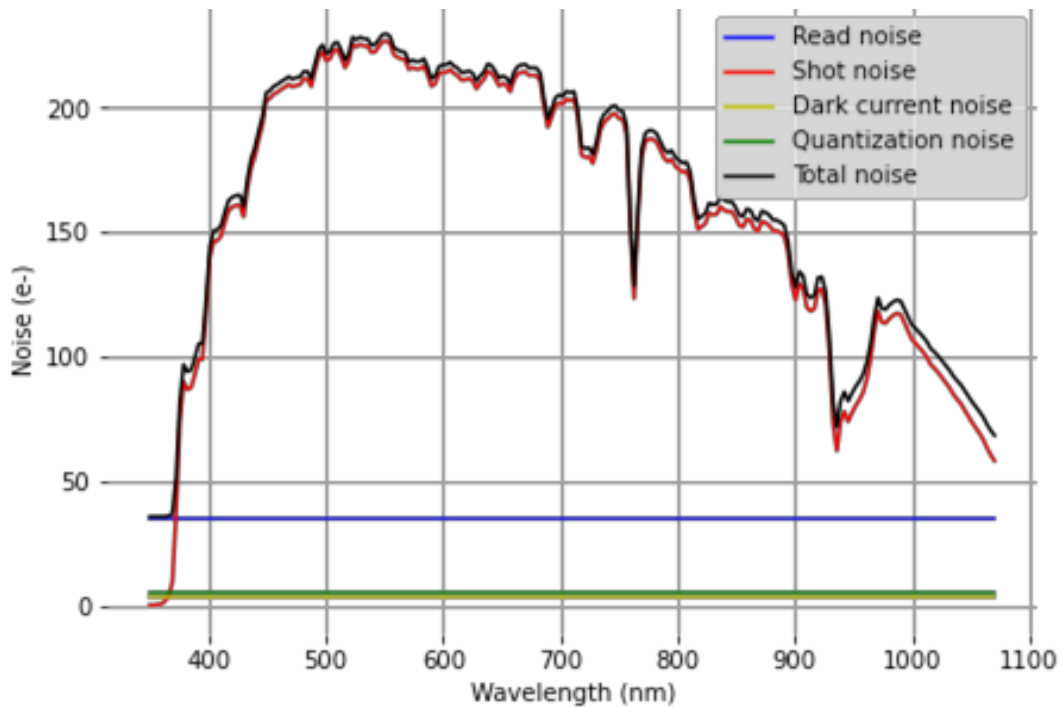


Figure 5-3: Instrument noise sources.

5.3 Instrument calibration

Accurate retrieval of water column parameters requires the basic spectroscopic radiance measurement to be of high fidelity. This requires attention to diverse aspects of instrument design and operation, as well as ensuring good spatial uniformity and accurate spectral and radiometric calibration. The process begins with the instrument design itself, and continues throughout the laboratory alignment and calibration experiments, as well as on-orbit calibration.

It is critical to select an optical design which enables high spatial uniformity by minimising aberrations and facilitating accurate alignment in the laboratory. Errors in alignment can result in spatial nonuniformities such as smile or keystone—effects which cannot be perfectly compensated in postprocessing and can cause large errors in downstream processing (Thompson et al., 2021). Even slight spectral miscalibrations—well within the envelope of acceptable smile distortions for many current missions—can result in phytoplankton pigment estimation errors that exceed those due to instrument noise.

Fortunately, with modern laboratory alignment procedures, spatial nonuniformities can be driven so low that they are negligible for downstream users. This obviates the need for fragile and uncertain smile correction operations. We recommend a procedure similar to the calibration process for imaging spectrometers like EMIT, the Compact Wide-swath Imaging Spectrometer (CWIS), and AVIRIS-3 (Moore et al., 2020). Here, response functions are measured independently in the cross-track, along-track, and spectral dimensions. This information, acquired multiple times throughout the alignment process, helps to ensure

optimal positioning of the optical components. Lasers with known wavelengths are used to measure the instrument's channel-to-wavelength mapping.

Even after this laboratory calibration process, post-launch spectral calibration is still necessary because the channel-to-wavelength alignment is highly sensitive and the spectrometer readily measures even small changes, such as might occur due to launch stresses, thermal cycling or the absence of gravity load. Recent airborne and orbital missions have been quite successful measuring spectral offsets from features of the atmosphere; sharp gas absorption features provide a known standard for understanding the center wavelength and response function for each channel. This process, based on fitting an atmospheric radiative transfer model including atmospheric constituents and surface reflectance, can yield wavelength calibration with precisions better than 1% of a channel width (Thompson et al., 2024). This means that costly and complex onboard wavelength standards are not necessary.

Finally, radiometric calibration is vitally important for remote sensing of water quality and aquatic ecosystems. Even spectrally uniform calibration errors can still have deleterious effects because the radiance signal is dominated by an additive path radiance term. This additive term first must be modelled and subtracted to reveal the water-leaving reflectance signal. Calibration begins in the laboratory with the use of SI-traceable radiometric standards imaged with known geometry. Techniques such as varying integration times and the use of multiple sources can be used to characterise the detector linearity. On orbit, vicarious calibration experiments based on field reference surfaces can be used to update and maintain radiometric calibration. Such approaches tend to produce better reflectance spectra, because multiplicative radiative transfer modelling errors 'divide out' when a vicariously calibrated radiance measurement is then used to retrieve reflectance spectra. Instruments like EMIT have demonstrated that vicarious calibration can be an effective solution to obtain accurate radiometry without the complexity and additional uncertainties created by onboard calibration standards (Thompson et al., 2024).

The spatial dimension of radiometric calibration, commonly called a 'flat field', measures the spatial deviation in radiometric response of different FPA elements. The flat field tends to drift slightly over time at the sub-1% level due to tiny changes in electronic state, an amount which seems benign at first glance but can cause obvious visual striping in pushbroom images. The flat field can also be updated vicariously by using signal processing techniques and long-timeframe averages to smooth out the spatial field presented to the sensor, as in the EMIT mission (Bruegge et al., 2021).

5.4 Instrument implementation

In this section, we present a high-level description of the instrument that implements the requirements as stated in previous sections.

5.4.1 Optics

The optical system is designed to the requirements specified in the ATM. It features an F# of 1.8 and an effective telescope aperture of 110 mm, paired with a slit measuring 0.018 mm x 54 mm. The telescope uses a three-mirror anastigmat (TMA) configuration, as shown in Figure 8-1.

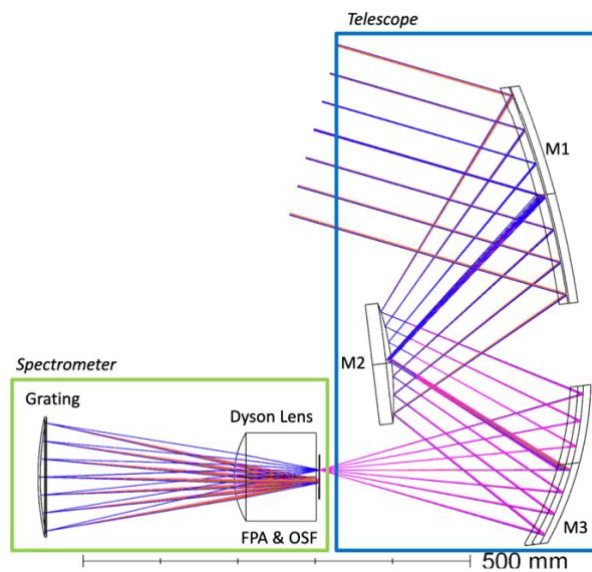


Figure 5-4: High-level optical design rendering of telescope and spectrometer.

The mirrors are silver-coated and made from low-expansion glass ceramic, such as Ohara CLEARCERAM-Z. The mirrors are freeform, as follows:

- M1 (y-decentered, freeform)
- M2 (freeform)
- M3 (y-decentered, freeform).

The Dyson spectrometer has following parameters and elements:

- Aspheric Plano-convex CaF₂ Dyson Lens, AR coated
- Lithographic slit (18 μm width, 54 mm length)
- Zero Order Light Trap (ZOLT) for suppression of the 0th order light
- Conic Diffraction grating (BK7), 13.7 cm diameter
- Order sorting filter (OSF).

The concave grating substrate is glass, and the blazed groove profile is shaped using E-beam grayscale lithography to optimise efficiency over the blue range. The grating operates on the -1 order.

The current design tracks key performance metrics, including the along-track response function (ARF), spectral response function (SRF), crosstrack response function (CRF), smile, and keystone (see Figure 5-5). The instrument requirements were flown down to these metrics and the implementation allows for a margin beyond the specified requirements (see Table 5-1).

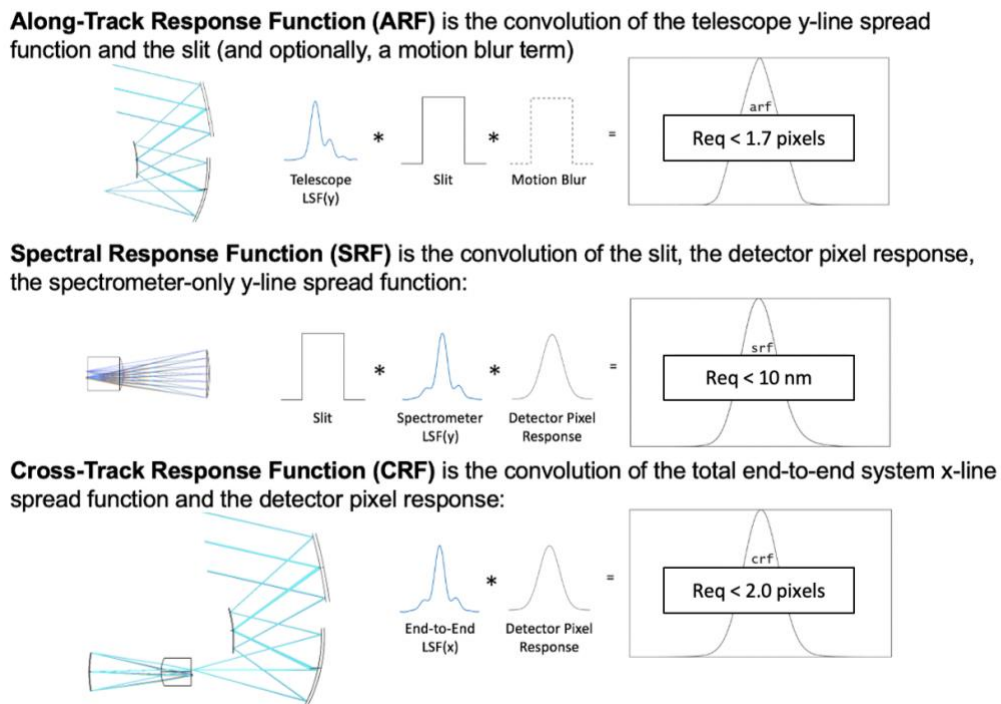


Figure 5-5: Key performance parameters satisfied by the current optical design.

Table 5-1: Key performance metrics for the optical system.

| Property | Requirement | Design Value | CBE with tolerances |
|----------|--------------|--------------|---------------------|
| ARF | < 1.7 pixels | 1.07 | 1.42 |
| SRF | < 10 nm | 4.61 | 5.33 |
| CRF | < 2.0 pixels | 1.24 | 1.85 |
| Smile | < 15% pixel | 2.5% | 5.6% |
| Keystone | < 15% pixel | 2.0% | 5.0% |

5.4.2 Detector and associated electronics

A block diagram of the electronics subsystem is shown in Figure 5-6. The combination of fine spatial resolution and wide swath is enabled using a large-format, digital-output detector array from Teledyne Imaging Sensors. The CHROMA-D/GeoSnap array (Jerram and Beletic, 2018) with 3072 spatial rows by 512 spectral columns, with 18 μm pixels, consists of a silicon photodiode array hybridised to a silicon readout integrated circuit (ROIC). The detector array is operated in deep depletion mode for high quantum efficiency out to 1050 nm. The array is operated near 250 K to mitigate dark current. To increase the SNR, the spectrum is sampled at 3.2 nm per row and co-added onboard the payload to 6.4 nm resolution.

The unit cell of the ROIC is a capacitive transimpedance amplifier (CTIA) with correlated double sampling for high linearity and low read noise. The ROIC contains an analog-to-digital converter (ADC) in each column, so all the pixels in each spectrum are converted by the same channel. Integrating the ADC into the ROIC minimises the length of the analog signal chain, which reduces the susceptibility of the science data to electronic noise and thermal effects. It also offers lower mass and power than external analog-to-digital electronics would require. The conversion result is serialized into high-speed differential outputs that can interface directly with an FPGA.

External electronics receive the detector data, perform spectral co-adding and buffering of the data, provide power and control signals for the detector, monitor temperature sensors, control operational heaters, and provide the power and data interfaces to the spacecraft. The data handling functions are performed by a Xilinx Ultrascale FPGA (XQRKU060); Jongeling et al. (2022) details its application to instrument electronics. The electronics providing power and control signals to the detector would be similar to those described in Sullivan et al. (2023). A microprocessor or microcontroller would be responsible for command processing, housekeeping, fault detection, and thermal control. A similar architecture is currently being developed for the Surface Biology and Geology-Visible Shortwave Infrared (SBG-VSWIR) mission (Green et al., 2022).

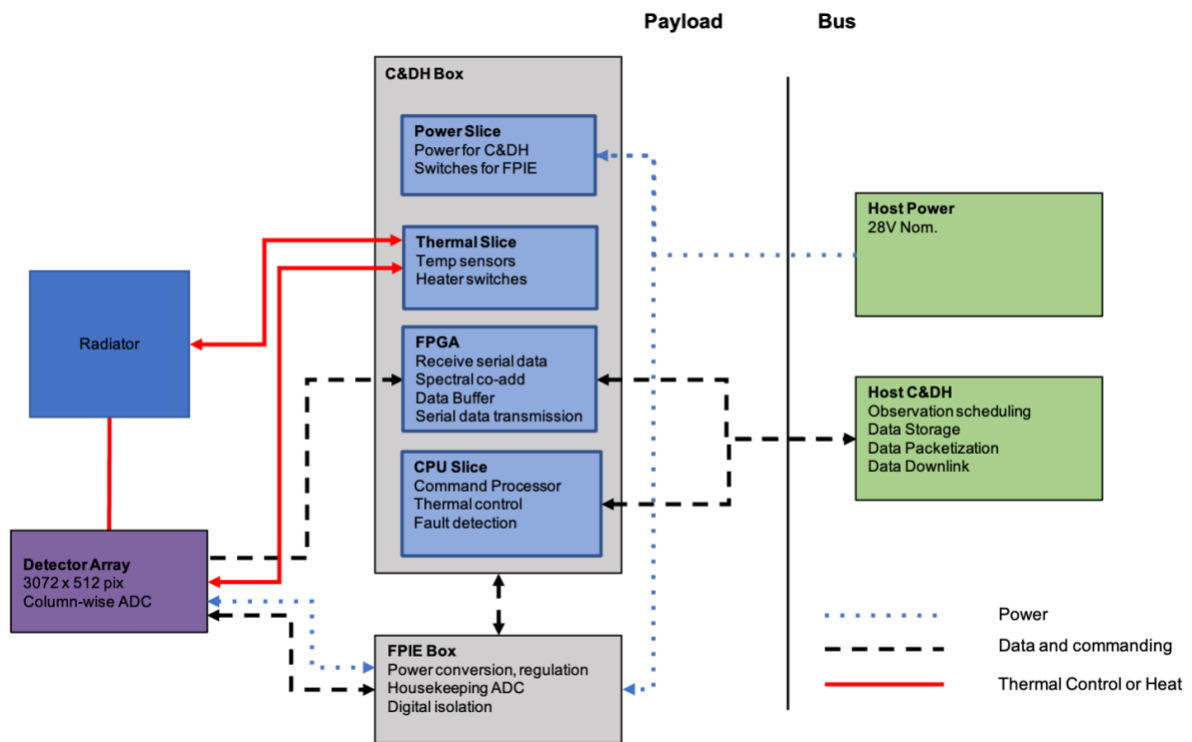


Figure 5-6: Block diagram of the electronics subsystem, which is split into two assemblies—the focal plane electronics and a command and data handling unit.

5.4.3 Thermal solution

The AquaSat-1 instrument is passively cooled and must function under challenging thermal conditions. The mission’s orbital parameters, combined with the requirement of $\pm 30^\circ$ off-nadir rotations in both the roll and pitch axes at any time and for unlimited duration, mean that the instrument radiators must accommodate significant solar exposure at various points in the orbit. At the same time, the instrument’s detector and spectrometer must be maintained at $250\text{ K} \pm 1\text{ K}$ and $273\text{ K} \pm 1\text{ K}$, respectively. To provide margin against requirements, the thermal design, as shown in Figure 5-7, assumes $\pm 35^\circ$ off-nadir rotations and $\pm 0.1\text{ K}$ thermal stability.

The thermal concept uses two passive radiator stages to remove thermal energy from the instrument: a warm stage for the spectrometer and a cold stage for the detector. Temperature-controlled trim heaters are used to maintain the required temperatures for both the spectrometer and detector during operation. The spectrometer and detector radiators are each split into equal area panels, one each on the port and starboard sides, for a total of four instrument radiator panels. An additional nadir-facing radiator rejects heat from the direct-mounted instrument electronics and requires only a survival heater.

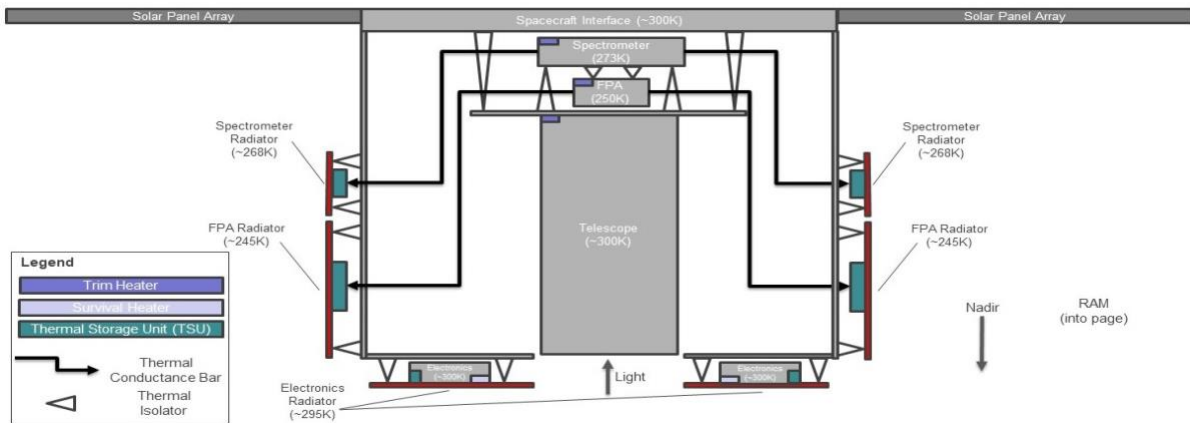


Figure 5-7: Schematic thermal design. The electronics boxes are attached to the nadir radiator. The side panels need thermal isolation from the spacecraft and each other. The design assumes PID-controlled trim heaters on the FPA and spectrometer, requiring ± 0.1 K stability; survival heaters can be ON/OFF. The design assumes that the solar panel dimensions are 1063 mm (length) x 1055 (width) mm.

The spectrometer and detector are thermally connected to their respective radiator panels using solid conductor bars or heat pipes, each assumed to have a thermal conductance of 1 W/K each. With this radiator arrangement, solar loading on either the port or starboard radiators—due to either drift in orbit or off-nadir spacecraft attitudes—can be rejected through the conductance bars to the opposite radiator, which is oriented toward deep space and the Earth. This configuration is illustrated in the example orbits shown in Figure 5-8. The radiators and conductance bars must be both oversized relative to the instrument loads and have sufficient heat capacity to maintain the instrument set points during these solar exposures. Z93 white paint is used for all radiators to minimise solar loads. Note that the Earth infrared load on the instrument radiators is negligible due to their relatively high temperatures.

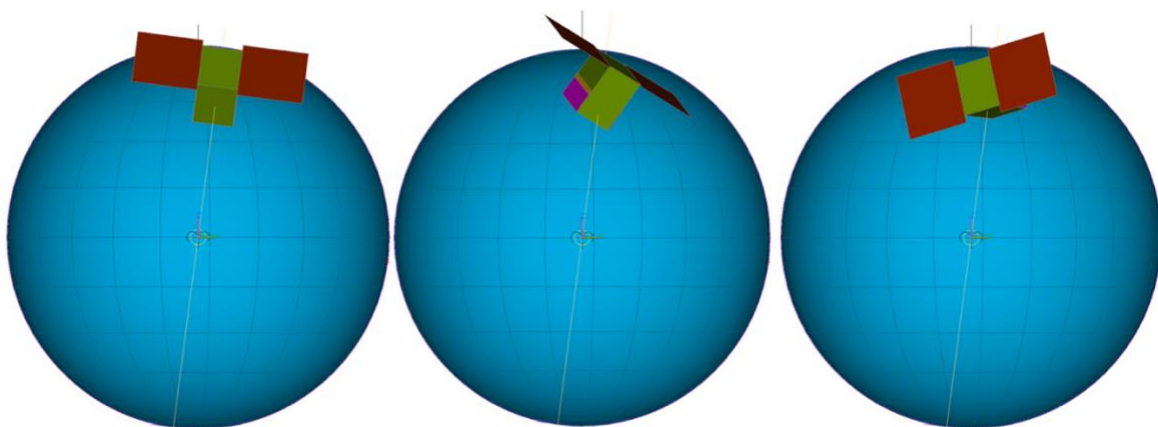


Figure 5-8: Example orbits (viewed from the sun) depicting baseline and extrema spacecraft attitudes. Left panel: pitch=0° and roll=0° (nadir pointing telescope). Middle panel: pitch=-35° and roll=-35°. Right panel: pitch=+35° and roll=+35°. The orbital position in the middle panel shows the port side instrument radiators exposed to the sun and the starboard panels viewing the Earth and deep space. Purple=spacecraft panels; red=solar arrays; pink=detector radiators; orange=spectrometer radiators.

To reduce overall mass of the thermal control system, the radiators must be constructed from high specific heat capacity materials. Two radiator options are explored here: aluminum-only and aluminum backed with paraffin thermal storage units (TSUs). Note that the latter utilises the high sensible specific heat of paraffin relative to aluminum rather than its latent heat.

A thermal model of the AquaSat-1 instrument is used to estimate loads that must be managed by the conductor bars and radiators to maintain the detector and spectrometer setpoint temperatures. The model considers radiative and conductive parasitics within the thermal system, as well as active dissipation in the detector. The resulting loads for each radiator are detailed in Table 5-2. Radiator sizing is determined using a thermal desktop model that accounts for solar irradiance, Earth infrared radiation, Earth albedo, and solar panel array loading on the radiator panels at the specified orbit and extrema spacecraft attitude.

Results from the model, detailed in Table 5-2, show that the proposed passive thermal control system can maintain the instrument’s set point temperatures under the specified orbital and attitude constraints while keeping mass, radiator area, and trim heater power budgets within reasonable limits. In particular, the model estimates that the radiator areas are compact enough to fit within the boundaries of the mechanical design. Additionally, using high specific heat capacity materials to absorb solar loading on the radiators offers substantial mass savings compared to an aluminium-only design.

Table 5-2: Thermal model results.

| Component | Temperature range [K] | Radiator load [W] (included margin [%]) | Total radiator surface area [cm ²] | Thermal control system mass [kg] | | Orbital maximum trim heater power [W] |
|--------------|-----------------------|---|--|----------------------------------|--------------------------------|---------------------------------------|
| | | | | Aluminium-only radiators | Aluminium & paraffin radiators | |
| Detector | 250 ± 0.1 | 7.9 (150) | 5740 | 11.3 | 3.2 + 2.2 | 27.8 |
| Spectrometer | 273 ± 0.1 | 6.5 (150) | 1320 | 3.3 | 1.1 + 0.7 | 11.0 |
| Electronics | 284 to 313 | 64.1 (40) | 4040 | 6.3 | 4.1 + 0.2 | 0.0 |
| Total | - | - | 11100 | 21.0 | 11.5 | 42.9 |

5.4.4 Mechanical configuration

The mechanical design of the instrument features a detached payload architecture, enabling a modular system that separates the interfaces of its key components: the payload chassis, telescope housing, telescope optical bench assembly (TOBA), spectrometer, and electronics. This modular approach allows the telescope, spectrometer, and chassis to be manufactured independently before being integrated with the aligned TOBA. This approach reduces complexity, enhances robustness, and maintains flexibility within the architecture.

The payload chassis and telescope housing are constructed from lightweight aluminium and are covered with white-coated radiator panels. For this configuration, we assume that the thermal solution will not use TSUs. The spectrometer is mounted to the telescope housing using titanium bipods and struts, forming the TOBA. Titanium bipods and struts are also used to mount the TOBA to the payload chassis. Optical alignment of mirrors is performed at near-room temperature using titanium bipods bonded to the telescope housing. This design minimises thermal mismatches and has a negligible impact on the optical alignment during operations.

The instrument's mass is estimated at 103.04 kg, which includes 15% mass growth allowance, and its nominal dimensions are 1148 mm x 796 mm x 991 mm, including a 20% size growth allowance. These allowances accommodate structural, thermal, and optical refinements needed to meet performance requirements. A notional configuration of the instrument is illustrated in Figure 5-9.

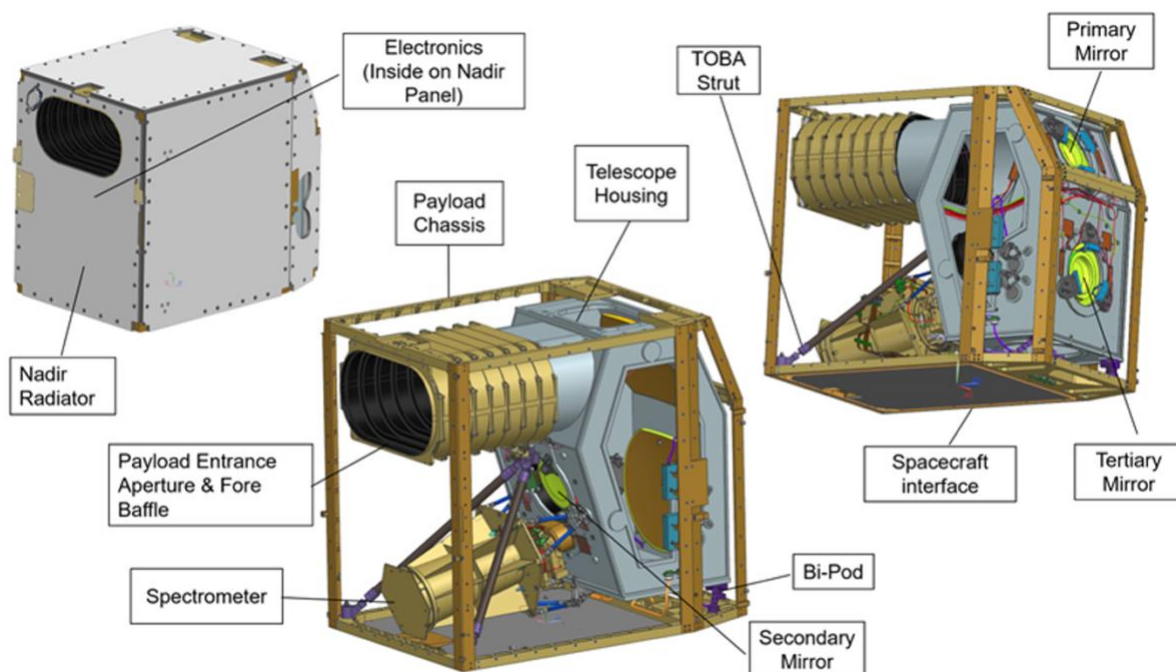


Figure 5-9: Mechanical configuration of the AquaSat-1 instrument.

5.5 Instrument accommodation requirements

Table 5-3 lists the maximum expected values (MEV) for key accommodation parameters for the complete payload. These were used as input for the platform evaluation (see Section 6).

Table 5-3: Payload accommodation requirements, with MEV at time of issuing this report.

| Parameter | MEV |
|--|---|
| Payload mass | 103.04 kg |
| Dimensions | 1148 mm x 796 mm x 991 mm |
| Operational mode timeline per orbit (95 min) | Science Imaging: 1 min; Standby: 90 min |
| Payload power demand (400 fps) | OAP: 74.3 W |
| | Peak: 90.2 W |
| | Science/Data to satellite platform: 90.2 W |
| | Safe/Boot: 60.7 W |
| | idle/Ready: 90.2 W |
| Data rate per mode | Science pushbroom mode: 2.9 Gbps |
| Total data in 24 hrs | 80 GB |
| Electrical interfaces to satellite platform | RS-422 – Commanding; Camera Link (4 Gbps)– Data Transfer; 28 V - Power |
| Instrument thermal control | All parts passively cooled with 2 radiators each for electronics (0.3 m ² total), spectrometer (0.1 m ² total), FPA (0.5 m ² total) thermally isolated from the platform structure |
| Platform stabilization requirements | Pointing: 3-axis stabilization with nadir pointing; |
| | Accuracy: 1/3 swath = 18 km = 2.6° |
| | Drift: <±0.5 pixel per 25 pixel travel = ±4 arcsec per 225 arcsec travel. |
| | Jitter: 1/10 pixel per GMC integration = 0.9" per 25 ms |
| | Knowledge: 0.5 pixel - 4" |
| Observational geometry requirements | Nadir pointing, 30° FOR. If pushbroom, ±10° off-nadir along-track |
| Launch vibration constraints | All AquaSat-1 components are expected to survive a NASA GEVS type launch environment |
| EMI/EMC requirements | Not derived |

5.6 Instrument trades

During the study, the team performed several instrument trades to optimise the baseline design. These are specified in Table 5-4.

Table 5-4: Instrument trades considered during this feasibility study.

| Topic | Options | Key parameters | Selection and rationale |
|-------------------------------------|----------------------------------|--|---|
| Spectral sampling | 1.6 nm/3.2 nm/6.4 nm | SNR, spectral feature width | 3.2 nm native 6.4 nm coadded on board: maximise SNR |
| Detector | CHROMA-D/Chroma-640 (CPM) | Tech. maturity; Pixel size Digital/Analog, swath size | CHROMA-D: Large swath, small pixel, digital electronics |
| Electronics | Pushbroom only/GMC- only/Both | Power, payload flexibility | Both: Want to keep pushbroom capability, SSDR can handle higher data rate |
| Mechanical | Aluminum/composite | Cost, thermal uniformity and validation, lead times, heritage | Aluminum: higher mass but better thermal validation and shorter lead times. |
| Thermal system - cooling | Cryocooler/No-Cryo | Detector/Spectrometer temperature, complexity, cost, mass allocation, volume | No cryocooler: cost and complexity |
| Thermal system - heat pipes | Heat pipes/No heat pipes | | Heat pipes: effective and low cost |
| Thermal system - Earth shielding | Yes/No | | No: not needed |

6 Satellite platform description

This section summarises the outputs of a satellite platform evaluation performed by UNSW Canberra Space under contract to CSIRO. UNSW Canberra Space operates the Australian National Concurrent Design Facility, which is a national asset designed to support the Australian space ecosystem and provides expertise and capability in early concept satellite design.

The purpose of the platform evaluation was to determine driving requirements, establish a baseline major resource budget (SWaP – size, weight, and power) and identify any major risks in the satellite platform. Figure 6-1 highlights the scope of the platform evaluation, which included the following activities:

- satellite configuration development
- structural evaluation
- power budget and power subsystem evaluation
- pointing budget and attitude and orbit control system (AOCS) evaluation
- propellant budget and propulsion subsystem evaluation
- data budget and computer subsystem evaluation
- link budget and communications subsystem evaluation
- ground segment evaluation
- launch vehicle evaluation
- assessment of commercially available platform options.

Key inputs were the AquaSat-1 mission requirements (see Section 3.6), concept of operations (see Section 4.1) and instrument accommodation requirements (see Section 5.5).

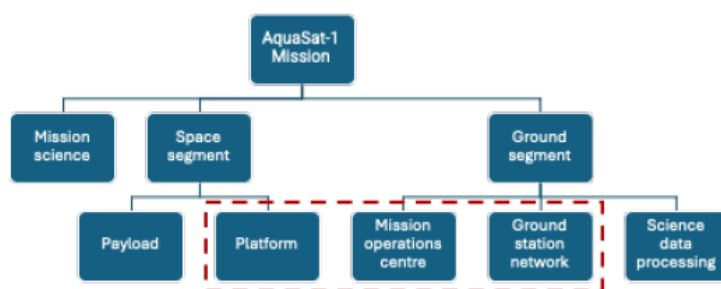


Figure 6-1: AquaSat-1 system elements (red-dashed box indicates the scope of the platform evaluation).

The evaluation concluded that the satellite platform manufacture is feasible with no significant subsystem development activities required. With an estimated total wet mass of approximately 330 kg, the mission could be implemented using a tailored small satellite platform, of which several space-qualified examples exist. Full details can be found in the accompanying AquaSat-1 Platform Evaluation Report (UNSW Canberra Space, 2024).

6.1 Platform requirements

As part of the platform evaluation, the mission requirements listed in Section 3.6 were expanded to a set of 50 derived requirements on the platform and subsystems. These derived requirements can be found in UNSW Canberra Space (2024). These requirements are stated solely for the purpose of the platform evaluation and do not form contractual requirements for subsequent work.

6.2 Platform concept design

This section provides a summary of the driving platform subsystem selections, as well as the technical budgets that were derived through the platform evaluation process.

The space segment consists of one satellite comprising the payload described in Section 5, and the supporting platform outlined here. The generic satellite architecture can be seen in Figure 6-2.

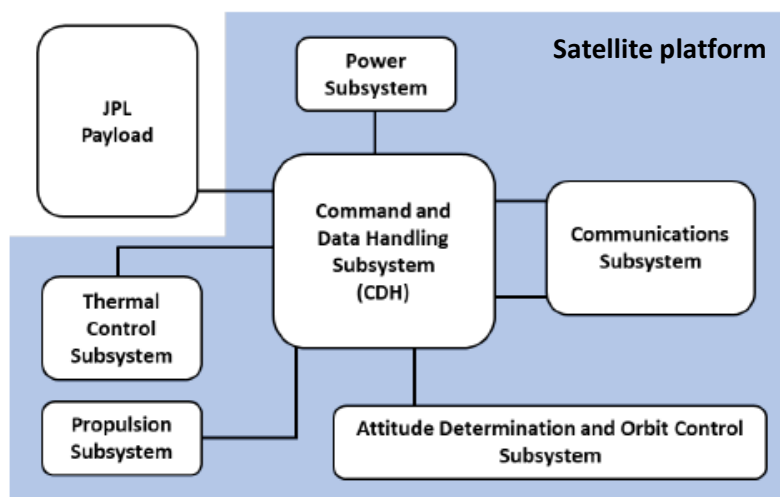


Figure 6-2: AquaSat-1 conceptual design architecture (UNSW Canberra Space, 2024).

6.2.1 Attitude and orbit control system (AOCS)

To execute its mission functions, the satellite is required to slew between target sites. Based on the concept of operations in Section 4.1, the following slew manoeuvres need to be performed:

- slew to next target
- dwell on current target
- slew to celestial calibration target
- point to nadir.

The agility and control of the satellite shall be sufficient to achieve a dwell factor of 10:1 to accommodate the GMC imaging strategy described in Section 4.1. This is a minimum of 1.1

deg/s about the pitch axis during imaging. The agility of the satellite also contributes to the time it takes to slew to the next target, which impacts the number of imaging opportunities for any given overpass of Australia or the US. This requirement is captured in AS1-MIS-18 (Section 3.6), which specifies that the platform shall achieve a slew rate > 3 deg/s. Slewing to celestial calibration targets and nadir pointing are not considered to drive the spacecraft agility requirements. This means that the driving requirement for the platform is AS1-MIS-18. The agility performance of the reference design is presented in Table 6-1.

Table 6-1: Satellite agility performance summary (UNSW Canberra Space, 2024).

| Parameter | Value | Notes |
|---|--------------|-------------------------|
| Settling Time | 3 s | Based on UNSW modelling |
| Settling-time margin | 100% | |
| Specified settling time | 6 s | Including margin |
| Maximum slew rate | 4.24 deg/s | Pitch |
| Maximum angular acceleration | 0.33 deg/s/s | Pitch |
| Specified rapid slew time from look angle of -30° to +30° | 37.4 s | |

6.2.2 Propulsion and delta-V budget

The delta-v budget for orbit control is driven by the mission lifetime requirements (AS1-MIS-6 and AS1-MIS-7), spatial resolution tolerance (AS1-MIS-16), orbit LTDN (AS1-MIS-5), and required de-orbit maneuvers (AS1-MIS-8). A trade study on electric versus chemical propulsion systems⁸ concluded that chemical propulsion is more suitable for this mission, as the reduced propellant mass for an electric propulsion system is overshadowed by negative performance impacts on the power subsystem, satellite agility, and thermal dissipation. The derived delta-V requirements for the chemical propulsion system are summarised in Table 6-2.

Table 6-2: Mission delta-V requirements for chemical propulsion (UNSW Canberra Space, 2024).

| Manoeuvre | Delta-V (m/s) |
|----------------------------|---------------|
| Orbit insertion correction | 10 |
| Altitude maintenance | 168 |
| Orbit plane maintenance | 17 |
| Collision avoidance | 20 |
| De-orbit | 95 |
| Total | 310 |

Key performance specifications for the propulsion system are shown in Table 6-3. The reference design uses Dawn Aerospace’s SmallSat propulsion system that consists of a bipropellant thruster that uses nitrous oxide as an oxidiser and propene as a fuel. Both are readily available fluids, are non-toxic, and thus do not require extensive safety requirement to handle. The reference design does not preclude the use of alternative propulsion systems if this mission proceeds to implementation.

Table 6-3: Key specifications of the propulsion system (UNSW Canberra Space, 2024).

| Parameter | Value |
|------------------|---|
| Thruster | Dawn Aerospace B20 |
| Oxidiser | Tank: Dawn Aerospace 3D printed titanium Propellant: Nitrous Oxide |
| Fuel | Tank: Dawn Aerospace 3D-printed titanium Propellant: Propene |
| Specific Impulse | 250-280 s |
| Thrust | 20 N |
| Propellant | 40.7 kg |
| Delta-V | 310 m/s |
| Dry Mass | 23.5 kg |
| Wet Mass | 64.2 kg |

⁸ Here we consider chemical propulsion to include any system that produces thrust using thermal expansion of a fluid.

6.2.3 Data budget

The science data budget can be seen in Table 6-4. These values utilise the instrument data collection rate combined with the maximum acquisition duty across an orbit. This provides a worst-case data budget, which was used to derive data storage requirements and the link budget. This data informs the design of the communications subsystem and ground segment, leading to specification of an X-band radio link for payload data and S-band for telemetry, tracking, and command (TT&C) (see Section 6.2.7).

Table 6-4: The science data budget (UNSW Canberra Space, 2024).

| Parameter | Value | Comments |
|---|--|--|
| Payload data rate (before compression) | 2900 Mbps | |
| Orbit acquisition duty cycle | 5.3% | |
| Mean raw data volume | 153.8 Mbps 1661 GB/day | Product of operating output data rate and operating duty cycle. The output data if the instrument was producing the same volume of data, but at a constant rate 100% of the time. |
| Coaddition reduction factor | 10x | 10x GMC (coadding occurs onboard the instrument). |
| Mean data volume collected from target site imaging (before compression) | 15.4 Mbps 166.1 GB/day 10.7 GB/orbit | Reduced by coaddition reduction factor. |
| Dark calibration data | 0.375 GB/orbit | See AQ1-MIS-45 = 3 Gbit/orbit; Note: assume the same compression is applicable. |
| Mean dark calibration data volume | 0.54 Mbps | |
| Mean data volume – target site imaging and calibration (before compression) | 15.9 Mbps 11.1 GB/orbit | Target data volume plus dark calibration target volume. |
| Data compression ratio | 2:1 | From instrument accommodation requirements. |
| Average data volume (compressed) | 7.96 Mbps 5.53 GB/orbit 85.9 GB/day | Collected data volume/compression ratio. |
| Overheads | 10% | Total overheads on the compressed data above, before it is encoded and modulated. Includes metadata, formatting, and any packetization and framing not included in the modulation and coding scheme. Assumed reasonable value; may be refined. |
| Required data downlink volume | 94.5 GB/day | Overhead amount added to previous. |
| Margin | 10% | Assumed. |
| Required downlink data volume (with margin) | 104 GB/day 6.69 GB/orbit | Margin added to previous. |
| Mean required downlink data rate | 9.6 Mbps | Previous value in different units; the data rate required if it was transferred at a constant rate 100% of the time. |

6.2.4 Power budget

The satellite power budget is shown in Table 6-5. The concept design incorporates deployable solar panels (see Section 6.2.6), with a minimum area of 1.5 m² of space grade commercial solar cells with significant flight heritage. No additional articulation is required. Battery options are presented in UNSW Canberra Space (2024) with several commercial off-the-shelf (COTS) Li-Ion options with significant flight heritage available that meet the power and lifetime requirements.

Table 6-5: Power budget for each operating mode (UNSW Canberra Space, 2024).

| Subsystem | Power consumption by operating mode | | | | |
|--|-------------------------------------|--------------|--------------|--------------|-------------|
| | Standby | Acquisition | Rapid slew | Downlink | Thrust |
| Payload | 86.6 | 104.1 | 86.6 | 93.6 | 82.4 |
| AOCS | 42.4 | 55.9 | 174.1 | 46.3 | 52.0 |
| CDH | 4.8 | 14.4 | 4.8 | 14.4 | 4.8 |
| Communications | 5.0 | 5.0 | 5.0 | 140.3 | 5.0 |
| Power | 10.5 | 10.5 | 10.5 | 10.5 | 10.5 |
| System margin | 20% | 20% | 20% | 20% | 20% |
| TOTAL incl. margin (consumption) | 179.2 | 227.9 | 337.2 | 366.1 | 86.8 |
| TOTAL incl. margin (heat dissipation) | 177.7 | 227.9 | 337.2 | 329.1 | 86.8 |

6.2.5 Mass budget

The satellite concept mass budget is shown in Table 6-6, with margins applied at both the component level and system level. The effect of the propulsion system selection (chemical versus electric), as well as other subsystem selections can be seen in UNSW Canberra Space (2024).

Table 6-6: The satellite concept mass budget (UNSW Canberra Space, 2024).

| Subsystem | Mass excl. margin (kg) | Margin (%) | Mass incl. margin (kg) | % of total mass |
|---|------------------------|------------|------------------------|-----------------|
| Payload (incl. computer & data storage) | 89.6 | 15.0% | 103.0 | 42.4% |
| AOCS | 20.2 | 7.1% | 21.6 | 8.9% |
| CDH | 4.7 | 18.2% | 5.6 | 2.3% |
| Communications | 6.4 | 15.3% | 7.4 | 3.0% |
| Propulsion | 16.3 | 20.0% | 19.6 | 8.1% |
| Power | 13.3 | 15.9% | 15.5 | 6.4% |
| Structure | 58.6 | 19.8% | 70.3 | 28.9% |
| Thermal ⁹ | 0.0 | 0.0% | 0.0 | 0.0% |
| S/C dry mass incl. margins | 209.2 | 16.1% | 243.0 | 100.0% |
| System margin | | 20.0% | | |
| S/C dry mass incl. system margin | | | 291.5 | |
| Propellant mass incl. system margin | 37.0 | 10.0% | 40.7 | 12.2% |
| Total wet mass incl. all margins | | | 332.2 | |

⁹ The mass of the platform's thermal subsystem (mostly radiators) is accounted for in the structure subsystem.

6.2.6 Structure, thermal control system, and configuration

The satellite mass and volume are suitable for a standard ‘ESPA Class’ 24” launch vehicle adaptor. As with the payload mechanical configuration described in Section 5.4.4, a box frame with aluminium sandwich panels forms the platform structure. It is not expected that carbon fibre structure would be required for stiffness, strength or thermo-elastic purposes.

The length of the platform is driven by the required radiator area. A preliminary area of 1.2 m² is estimated based on the power budget and radiator location, with further transient thermal analysis required in a future phase of this project. The payload is thermally isolated from the platform with a dedicated thermal control system (see Section 5.4.3).

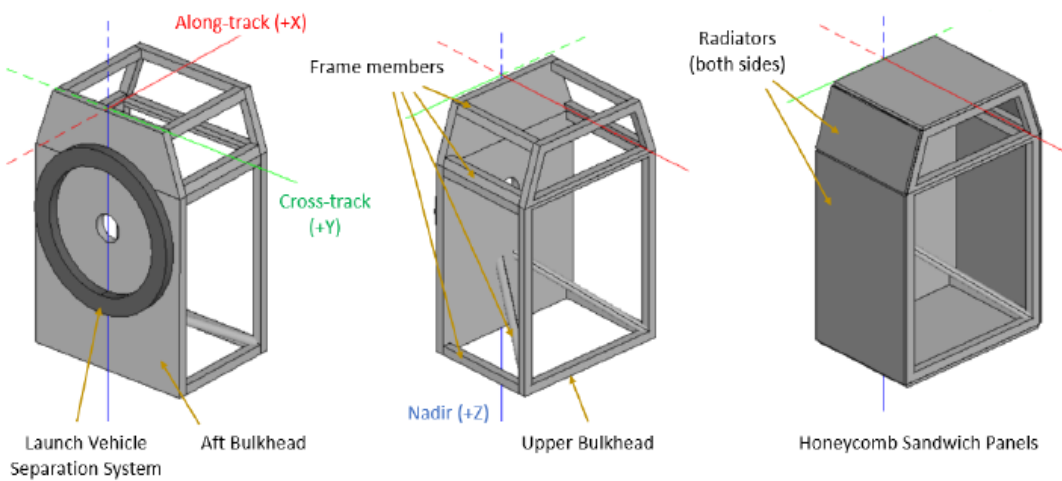


Figure 6-3: Proposed structural configuration of the satellite platform (UNSW Canberra Space, 2024).

6.2.7 Communications and ground segment

Separate communications links were assumed: bi-directional telemetry, tracking, and command (TT&C), and payload data downlink. Based on the data budget described in Section 6.2.3, UNSW Canberra Space (2024) selected an S-band (2200-2290 MHz) link for TT&C and an X-band link (8025-8400 MHz) for payload data downlink.

Several ground segment concepts were assessed in UNSW Canberra Space (2024). The data latency requirement (AS1-MIS-9) defined in Section 3.6 drives the location and requirements for the ground segment, in combination with the data budget. A single ground station at the Svalbard site in Norway, operated by Kongsberg Satellite Services (KSat), was chosen for the conceptual design. Table 6-7 summarises its specifications, including calculated access numbers based on the baseline mission orbit. Figure 6-4 shows the ground station coverage overlaid with the AquaSat-1 orbit ground track.

The period between contacts (7.7 hours) is part of the budget that informs compliance with the latency requirements. We note here that studies by the EMIT team (Olson-Duvall, personal communication, 14 June, 2024) show a distribution of latency values, with most of these smaller than 2 days. This suggests that the AquaSat-1 requirement (≤ 2 days) is achievable. However, further exploration of the AquaSat-1 data processing system, including the preliminary design of the science data system, is necessary to determine compliance with the requirement.

Table 6-7: Concept ground segment parameters (UNSW Canberra Space, 2024).

| Parameter | Value | Units |
|--|------------------|---------|
| Site | Svalbard, Norway | - |
| Latitude | 78.23 | °N |
| Longitude | 15.41 | °E |
| Gain-to-noise-temperature ratio (G/T)—X band | 29.2 | dB/K |
| Dish size | 7.3 | m |
| Access time (24-hour minimum) | 78 | min/day |
| | 5.4 | % |
| Access time (average) | 84 | min/day |
| | 5.8 | % |
| Longest period between contacts | 7.73 | hours |

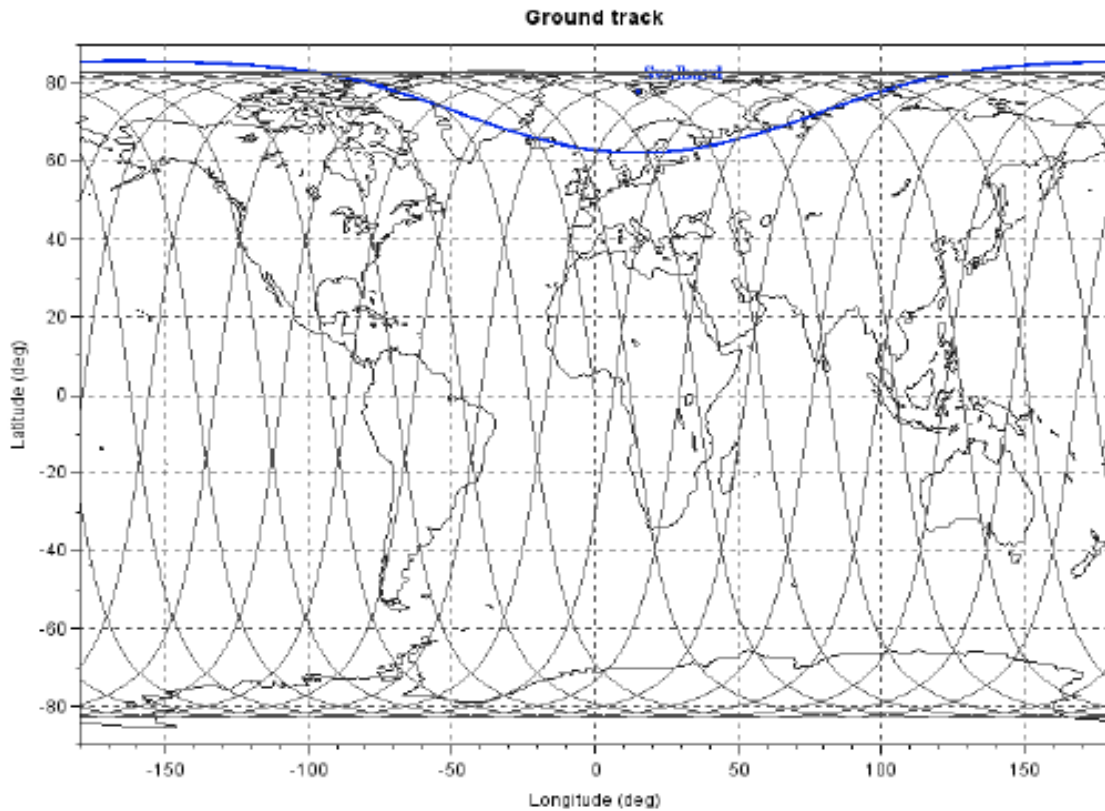


Figure 6-4: Svalbard ground station coverage for the 400 km orbit to 5° elevation, overlaid with the AquaSat-1 reference ground track over one day (UNSW Canberra Space, 2024).

6.2.8 Subsystem down-selection

The platform concept design was assessed against widely available commercial subsystems and components, with down-selected components presented in Table 6-8. It should be noted that the purpose of this effort was to validate that the platform can be manufactured without significant development activities that would drive the risk and schedule of the satellite manufacture. This design may not present the optimal solution for satellite manufacture and does not form a recommended industrial structure. An overview of this platform concept design can be seen in Figure 6-5 and Figure 6-6.

Table 6-8: Down-selected components for the platform concept that meet requirements (UNSW Canberra Space, 2024).

| Subsystem | Component | Vendor | Model | Maturity | Comments |
|--|-----------------------------|---|---|---|--|
| Command and data handling | Computer | Not yet selected | Not yet selected | TBD | To co-add GMC data and provide 2:1 compression. Component selection deferred until later design phase. |
| On-board storage | Memory | Mercury | RH3440 | Flight heritage | 440 GB capacity for payload data storage. |
| AOCS | Computer | Custom (based on Berlin Space Technologies ACC-110) | | Flight heritage | No suitable COTS option could be found. This computer is for the AOCS subsystem only. |
| | Reaction wheels | Blue Canyon | RW4 | Flight heritage | High torque, moderate momentum, low weight, and compact size. |
| | Magnetorquers | Sinclair Interplanetary | TQ-40 | Flight heritage | High torque and low weight. |
| | Star Trackers | RocketLab | ST-16RT2, Mid-Baffle | Flight heritage | High accuracy, low weight & power, moderate maximum slew rate, and moderate sun exclusion angle. |
| | GNSS Receiver | Berlin Space Technologies | GPS-110 | Flight heritage | Lightweight, low power, and good accuracy. |
| | IMU | Safran | STIM380H | Flight heritage | Compact, lightweight, space applicable, and ITAR free. |
| | Magnetometer | MEDA | TAM-2 | Flight heritage | Space-specific magnetometer. |
| | EHS | CubeSense | Earth | Flight heritage | Compact with good FoV. |
| Propulsion | Chemical thruster | Dawn Aerospace | SatDrive | Flight heritage | Nitrous oxide & propene Thrust = 6.1-16.7 N. I_{sp} = 250-280 s. |
| Communications - payload data downlink | Radio | L3Harris | T-748 High Data Rate Transmitter (X Band) | Flight heritage | X-band |
| | Antenna | Beyond Gravity | X-band gen 2 helix data downlink antenna | Not stated, but generation 1 antennas have flight heritage. | EOC 55°, 8.2 GHz variant |
| Communications - TT&C | Radio | Rocket Lab | Frontier-S-LEO-ST | Flight heritage | S-band |
| | Antenna | Not specified | Patch antenna | TBD | This component is simple and widely available. |
| Power | Solar Arrays | Airbus Defence & Space | SparkWing | Flight heritage | Azur Space 3G30A cells; CFRP skin with aluminium honeycomb core. |
| | Batteries | Saft | 4S1P VES16 | Flight heritage | Li-ion, 512 Wh. |
| Ground-stations network | Ground station as a service | KSat | N/A | Currently in use | Class of solution with a mature vendor identified. |

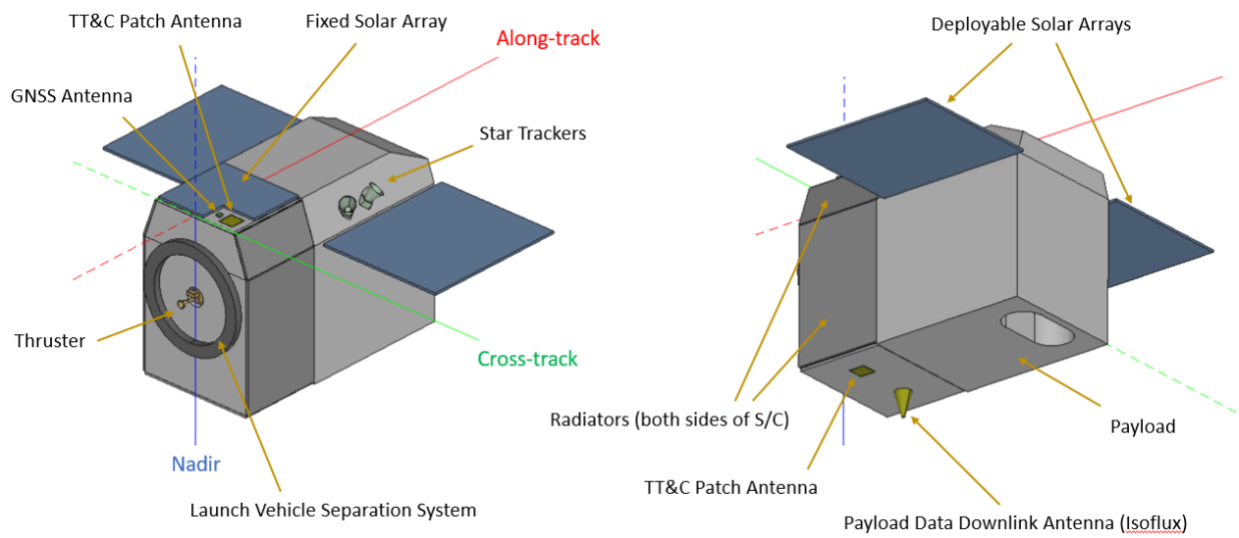


Figure 6-5: Platform concept design overview with a dedicated platform assembled to suit the payload (UNSW Canberra Space, 2024).

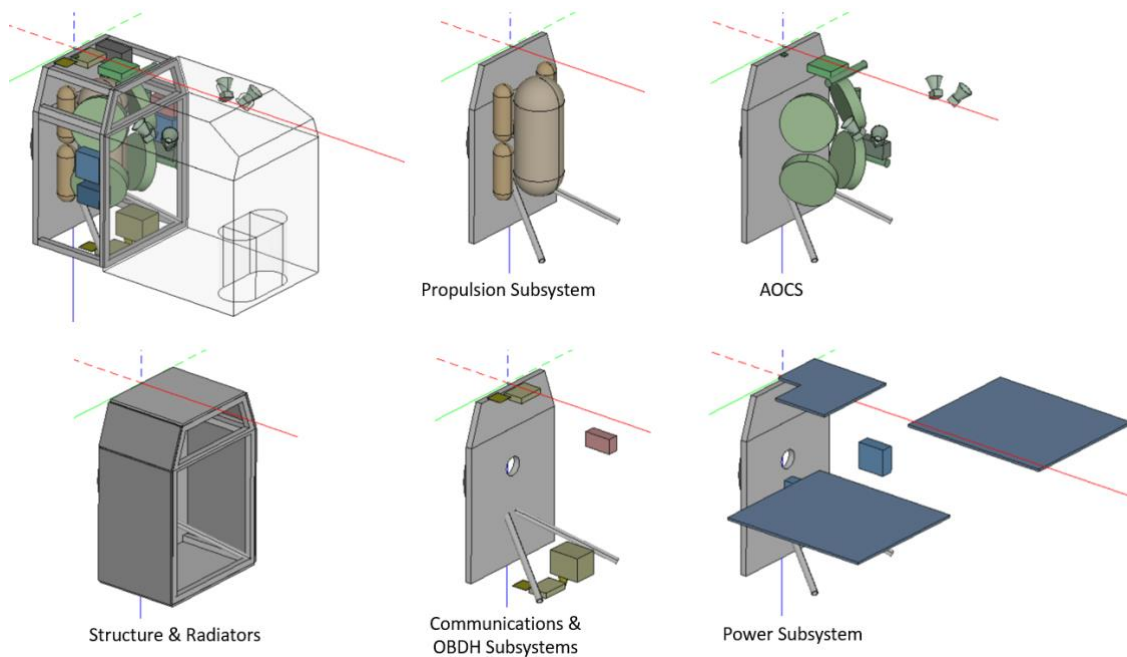


Figure 6-6: Platform subsystem overview (UNSW Canberra Space, 2024). In addition to structural and thermal interfaces between the instrument and platform, the AOCs and power subsystems require additional interfaces on the payload.

6.2.9 Platform selection

The most feasible industrial structure for AquaSat-1 is to utilise an existing satellite platform. It was found unlikely that a fully COTS small satellite platform could meet or exceed the AquaSat-1 platform requirements due to the unique size and shape of the payload. However, several commercial providers offer customisable satellite platform solutions.

Figure 6-7 shows two variations of a Surrey Satellite Technology Limited (SSTL) platform, each with a launch mass of approximately 430 kg, in the region of AquaSat-1. A study led by SSTL commenced in May 2024 to investigate this as a potential option for AquaSat-1. Other satellite manufacturers provide similar customisable platforms and are discussed in UNSW Canberra Space (2024).



Figure 6-7: NovaSAR-1 and SSTL S1-4, both based on the SSTL-MINI platform (approximately 430 kg launch mass each). Image credit: SSTL.

6.3 Platform trades

6.3.1 Altitude trade

UNSW Canberra Space (2024) assesses the impact of increasing the specified orbit altitude from 400 km to 600 km. The required delta-V is smaller at the higher altitude. However, to maintain the required 18 m GSD, the instrument needs to be significantly increased in size (approximately 50% in all dimensions), mass (approximately 80%) and inertia (approximately 4.5x). Table 6-9 summarises the platform impacts.

Table 6-9: Impact of orbit altitude on satellite platform (UNSW Canberra Space, 2024).

| Design parameter | 400 km altitude | 600 km altitude | Change |
|--|-------------------------|-------------------------|------------------|
| Orbit | | | |
| Type / LTDN | Sun-synchronous / 12:00 | Sun-synchronous / 12:00 | None |
| Orbit altitude [km] | 399.5 | 602.5 | +51% |
| Repeat cycle duration [days] | 13 | 15 | +15% |
| Number of orbits per cycle | 202 | 223 | +10% |
| Orbit period [mins] | 92.67 | 96.86 | +5% |
| Satellite configuration | | | |
| Total wet mass [kg] | 332.2 | 526.8 | +59% |
| Dimensions [mm] | 1661 x 898 x 1314 | 2107 x 1243 x 1888 | +27% x 40% x 44% |
| Launch vehicle adaptor [inch] | 24 | 36.89 | - |
| Propulsion system | | | |
| Propulsion type | Chemical bi-propellant | Chemical bi-propellant | None |
| Delta-V [m/s] | 310.3 | 211.0 | -32% |
| Propellant mass [kg] | 40.7 | 44.8 | +10% |
| AOCS | | | |
| Reaction wheel size [N.m.s/N.m] | 4 / 0.25 | 8 / 0.25 | +100% / - |
| Max. slew rate [deg/s] | 4.24 | 2.68 | -37% |
| Max. angular acceleration [deg/s/s] | 0.32 | 0.1 | -69% |
| Electrical power system | | | |
| Orbit average power [W] | 184.3 | 195.3 | +6% |
| Solar array area [m ²] | 1.4 | 1.5 | +7% |
| Battery capacity [W.h] | 550 | 550 | None |
| Minimum continuous discharge current [A] | 38.4 | 38.4 | None |
| Communications system | | | |
| Data volume [GB/day] | 104 | 126 | +21% |
| RF band | X | X | None |
| Downlink time per orbit [mins] | 5 | 7.6 | +52% |

6.3.2 Imaging strategy trade

The GMC imaging strategy discussed in Section 4.1 could also influence the platform design, when compared against a more traditional pushbroom strategy. The instrument analysis in Section 5 identifies the SNR requirements for the three applications objectives in Section 3. As noted in Section 3.5, GMC is required to meet the SNR requirements for application objective 3. On the other hand, the GMC imaging strategy results in a reduction in the number of imaged targets due to the increased overpass time required for each target image. This is particularly significant where target sites are in close proximity.

An analysis of the imaging duty-cycle for the satellite was performed in UNSW Canberra Space (2024) considering a representative overpass of targets in the US and two imaging strategies: 10x GMC mode and pushbroom mode.

Table 6-10 compares the duty cycles of the two imaging modes. As expected, pushbroom mode permits considerably more imaging coverage, increasing from 174 km per orbit for GMC mode to 1103 km per orbit for pushbroom mode. This corresponds to an absolute instrument imaging duty-cycle of 4.3% for GMC mode and 2.7% for pushbroom mode. The duty cycle is smaller in pushbroom mode because the distance the satellite travels while imaging is smaller (1103 km) than in GMC mode (1740 km).

Table 6-10: Duty cycle comparison between GMC and pushbroom imaging modes (UNSW Canberra Space, 2024).

| Mode | Pushbroom time per mode (s) | 10× GMC visibility-window duty cycle per mode | Pushbroom visibility-window duty cycle per mode | 10× GMC orbital duty cycle per mode | Pushbroom orbital duty cycle per mode |
|--------------------|-----------------------------|---|---|-------------------------------------|---------------------------------------|
| Inter-imaging slew | 185.6 | 28.9% | 46.4% | 2.1% | 3.3% |
| Imaging | 151.0 | 59.5% | 37.7% | 4.3% | 2.7% |
| Idle or other mode | 3.4 | 11.6% | 15.8% | 93.6% | 93.9% |

Table 6-11 compares the platform specifications impacted by the observing mode for GMC-only and pushbroom-only imaging. Here we are assuming that during GMC operations, the data for a given target is coadded on-board by the satellite platform. Because of this, in pushbroom mode the total data volume that needs to be downlinked increases by approximately 6.5x, with significant impacts on the communications subsystem and the ground segment. UNSW Canberra Space (2024) proposed tripling the number of ground stations and enhancing the on-board radio. The resulting increase in radio output power along and downlink operations drives an increased battery capacity and solar array area.

The UNSW Canberra Space (2024) study presents additional minor impacts of imaging strategy on the satellite platform. Notably, the AOCs design is driven by the inter-imaging slew operations and not impacted by the imaging strategy. The data recorder proposed in Section 6.2.8 is compliant with both imaging strategies.

Table 6-11: Platform comparison for GMC-only and pushbroom-only imaging modes (UNSW Canberra Space, 2024).

| Design parameter | GMC-only imaging | Pushbroom-only imaging | Change |
|--|------------------|------------------------|--------|
| Communications system | | | |
| Data volume [GB/day] | 104 | 686 | +560% |
| RF band | X | X | None |
| Downlink time per orbit [mins] | 5 | 14 | +180% |
| Electrical power system | | | |
| Orbit average power [W] | 196.6 | 234.7 | +27% |
| Solar array area [m ²] | 1.5 | 1.9 | +27% |
| Battery capacity [W.h] | 550 | 875 | +59% |
| Minimum continuous discharge current [A] | 38.4 | 38.4 | None |

7 Technology readiness level and technical risks

Given the heritage of the imaging spectrometers at JPL (see Section 5.1), all systems in AquaSat-1 are technology readiness level (TRL) ≥ 6 or assessed to be standard engineering (NASA, 2020). Here we list the top 4 technical risks identified during the study and map them to a risk matrix in Figure 7-1. The likelihood and consequence (on performance only) use the standard NASA definitions (NASA, 2017). The top 4 technical risks are as follows:

1. System

a. Mechanical:

- If the first mode frequency with $>10\%$ mass participation is low compared to launch requirements, due to the payload mass distribution, resonances may be induced during launch, resulting in payload damage

Likelihood: 3 – Default without further analysis

Consequence: 4

Rationale and potential mitigation: Previous experience has shown that management of the first mode frequency may require the addition or modification of mechanical elements. To mitigate, perform a mechanical analysis of the integrated payload and platform system and modify the location or mass of payload elements accordingly.

b. Mission:

- If the sensitivity performance of the GMC mode is not as large as expected, due to glint and target configuration issues (presence of trees, canyons, etc.), physical parameters will not be obtained with the required uncertainty.

Likelihood: 3 – Default without further analysis

Consequence: 3

Rationale and potential mitigation: The satellite maneuverability reduces the likelihood of glint and the impact of terrain obstacles. The margin between instrument requirements and instrument performance provides a built-in mitigation. To mitigate, perform further analysis of the performance of the GMC mode in challenging terrain or in the presence of glint.

2. Instrument

a. Electronics:

- If the FPGA board that has been baselined is not available in time, due to development delays in SBG, a new board will need to be designed, fabricated, and tested, leading to schedule delays and potential cost increases.

Likelihood: 3 – Default without further analysis

Consequence: 4

Rationale and potential mitigation: The FPGA board is being developed as part common instrument electronics R&TD effort, in the context of SBG Thermal Infrared (TIR) concept. This development will need to be adapted to AquaSat-1. The use of this FPGA will need to be re-examined if AquaSat-1 enters formulation.

b. Radiators:

- If heat is not spread uniformly over the radiator surfaces, due to thermal design problems, the effectiveness of the heat transport may be compromised, resulting in poor control authority over the temperature of the parts.

Likelihood: 3 – Default without further analysis

Consequence: 3

Rationale and potential mitigation: The effectiveness of the system (internal temperature gradients) has not been fully analysed. The design may require additional radiator mass or internal heat pipes to spread heat over the radiator surface. Effects on the temperature control authority related to the detailed spectrometer and detector geometry have yet to be analysed.

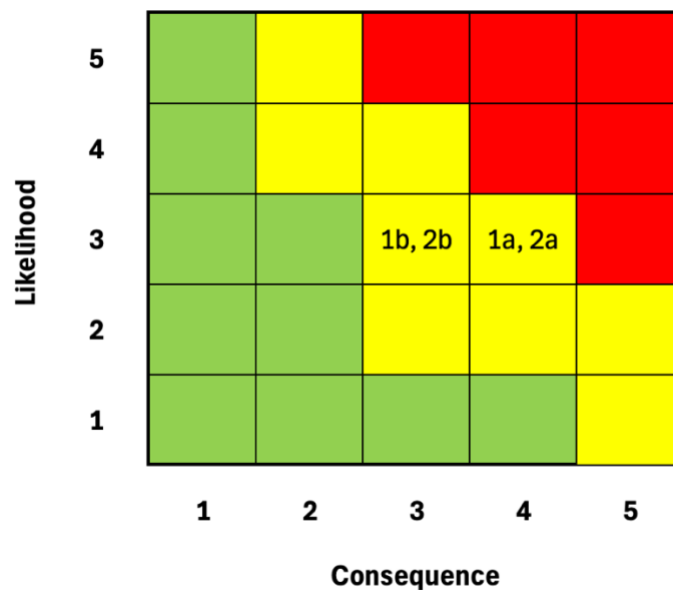


Figure 7-1: Risk fever chart for AquaSat-1, showing the top four technical risks.

8 Relationship between AquaSat-1 and other missions

Figure 8-1 compares AquaSat-1 specifications to those of existing and planned Earth observing missions, focussing on GSD and number of spectral bands relevant to aquatic imaging. Additional comparison parameters for featured missions are detailed in Table 8-1.

AquaSat-1 occupies a unique position in the spatial resolution parameter space, providing access to small water bodies that are not resolved by current ocean-imaging systems. While AquaSat-1 matches land imagers in terms of number of bands and spatial resolution, it benefits from enhanced sensitivity due to its use of ground motion compensation (GMC), effectively increasing its etendue (see Table 8-1). This additional sensitivity enables applications not possible with other systems.

Each mission listed in Figure 8-1 and Table 8-1 is optimised for specific objectives. However, AquaSat-1 stands out as the only mission focused on inland and coastal water applications, meeting the 'H4' criteria—high spatial, spectral, and temporal resolution with high radiometric quality—identified by Muller-Karger (2018) as essential for monitoring inland and coastal ecosystems.

AquaSat-1 complements NASA's upcoming SBG-VSWIR mission, which aims to 'quantify the global distribution of the functional traits, functional types, and composition of vegetation spatially and over time' (JPL, 2024c). Like AquaSat-1, the SBG-VSWIR instrument is an imaging spectrometer, although with a larger spectral range and coarser spatial resolution. SBG will provide global observations to help us understand regional and global trends, but at a longer time step. Following SBG observations, AquaSat-1 will allow us to target societally relevant water bodies with H4 sensing to support science to Earth action needs.

The planned Geostationary Littoral Imaging and Monitoring Radiometer (GLIMR) mission will offer high temporal resolution for dynamic analysis, but focuses primarily on the Gulf of Mexico (NASA, 2024b). Its 1 km spatial resolution does not permit resolution of water supply-relevant water bodies, except for the US Great Lakes.

The Ocean Color Instrument (OCI) of the Plankton, Aerosol, Cloud, ocean Ecosystem (PACE) mission is devoted to the open ocean, and includes identification of potentially harmful algal blooms as an objective (NASA, 2024c). Like GLIMR, PACE provides rapid revisit, but with a spatial resolution unsuitable for inland and coastal waters.

In summary, AquaSat-1 provides unique complementarity to the program of record by advancing H4 requirements in remote sensing. A full suite of missions monitoring land and oceans with a variety of capabilities is crucial to understand the dynamics of our changing planet.

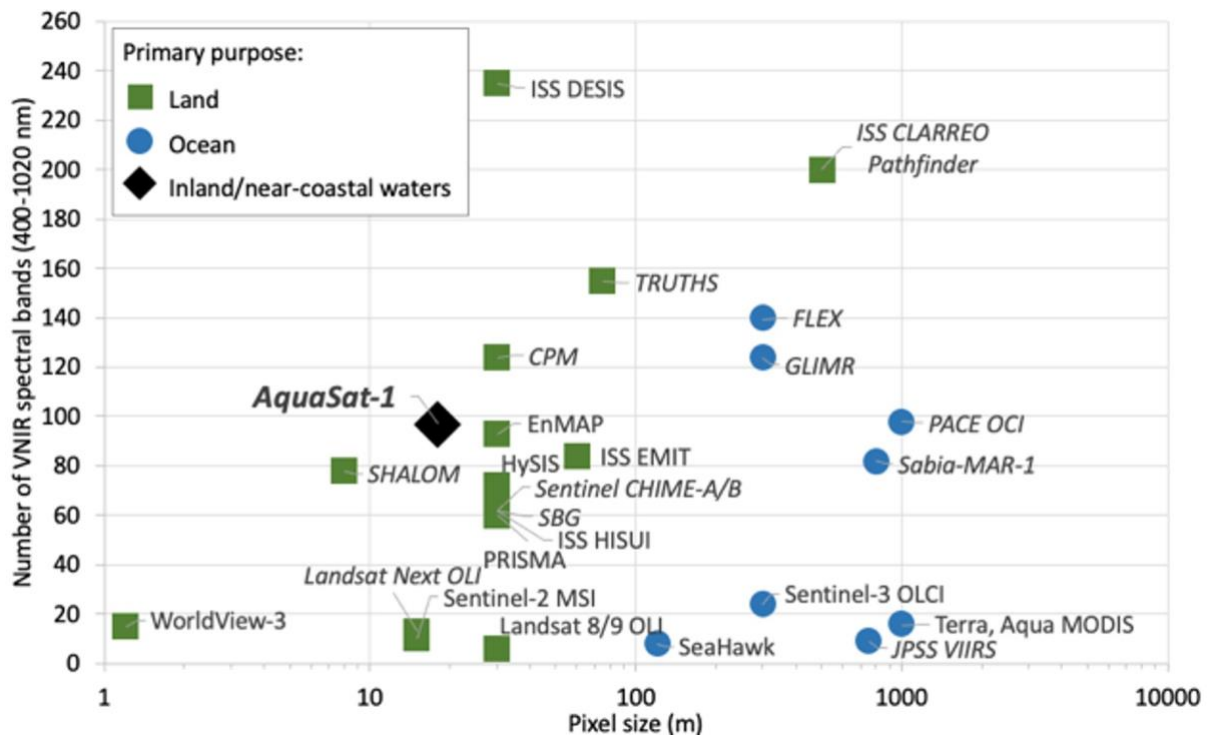


Figure 8-1: AquaSat-1 is the only mission concept primarily designed for inland and near-coastal waters (so far), with a spatial resolution 1-2 orders of magnitude higher than current/planned ocean imagers. The concept provides high spectral resolution across the full VNIR range, allowing discrimination of variables not possible with multispectral imagers. The combination of high optical throughput, tailored concept of operations, and excellent spectral and spatial uniformity result in high SNR at this challenging spatial resolution.

Table 8-1: Comparison of AquaSat-1 specifications with NASA’s upcoming or recently launched aquatic missions.

| Design/specification | AquaSat-1 | SBG-VSWIR | GLIMR | PACE-OCI |
|---|---|--|---|--|
| Primary application | Inland and coastal water quality and aquatic ecosystems | Snow, coastal ecosystems, vegetation health, volcanic activity, and mineralogy | Ocean processes | Ocean and atmosphere carbon dioxide exchange |
| Spatial resolution (m) | 18 | 30 | 300 | 1000 |
| Spectral range (nm) | 350-1050 | 400-2500 | 340-1040 | 350-890 |
| Spectral response function or band width (nm) | 5.6 | 8-12 | 5-40 | 5 |
| Etendue (μm ² .sr) | Pushbroom: 78.5 GMC: 785* | 78.5 | 4.3 | 368 |
| Revisit (days) ** | 4 | 16 | <1 | 1-2 |
| Orbit | Sun-synchronous | Sun-synchronous | Geostationary | Sun-synchronous |
| Coverage | Inland and coastal water target sites (globally, with priority to sites in Australia and western US). | Global | Gulf of Mexico, the southeastern US coastline and Amazon River plume. | Global |
| <p>* GMC operations increase the exposure time per GSD by 10x, and therefore the system sensitivity. We capture this effect as an increase in the etendue.</p> <p>** This is the revisit provided to the coverage area by the satellite orbit. It does not account for cloud cover, sun glint, or target site conflicts (where applicable).</p> | | | | |

9 Conclusions

By developing the AquaSat-1 mission concept, this study has shown that a JPL imaging spectrometer can provide space-based observations that can be used to deliver actionable information on water quality and aquatic ecosystems. The concept is proposed as the first Earth observing mission to demonstrate wide-swath ground motion compensation and ‘H4’ imaging, pushing the boundaries of aquatic measurements from space. Further development of this concept will require alignment with a specific sponsor and flight opportunity, with recommendations for future work detailed in Appendix A.

The development of this mission concept was guided by three end-user driven application objectives: to detect potentially harmful algal blooms, monitor invasive aquatic vegetation, and assess coral reef ecosystem condition. Simulations show that the AquaSat-1 instrument and concept of operations—in terms of spectral, spatial, radiometric and temporal performance—meets the needs of each application objective. This capability addresses significant gaps in current aquatic monitoring technologies. Data collected by AquaSat-1 would be processed by a science data system and analysed through the AquaWatch data analytics platform to provide actionable insights to end-users.

The mission concept aligns with NASA’s Earth Science to Action strategy and addresses the unallocated targeted observable on Aquatic-Coastal Biogeochemistry, specified in the most recent US National Academies Decadal Survey for Earth Sciences and Applications from Space (ESAS 2018). AquaSat-1 requirements are traceable to goals of CSIRO’s AquaWatch program, NASA’s WWAO, and four ‘important’ and ‘most important’ ESAS 2018 objectives.

The AquaSat-1 instrument is a state-of-the-art VNIR imaging spectrometer, which builds on the heritage of JPL’s AVIRIS, EMIT, CPM, and CRISM instruments. The challenging combination of high spatial, spectral, and temporal resolution, as well as high radiometric quality is achieved through a tailored concept of operations, high optical throughput, and excellent spectral and spatial uniformity. The satellite platform required to support the concept of operations and instrument is low risk with no significant development activities needed.

The AquaSat-1 mission concept is both cross-sectoral and highly relevant for societal applications and science priorities. Current involvement of Australia and the US, with growing international interest, underscores the mission’s global relevance and potential for widespread impact. Leveraging international collaboration and cutting-edge technology, AquaSat-1 establishes a next-generation capability for space-based water quality and aquatic ecosystem monitoring to address local, regional, and global needs.

10 References

- Adjovu GE, Stephen H and Ahmad S (2023) Spatial and temporal dynamics of key water quality parameters in a thermal stratified lake ecosystem: the case study of Lake Mead. *Earth* 4(3), 461-502.
- Allen GH and Pavelsky TM (2018) Global extent of rivers and streams. *Science* 361(6402), 585-588.
- Altenau EH, Pavelsky TM, Durand MT, Yang X, Frasson RPdM and Bendezu L (2021) The Surface Water and Ocean Topography (SWOT) Mission River Database (SWORD): A global river network for satellite data products. *Water Resources Research* 57(7), e2021WR030054.
- ANZECC A (2000) Australian and New Zealand guidelines for fresh and marine water quality, Volume 1. Australian and New Zealand Environment and Conservation Council and Agriculture and Resource Management Council of Australia and New Zealand, Canberra.
- Asner GP, Vaughn NR, Heckler J, Knapp DE, Balzotti C, Shafron E, Martin RE, Neilson BJ and Gove JM (2020) Large-scale mapping of live corals to guide reef conservation. *Proceedings of the National Academy of Sciences* 117(52), 33711-33718. DOI: doi:10.1073/pnas.2017628117.
- Australian Government (2024a) About: National water quality management strategy. Viewed 1 June 2024, <[>](https://www.waterquality.gov.au/about#:~:text=The%20purpose%20of%20the%20NWQMS,and%20urban%20communities%2C%20and%20industry.>>.</p><p>Australian Government (2024b) Australian and New Zealand guidelines for fresh and marine water quality. Viewed 1 June 2024, <<a href=).
- Beck MW, Losada IJ, Menéndez P, Reguero BG, Díaz-Simal P and Fernández F (2018) The global flood protection savings provided by coral reefs. *Nature communications* 9(1), 2186. DOI: 10.1038/s41467-018-04568-z.
- Bolch EA, Hestir EL and Khanna S (2021) Performance and feasibility of drone-mounted imaging spectroscopy for invasive aquatic vegetation detection. *Remote Sensing* 13(4), 582.
- Bolch EA, Santos MJ, Ade C, Khanna S, Basinger NT, Reader MO and Hestir EL (2020) Remote detection of invasive alien species. In: Cavender-Bares J, Gamon JA and Townsend PA (eds) *Remote Sensing of Plant Biodiversity*. Springer International Publishing, Cham, 267-307.
- Bouvet M, Thome K, Berthelot B, Bialek A, Czapla-Myers J, Fox NP, Goryl P, Henry P, Ma L and Marcq S (2019) RadCalNet: A radiometric calibration network for Earth observing imagers operating in the visible to shortwave infrared spectral range. *Remote Sensing* 11(20), 2401.

- Boyden J, Wurm P, Joyce KE and Boggs G (2019) Spatial dynamics of invasive para grass on a monsoonal floodplain, Kakadu National Park, Northern Australia. *Remote Sensing* 11(18), 2090.
- Bruegge CJ, Arnold GT, Czaplá-Myers J, Dominguez R, Helmlinger MC, Thompson DR, Van den Bosch J and Wenny BN (2021) Vicarious calibration of eMAS, AirMSPI, and AVIRIS sensors during FIREX-AQ. *IEEE Transactions on Geoscience and Remote Sensing* 59(12), 10286-10297.
- CEOS (2018) Feasibility study for an aquatic ecosystem Earth observing system. CSIRO, Canberra, Australia.
- Convention on Wetlands (2021) Global wetland outlook: Special edition 2021. Secretariat of the Convention on Wetlands Gland, Switzerland, Gland, Switzerland.
- Cruse L and Gillespie R (2008) The impact of water quality and water level on the recreation values of Lake Hume. *Australasian Journal of Environmental Management* 15(1), 21-29.
- CSIRO (2023) AquaWatch Australia science, technology and implementation roadmap.
- CSIRO (2024) AquaWatch Australia. Viewed 15 August 2024, <<https://www.csiro.au/en/about/challenges-missions/aquawatch>>.
- Dekker AG and MacLeod A (2021) AquaWatch Australia end-user consultation report. CSIRO and SmartSat CRC, Canberra, Australia. <<https://smartsatcrc.com/smartsat-publications/technical-report-aqw-2-end-user-consultation-report/>>.
- Dierssen H, McManus GB, Chlus A, Qiu D, Gao B-C and Lin S (2015) Space station image captures a red tide ciliate bloom at high spectral and spatial resolution. *Proceedings of the National Academy of Sciences* 112(48), 14783-14787. DOI: doi:10.1073/pnas.1512538112.
- Dierssen HM, Ackleson SG, Joyce KE, Hestir EL, Castagna A, Lavender S and McManus MA (2021) Living up to the hype of hyperspectral aquatic remote sensing: science, resources and outlook. *Frontiers in Environmental Science* 9. DOI: 10.3389/fenvs.2021.649528.
- Drayson N, Anstee J, Botha H, Kerrisk G, Ford P, Wojtasiewicz B, Clementson L, McLaughlin J and Hutton M (2022) Australian aquatic bio-optical dataset with applications for satellite calibration, algorithm development and validation. *Data in Brief* 44, 108489. DOI: 10.1016/j.dib.2022.108489.
- Edalat MM and Stephen H (2019) Socio-economic drought assessment in Lake Mead, USA, based on a multivariate standardized water-scarcity index. *Hydrological sciences journal* 64(5), 555-569.
- Emery-Butcher HE, Beatty SJ and Robson BJ (2020) The impacts of invasive ecosystem engineers in freshwaters: A review. *Freshwater Biology* 65(5), 999-1015.
- European Commission (2023) Complete ERA5 global atmospheric reanalysis. Viewed 1 June 2024, <<https://cds.climate.copernicus.eu/cdsapp#!/dataset/reanalysis-era5-complete?tab=overview>>.

- Feng D, Gleason CJ, Lin P, Yang X, Pan M and Ishitsuka Y (2021) Recent changes to Arctic river discharge. *Nature communications* 12(1), 6917.
- Feng D, Gleason CJ, Yang X and Pavelsky TM (2019) Comparing discharge estimates made via the BAM algorithm in high-order Arctic rivers derived solely from optical CubeSat, Landsat, and Sentinel-2 data. *Water Resources Research* 55(9), 7753-7771.
- Fernandes MR, Aguiar FC, Silva JMN, Ferreira MT and Pereira JMC (2013) Spectral discrimination of giant reed (*Arundo donax* L.): A seasonal study in riparian areas. *ISPRS Journal of Photogrammetry and Remote Sensing* 80, 80-90. DOI: 10.1016/j.isprsjprs.2013.03.007.
- Frasson RPD, Pavelsky TM, Fonstad MA, Durand MT, Allen GH, Schumann G, Lion C, Beighley RE and Yang X (2019) Global relationships between river width, slope, catchment area, meander wavelength, sinuosity, and discharge. *Geophysical Research Letters* 46(6), 3252-3262.
- Frasson RPM, Ardila DR, Pease J, Hestir E, Bright C, Carter N, Dekker AG, Thompson DR, Green RO and Held A (2024) The impact of spatial resolution on inland water quality monitoring from space. *Environmental Research Communications*.
- GBRMPA (2013) Coastal ecosystems management-case study: water management. Townsville.
- GEOS (2014) The GEOSS water strategy: From observations to decisions. The Japan Aerospace Exploration Agency, Tokyo, Japan.
<https://ceos.org/document_management/Ad_Hoc_Teams/WSIST/WSIST_GEOSS-Water-Strategy-Full-Report_Jan2014.pdf>.
- Gleason CJ and Smith LC (2014) Toward global mapping of river discharge using satellite images and at-many-stations hydraulic geometry. *Proceedings of the National Academy of Sciences* 111(13), 4788-4791.
- Gleason CJ, Smith LC and Lee J (2014) Retrieval of river discharge solely from satellite imagery and at-many-stations hydraulic geometry: Sensitivity to river form and optimization parameters. *Water Resources Research* 50(12), 9604-9619.
- Green RO, Sen A, Pearson JC, Mouroulis P, Patel S, Sullivan P, Werne T, Brenner M, McKinley I, Liggett E, Rodriguez J, Eastwood M, Smith ST, Diaz E, Bennett M, Pollock R and Walch M (2022) Surface Biology and Geology (SBG) visible to short wavelength infrared (VSWIR) wide swath instrument concept. *IEEE Aerospace Conference*.
- Guanter L, Kaufmann H, Segl K, Foerster S, Rogass C, Chabrilat S, Kuester T, Hollstein A, Rossner G and Chlebek C (2015) The EnMAP spaceborne imaging spectroscopy mission for Earth observation. *Remote Sensing* 7(7), 8830-8857.
- Guy-Haim T, Lyons DA, Kotta J, Ojaveer H, Queirós AM, Chatzinikolaou E, Arvanitidis C, Como S, Magni P and Blight AJ (2018) Diverse effects of invasive ecosystem engineers on marine biodiversity and ecosystem functions: A global review and meta-analysis. *Global Change Biology* 24(3), 906-924.
- Hagemann M, Gleason C and Durand M (2017) BAM: Bayesian AMHG-Manning inference of discharge using remotely sensed stream width, slope, and height. *Water Resources Research* 53(11), 9692-9707.

- Hannoun D and Tietjen T (2023) Lake management under severe drought: Lake Mead, Nevada/Arizona. *JAWRA Journal of the American Water Resources Association* 59(2), 416-428.
- Hardy FJ, Bouchard D, Burghdoff M, Hanowell R, LeDoux B, Preece E, Tuttle L and Williams G (2016) Education and notification approaches for harmful algal blooms (HABs), Washington State, USA. *Harmful Algae* 60, 70-80. DOI: 10.1016/j.hal.2016.10.004.
- Havel JE, Kovalenko KE, Thomaz SM, Amalfitano S and Kats LB (2015) Aquatic invasive species: challenges for the future. *Hydrobiologia* 750, 147-170.
- Hedley JD, Roelfsema CM, Phinn SR and Mumby PJ (2012) Environmental and Sensor Limitations in Optical Remote Sensing of Coral Reefs: Implications for Monitoring and Sensor Design. *Remote Sensing* 4(1), 271-302.
- Hestir E and Dronova I (2023) Remote sensing of primary producers in the Bay–Delta. *San Francisco Estuary and Watershed Science* 20(4).
- Hestir EL, Khanna S, Andrew ME, Santos MJ, Viers JH, Greenberg JA, Rajapakse SS and Ustin SL (2008) Identification of invasive vegetation using hyperspectral remote sensing in the California Delta ecosystem. *Remote Sensing of Environment* 112(11), 4034-4047. DOI: 10.1016/j.rse.2008.01.022.
- Hestir EL, Schoellhamer DH, Greenberg J, Morgan-King T and Ustin SL (2016) The effect of submerged aquatic vegetation expansion on a declining turbidity trend in the Sacramento-San Joaquin River Delta. *Estuaries and Coasts* 39, 1100-1112.
- Hogan JF (2013) Water quantity and quality challenges from Elephant Butte to Amistad. *Ecosphere* 4(1), 1-16.
- Hunter PD, Tyler AN, Présing M, Kovács AW and Preston T (2008) Spectral discrimination of phytoplankton colour groups: The effect of suspended particulate matter and sensor spectral resolution. *Remote Sensing of Environment* 112(4), 1527-1544. DOI: 10.1016/j.rse.2007.08.003.
- IOCCG (2014) Phytoplankton functional types from space. <https://ioccg.org/wp-content/uploads/2018/09/ioccg_report_15_2014.pdf>.
- IWG-HABHRCA (2017) Harmful algal blooms and hypoxia in the Great Lakes research plan and action strategy: An interagency report. National Science and Technology Council. <<https://hab.who.edu/wp-content/uploads/2019/08/Harmful-Algal-Blooms-Report-FINAL-August.2017.pdf>>.
- Jackson N, Cudney D, DiTomaso J, Benefield C, Lee V, Drewitz J, Bossard S, Randall L, Hansen-Winter B and Faber P (2006) Invasive plants of California's wildland.
- Jerram P and Beletic J (2018) Teledyne's high performance infrared detectors for space missions. International Conference on Space Optics — ICSO 2018. International Society for Optics and Photonics, Chania, Greece.
- Jongeling A, Walsh W, Kilzer M, Pugh M, Kobayashi MM, Gayle J, Hawkins D and Kuperman I (2022) A swift approach to a flexible instrument processor. *IEEE Aerospace Conference*.

- JPL (2006) PIA09343: CRISM's first 'targeted' observation of Mars. Viewed 1 June 2024, <<https://photojournal.jpl.nasa.gov/catalog/PIA09343>>.
- JPL (2022) Imaging spectroscopy. Viewed 1 June 2024, <<https://microdevices.jpl.nasa.gov/capabilities/imaging-spectroscopy/>>.
- JPL (2024a) AVIRIS Airborne Visible/Infrared Imaging Spectrometer. Viewed 7 June 2024, <<https://aviris.jpl.nasa.gov/index.html>>.
- JPL (2024b) Earth Surface Mineral Dust Source Investigation (EMIT). Viewed 1 June 2024, <<https://earth.jpl.nasa.gov/emit/>>.
- JPL (2024c) Surface Biology and Geology. Viewed 1 June 2024, <<https://sbg.jpl.nasa.gov/>>.
- JPL and John Hopkins Applied Physics Laboratory (2018) CRISM: Compact Reconnaissance Imaging Spectrometer for Mars. Viewed 1 June 2024, <<http://crism.jhuapl.edu/>>.
- Julien M, Griffiths M and Stanley J (2001) Biological control of water hyacinth 2: The moths *Niphograpta albiguttalis* and *Xubida infusellus*: biologies, host ranges, and rearing, releasing and monitoring techniques for biological control of *Eichhornia crassipes*. Australasian Centre for International Agricultural Research.
- Keller RP, Masoodi A and Shackleton RT (2018) The impact of invasive aquatic plants on ecosystem services and human well-being in Wular Lake, India. *Regional Environmental Change* 18(3), 847-857. DOI: 10.1007/s10113-017-1232-3.
- Khanna S, Gaeta JW, Conrad JL and Gross ES (2023) Multi-year landscape-scale efficacy analysis of fluridone treatment of invasive submerged aquatic vegetation in the Sacramento–San Joaquin Delta. *Biological Invasions* 25(6), 1827-1843. DOI: 10.1007/s10530-023-03013-7.
- Koweek D, Dunbar RB, Rogers JS, Williams GJ, Price N, Mucciarone D and Teneva L (2015) Environmental and ecological controls of coral community metabolism on Palmyra Atoll. *Coral Reefs* 34, 339-351.
- Kravitz J, Matthews M, Lain L, Fawcett S and Bernard S (2021) Potential for high fidelity global mapping of common inland water quality products at high spatial and temporal resolutions based on a synthetic data and machine learning approach. *Frontiers in Environmental Science* 9. DOI: 10.3389/fenvs.2021.587660.
- Kudela RM, Palacios SL, Austerberry DC, Accorsi EK, Guild LS and Torres-Perez J (2015) Application of hyperspectral remote sensing to cyanobacterial blooms in inland waters. *Remote Sensing of Environment* 167, 196-205. DOI: 10.1016/j.rse.2015.01.025.
- Laćan I and Resh VH (2016) A case study in integrated management: Sacramento–San Joaquin Rivers and Delta of California, USA. *Ecohydrology & Hydrobiology* 16(4), 215-228.
- Lain LR, Kravitz J, Matthews M and Bernard S (2023) Simulated inherent optical properties of aquatic particles using the equivalent algal populations (EAP) model. *Scientific Data* 10(1), 412. DOI: 10.1038/s41597-023-02310-z.

- Lawlor MP (2019) A multivariate analysis of the relationship between the water quality conditions and algal species composition of six mountain lakes in the North Cascades, WA, USA.
- Lee CM, Hestir EL, Tufillaro N, Palmieri B, Acuña S, Osti A, Bergamaschi BA and Sommer T (2021) Monitoring turbidity in San Francisco Estuary and Sacramento–San Joaquin delta using satellite remote sensing. *JAWRA Journal of the American Water Resources Association* 57(5), 737-751.
- Lyons MB, Murray NJ, Kennedy EV, Kovacs EM, Castro-Sanguino C, Phinn SR, Acevedo RB, Alvarez AO, Say C, Tudman P, Markey K, Roe M, Canto RF, Fox HE, Bambic B, Lieb Z, Asner GP, Martin PM, Knapp DE, Li J, Skone M, Goldenberg E, Larsen K and Roelfsema CM (2024) New global area estimates for coral reefs from high-resolution mapping. *Cell Reports Sustainability* 1(2), 100015. DOI: 10.1016/j.crsus.2024.100015.
- Macêdo RL, Haubrock PJ, Klippel G, Fernandez RD, Leroy B, Angulo E, Carneiro L, Musseau CL, Rocha O and Cuthbert RN (2024) The economic costs of invasive aquatic plants: A global perspective on ecology and management gaps. *Science of the Total Environment* 908, 168217. DOI: 10.1016/j.scitotenv.2023.168217.
- Madin JS, Baird AH, Bridge TC, Connolly SR, Zawada KJ and Dornelas M (2018) Cumulative effects of cyclones and bleaching on coral cover and species richness at Lizard Island. *Marine Ecology Progress Series* 604, 263-268.
- Malthus T (2024) Radiometric sensitivity requirements for monitoring live coral cover and associated benthic types from space. In Preparation.
- Manolakis DG, Shaw GA and Keshava N (2000) Comparative analysis of hyperspectral adaptive matched filter detectors. *Algorithms for Multispectral, Hyperspectral, and Ultraspectral Imagery VI*. SPIE.
- Matthews MW and Bernard S (2013) Using a two-layered sphere model to investigate the impact of gas vacuoles on the inherent optical properties of *Microcystis aeruginosa*. *Biogeosciences* 10(12), 8139-8157. DOI: 10.5194/bg-10-8139-2013.
- Messenger ML, Lehner B, Grill G, Nedeva I and Schmitt O (2016) Estimating the volume and age of water stored in global lakes using a geo-statistical approach. *Nature communications* 7(1), 13603.
- Moberg F and Folke C (1999) Ecological goods and services of coral reef ecosystems. *Ecological Economics* 29(2), 215-233. DOI: 10.1016/S0921-8009(99)00009-9.
- Moore LB, Bender HA, Bradley CL, Haag JM, Zandbergen S, Green RO and Mouroulis P (2020) Recent developments in tolerancing methods for imaging spectrometers. *Optical System Alignment, Tolerancing, and Verification XIII* 11488, 94-104.
- Morfin O Effects of system conservation on salinity in Lake Mead.
- Morrison TH, Hughes TP, Adger WN, Brown K, Barnett J and Lemos MC (2019) Save reefs to rescue all ecosystems. *Nature* 573(7774), 333-336.
- Mouroulis P and Green RO (2018) Review of high fidelity imaging spectrometer design for remote sensing. *Optical Engineering* 57(4). DOI: 10.1117/1.OE.57.4.040901.

- Muller-Karger FE, Hestir E, Ade C, Turpie K, Roberts DA, Siegel D, Miller RJ, Humm D, Izenberg N and Keller M (2018) Satellite sensor requirements for monitoring essential biodiversity variables of coastal ecosystems. *Ecological applications* 28(3), 749-760.
- Murchie SL, Arvidson RE, Bedini P, Beisser K, Bibring J-P, Bishop J, Boldt JD, Choo TH, Clancy RT, Darlington EH, Marais DD, Espiritu R, Fasold MJ, Fort D, Richard NG, Guinness E, John RH, Hash C, Heffernan KJ, Hemmler J, Heyler GA, Humm DC, Hutchison J, Izenberg NR, Lee RE, Lees J, Lohr DA, Malaret ER, Martin T, Morris RV, Mustard JF, Rhodes EA, Robinson MS, Roush TL, Schaefer ED, Seagrave GG, Silverglate PR, Slavney S, Smith MF, Strohbahn K, Taylor HW, Thompson PL and Tossman BE (2004) CRISM (Compact Reconnaissance Imaging Spectrometer for Mars) on MRO (Mars Reconnaissance Orbiter). *Proc.SPIE*.
- Murray–Darling Basin Authority (2023) Hume Dam. Viewed 1 June 2024, <<https://www.mdba.gov.au/water-management/infrastructure/hume-dam>>.
- Murray–Darling Basin Authority (MDBA) (2019) Independent assessment of the 2018-19 fish deaths in the lower Darling: Final report. <<https://www.mdba.gov.au/publications-and-data/publications/response-fish-deaths-lower-darling>>.
- NASA (2017) S3001: Guidelines for risk management. <https://www.nasa.gov/wp-content/uploads/2015/10/s3001_guidelines_for_risk_management_-_ver_g_-_10-25-2017.pdf>.
- NASA (2020) Technology readiness assessment best practices guide. <<https://ntrs.nasa.gov/citations/20205003605>>.
- NASA (2023) NASA systems engineering handbook. <<https://www.nasa.gov/reference/3-3-project-pre-phase-a-concept-studies/>>.
- NASA (2024a) Earth science to action strategy 2024-2034. Mary W. Jackson NASA Headquarters, Washington DC, 20546. <https://assets.science.nasa.gov/content/dam/science/esd/earth-science-division/earth-science-to-action/Earth_Science_to_Action_Strategy_2024-2034_May_24.pdf>.
- NASA (2024b) Geosynchronous Littoral Imaging and Monitoring Radiometer (GLIMR). Viewed 1 June 2024, <<https://science.nasa.gov/mission/glimr/>>.
- NASA (2024c) Plankton, Aerosol, Cloud, ocean Ecosystem (PACE). Viewed 1 June 2024, <<https://pace.oceansciences.org/>>.
- NASA Goddard Space Flight Centre (2023) NASA systems engineering processes and requirements updated w/change 2. <https://nodis3.gsfc.nasa.gov/displayDir.cfm?Internal_ID=N_PR_7123_001D_&page_name=AppendixG>.
- NASA WWAO (2020) Columbia River Basin needs assessment report: Tools for managing a precious resource. <<https://wwao.jpl.nasa.gov/documents/80/Water-Needs-Columbia-Report-2021.pdf>>.

- National Academies of Sciences E, and Medicine, (2018) *Thriving on a changing planet: A decadal strategy for Earth observation from space*. The National Academies Press, Washington, DC.
- NHMRC and NRMCC (2011) *Australian drinking water guidelines paper 6: National water quality management strategy*. National Health and Medical Research Council, National Resource Management Ministerial Council, Commonwealth of Australia, Canberra. <<https://www.nhmrc.gov.au/sites/default/files/documents/reports/aust-drinking-water-guidelines.pdf>>.
- Obura DO, Aeby G, Amornthammarong N, Appeltans W, Bax N, Bishop J, Brainard RE, Chan S, Fletcher P, Gordon TAC, Gramer L, Gudka M, Halas J, Hendee J, Hodgson G, Huang D, Jankulak M, Jones A, Kimura T, Levy J, Miloslavich P, Chou LM, Muller-Karger F, Osuka K, Samoily M, Simpson SD, Tun K and Wongbusarakum S (2019) *Coral Reef Monitoring, Reef Assessment Technologies, and Ecosystem-Based Management*. *Frontiers in Marine Science* 6. DOI: 10.3389/fmars.2019.00580.
- Perna C, Cappo M, Pusey B, Burrows D and Pearson RG (2012) *Removal of aquatic weeds greatly enhances fish community richness and diversity: An example from the Burdekin River floodplain, tropical Australia*. *River Research and Applications* 28(8), 1093-1104.
- Peterson MA, Collavo A, Ovejero R, Shivrain V and Walsh MJ (2018) *The challenge of herbicide resistance around the world: a current summary*. *Pest Management Science* 74(10), 2246-2259. DOI: 10.1002/ps.4821.
- Pimentel D, Lach L, Zuniga R and Morrison D (2000) *Environmental and economic costs of nonindigenous species in the United States*. *BioScience* 50(1), 53-65.
- Pitcairn MJ, Pratt PD, Villegas B, Popescu V, Borkent C and Reddy AM (2021) *Biological control of water hyacinth, Pontederia crassipes (C. Mart.) Solms (Pontederiaceae), in California: Release and re-distribution of biological control agents 1987–2006*. *The Pan-Pacific Entomologist* 97(2), 55-66.
- Ramsar (2023) *List of wetlands of international importance*.
- Rasmussen N, Conrad JL, Green H, Khanna S, Wright H, Hoffmann K, Caudill J and Gilbert P (2022) *Efficacy and Fate of Fluridone Applications for Control of Invasive Submersed Aquatic Vegetation in the Estuarine Environment of the Sacramento-San Joaquin Delta*. *Estuaries and Coasts* 45(7), 1842-1860. DOI: 10.1007/s12237-022-01079-5.
- Reid AJ, Carlson AK, Creed IF, Eliason EJ, Gell PA, Johnson PT, Kidd KA, MacCormack TJ, Olden JD and Ormerod SJ (2019) *Emerging threats and persistent conservation challenges for freshwater biodiversity*. *Biological reviews* 94(3), 849-873.
- Richardson RJ (2008) *Aquatic plant management and the impact of emerging herbicide resistance issues*. *Weed Technology* 22(1), 8-15.
- Rodgers CD (2000) *Inverse methods for atmospheric sounding: Theory and practice*. World scientific.
- Roelfsema C, Kovacs EM, Markey K, Vercelloni J, Rodriguez-Ramirez A, Lopez-Marcano S, Gonzalez-Rivero M, Hoegh-Guldberg O and Phinn SR (2021) *Benthic and coral reef*

- community field data for Heron Reef, southern Great Barrier Reef, Australia, 2002–2018. *Scientific Data* 8(1), 84.
- Roelfsema CM and Phinn SR (2017) Spectral reflectance library of healthy corals, bleached corals and other benthic features in Fiji. PANGAEA.
- Salau R (1995) Para grass in Kakadu National Park. Unpublished paper presented to Natural Resource Management, Australian Nature Conservation Agency.
- Sandin SA, Smith JE, DeMartini EE, Dinsdale EA, Donner SD, Friedlander AM, Konotchick T, Malay M, Maragos JE and Obura D (2008) Baselines and degradation of coral reefs in the Northern Line Islands. *PloS one* 3(2), e1548.
- Santos MJ, Khanna S, Hestir EL, Greenberg JA and Ustin SL (2016) Measuring landscape-scale spread and persistence of an invaded submerged plant community from airborne remote sensing. *Ecological applications* 26(6), 1733-1744. DOI: 10.1890/15-0615.
- Schaeffer BA and Myer MH (2020) Resolvable estuaries for satellite derived water quality within the continental United States. *Remote Sensing Letters* 11(6), 535-544.
- Seelos FP, Seelos KD, Murchie SL, Novak MAM, Hash CD, Morgan MF, Arvidson RE, Aiello J, Bibring J-P, Bishop JL, Boldt JD, Boyd AR, Buczkowski DL, Chen PY, Clancy RT, Ehlmann BL, Frizzell K, Hancock KM, Hayes JR, Heffernan KJ, Humm DC, Itoh Y, Ju M, Kochte MC, Malaret E, McGovern JA, McGuire P, Mehta NL, Moreland EL, Mustard JF, Nair AH, Núñez JI, O'Sullivan JA, Packer LL, Poffenbarger RT, Poulet F, Romeo G, Santo AG, Smith MD, Stephens DC, Toigo AD, Viviano CE and Wolff MJ (2024) The CRISM investigation in Mars orbit: Overview, history, and delivered data products. *Icarus* 419, 115612. DOI: 10.1016/j.icarus.2023.115612.
- Sequoia Scientific (2024) HydroLight. Viewed 1 August 2024, <<https://www.sequoiasci.com/product/hydrolight/>>.
- SmartSat (2021) Preliminary concept study for the satellite segment of AquaWatch Australia. SmartSat, Adelaide, Australia.
- Smith JE, Brainard R, Carter A, Grillo S, Edwards C, Harris J, Lewis L, Obura D, Rohwer F and Sala E (2016) Re-evaluating the health of coral reef communities: Baselines and evidence for human impacts across the central Pacific. *Proceedings of the Royal Society B: Biological Sciences* 283(1822), 20151985.
- Souter D, Planes S, Wicquart J, Logan M, Obura D and Staub F (2021) Status of coral reefs of the world: 2020 report.
- Sullivan P, Foster E, Green RO, Mckinley I, Nadgouda S, Shah N, Torousian S, Cardone J and Hellings J (2023) A comparison of imaging subsystems for analog- versus digital-output detector arrays. *IEEE Aerospace Conference*.
- Taitus Software (2024) SaVoir. Viewed 1 June 2024.
- Tanner J, Bailleul F, Bryars S, Doubell M, Foster N, Gaylard S, Gillanders B, Goldsworthy S, Huveneers C and James C (2019) Potential social, economic and ecological indicators for integrated ecosystem assessment of Spencer Gulf. Goyder Institute for Water Research Technical Report Series(19/32).

- Tanner JE and Connell JH (2022) Coral community data Heron Island Great Barrier Reef 1962–2016. *Scientific Data* 9(1), 617.
- Tebbett SB, Morais J and Bellwood DR (2022) Spatial patchiness in change, recruitment, and recovery on coral reefs at Lizard Island following consecutive bleaching events. *Marine Environmental Research* 173, 105537.
- Thompson DR, Brodrick PG, Cawse-Nicholson K, Dana Chadwick K, Green RO, Poulter B, Serbin S, Shiklomanov AN, Townsend PA and Turpie KR (2021) Spectral fidelity of Earth's terrestrial and aquatic ecosystems. *Journal of Geophysical Research: Biogeosciences* 126(8), e2021JG006273.
- Thompson DR, Green RO, Bradley C, Brodrick PG, Mahowald N, Dor EB, Bennett M, Bernas M, Carmon N and Chadwick KD (2024) On-orbit calibration and performance of the EMIT imaging spectrometer. *Remote Sensing of Environment* 303, 113986.
- Thompson DR, Natraj V, Green RO, Helmlinger MC, Gao B-C and Eastwood ML (2018) Optimal estimation for imaging spectrometer atmospheric correction. *Remote Sensing of Environment* 216, 355-373. DOI: 10.1016/j.rse.2018.07.003.
- UN (2023) The sustainable development goals report 2023: Special edition. <<https://unstats.un.org/sdgs/report/2023/The-Sustainable-Development-Goals-Report-2023.pdf>>.
- UN Department of Economic and Social Affairs (2024) Sustainable development: The 17 goals. <<https://sdgs.un.org/goals>>.
- UN Environment Programme (2024) Global Biodiversity Framework: 2030 targets (with guidance notes). <<https://www.cbd.int/gbf/targets>>.
- UN-Water (2021) Summary progress update 2021—SDG 6—water and sanitation for all. <<https://www.unwater.org/publications/summary-progress-update-2021-sdg-6-water-and-sanitation-all>>.
- Underwood E, Ustin S and DiPietro D (2003) Mapping nonnative plants using hyperspectral imagery. *Remote Sensing of Environment* 86(2), 150-161. DOI: 10.1016/S0034-4257(03)00096-8.
- UNESCO World Heritage Convention (2024) World heritage list. <<https://whc.unesco.org/en/list/>>.
- UNSW Canberra Space (2024) AquaSat-1 platform evaluation. <www.unsw.edu.au/canberra/our-research/our-facilities/australian-national-concurrent-design-facility>.
- US EPA (2015) Recommendations for public water systems to manage cyanotoxins in drinking water.
- USGS (2023) ECCOE test sites catalog.
- Villamagna A and Murphy B (2010) Ecological and socio-economic impacts of invasive water hyacinth (*Eichhornia crassipes*): A review. *Freshwater Biology* 55(2), 282-298.
- WHO (2021a) Guidelines on recreational water quality, Volume 1: Coastal and fresh waters. World Health Organization.

- WHO (2021b) Toxic cyanobacteria in water: A guide to their public health consequences, monitoring and management. CRC Press.
- WHO (2022) Guidelines for drinking-water quality: Fourth edition incorporating the first and second addenda.
- Wildman RA, Pratson LF, DeLeon M and Hering JG (2011) Physical, chemical, and mineralogical characteristics of a reservoir sediment delta (Lake Powell, USA) and implications for water quality during low water level. *Journal of environmental quality* 40(2), 575-586.
- Wolf P, Rößler S, Schneider T and Melzer A (2013) Collecting in situ remote sensing reflectances of submersed macrophytes to build up a spectral library for lake monitoring. *European Journal of Remote Sensing* 46(1), 401-416. DOI: 10.5721/EuJRS20134623.
- WWAO N (2016) Western water rapid needs assessment report: Tools for managing a precious resource. <<https://wwao.jpl.nasa.gov/documents/82/Western-Water-Rapid-Needs-Assessment-2016.pdf>>.
- Yang C and Everitt JH (2010) Mapping three invasive weeds using airborne hyperspectral imagery. *Ecological Informatics* 5(5), 429-439. DOI: 10.1016/j.ecoinf.2010.03.002.
- Zandbergen SR, Duren R, Giuliano P, Green RO, Haag JM, Moore LB, Shaw L and Mouroulis P (2022) Optical design of the Carbon Plume Mapper (CPM) imaging spectrometer. *SPIE Optical Engineering + Applications*.

Appendix A Recommendations for future work

The following are the recommendations for future work to follow on from this study.

- Requirement development:
 - Define requirements for the ground data system and effective delivery of actionable information to end-users.
 - Analyse the impact of decreasing the SRF (increasing the spectral resolution) on the application objectives. Explore spectral resolution requirements for challenging phytoplankton functional type situations (e.g., yellow tides, red tides) **(AO1)**.
 - Given the role of tides, analyse the impact of temporal sampling on observations of estuarine and coastal targets **(AO1, AO2, AO3)**.
 - Analyse the detectability of submerged vegetation feasibility on the challenging turbidity situations typical of inland waters **(AO2)**.
 - Model the impact of ocean floor slopes on the detectability of different types of benthic coverage. Explore the impact of the depth detectability limit on the area of coral reefs covered. **(AO3)**.
- Payload design:
 - Perform additional instrument iterations to reduce instrument size.
 - Given that water temperature is important for water managers, perform a trade study on the scientific, technical, and programmatic impact of the addition of a thermal radiometer.
 - Perform a trade study on the impact of a 1 μm vs 2.5 μm wavelength cutoffs for distinguishing IAV functional types.
- Concept of operations:
 - Develop a full design reference mission, including all potential targets over one year of observations.
 - Perform glint avoidance analysis to determine impact of sunglint on effective revisit.
 - Perform a complete analysis of the compliance with the latency requirement.
- Implementation:
 - Perform validation of GMC process and its applicability to extract water quality metrics either from an airborne platform or from space.
 - Generate example data products (based on airborne, PACE, or EMIT datasets) to demonstrate algorithm maturity.

Appendix B Additional revisit and cloud cover analysis

In the main text of this report, we presented an analysis of imaging opportunities and revisit times based on revisit means. Here we expand this analysis to consider the distributions in these quantities.

B.1 Distribution of imaging opportunities

The results presented in Figure B-1 show the distribution of the imaging opportunities presented Section 4.3.4. This figure shows the probability that a given revisit time will occur. The number of clear imaging opportunities that occur in 1 year for each target site for both a 1-satellite and 4-satellite constellation are shown in the subfigure headings. It should be noted that each subfigure bar has a width of 5 days.

The distribution of revisit time for each target site for both a 1-satellite and 4-satellite constellation is observed (Figure B-1). There is significant site variation in the distribution of revisit time, notably between Sacramento Delta and Palmyra Atoll. Increasing the constellation size from a 1-satellite to 4-satellite constellation increases the probability that a shorter revisit time occurs.

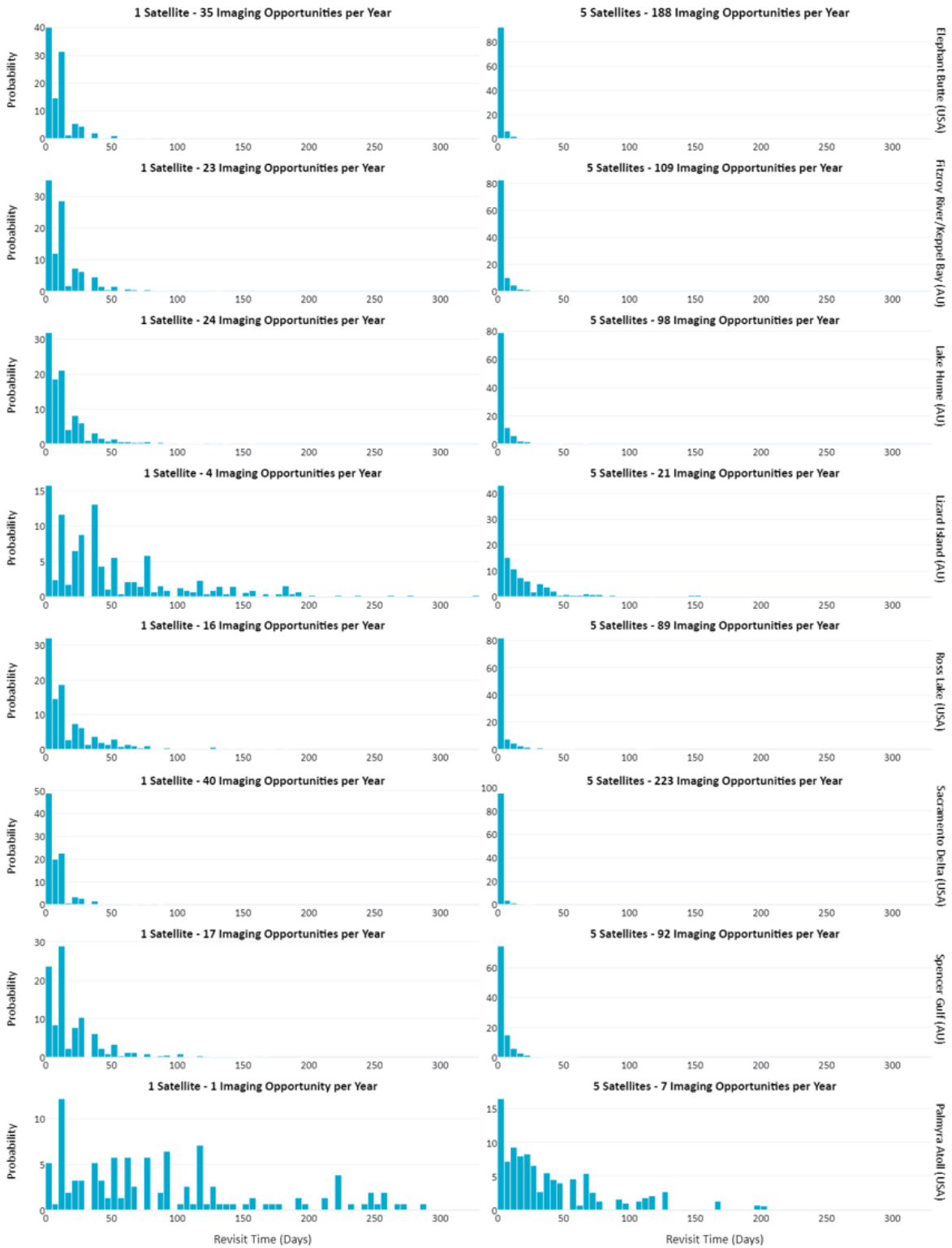


Figure B-1: Probability distribution for 1 and 5 satellite constellations. This plot shows the probability of a given revisit time occurring and presents the distribution of revisits for all target sites for a 1-satellite and a 4-satellite constellation. Each bar shown in this figure has a width of 5 days. This figure is presented as supplementary information to Section 4.3.4.

B.2 Temporal requirement probability

We generated a simulated dataset with information regarding the amount of time between consecutive observations for each site. This data was analysed through a statistical tool called the Empirical Cumulative Distribution Function (ECDF). The ECDF shows the cumulative probability of the revisit time being less than or equal to a certain value. For example, if the ECDF curve passes through the point (30 days, 0.8), it means there is an 80% probability that the revisit time for that site will be 30 days or less.

To relate this back to the temporal requirements, the results at specific points on the ECDF curve are summarised in Table B-1 and Figure B-2 for all target sites for a 1-satellite and 5-satellite constellation. These are presented for weekly (or better), monthly (or better) and quarterly (or better) revisit timeframes and show the probability of passes occurring with this frequency of revisit time.

For example, the probability of a monthly or better revisit for Spencer Gulf with one satellite is 81%. This means that, if we pick one month at random, there is an 81% chance that the satellite will observe the site at least once during that month. Over multiple months, this probability indicates consistent performance. Over the course of 10 months, we would expect the satellite to have made at least 8 observations with a revisit time of 1 month or better.

ASI-MSL-12 (see Section 3.6) states that the temporal requirement is monthly or better for HAB targets, monthly or better for IAV targets, seasonal or better for coral targets. The probability of meeting the requirement with a 1-satellite constellation is approximately 80% or better (except for Palmyra Atoll), and with a 5-satellite constellation it is approximately 99% or higher (except for Palmyra Atoll).

Table B-1: Cloud-free image probability for all target sites for a 1-satellite and 5-satellite constellation for weekly, monthly and quarterly timeframes.

| Target site | Cloud-free image probability (1 satellite) | | | Cloud-free image probability (5 satellites) | | |
|----------------------------------|--|----------|------------|---|----------|------------|
| | ≤weekly | ≤monthly | ≤quarterly | ≤weekly | ≤monthly | ≤quarterly |
| Sacramento Delta (US) | 49 | 98 | 100 | 97 | 100 | 100 |
| Elephant Butte (US) | 40 | 96 | 100 | 97 | 100 | 100 |
| Fitzroy River / Keppel Bay (Aus) | 35 | 90 | 100 | 90 | 99 | 100 |
| Lake Hume (Aus) | 42 | 89 | 100 | 87 | 99 | 100 |
| Spencer Gulf (Aus) | 24 | 81 | 97 | 85 | 99 | 100 |
| Ross Lake (US) | 34 | 81 | 97 | 85 | 98 | 100 |
| Lizard Island (Aus) | 16 | 47 | 84 | 54 | 86 | 99 |
| Palmyra Atoll (US) | 5.8 | 26 | 62 | 22 | 56 | 87 |

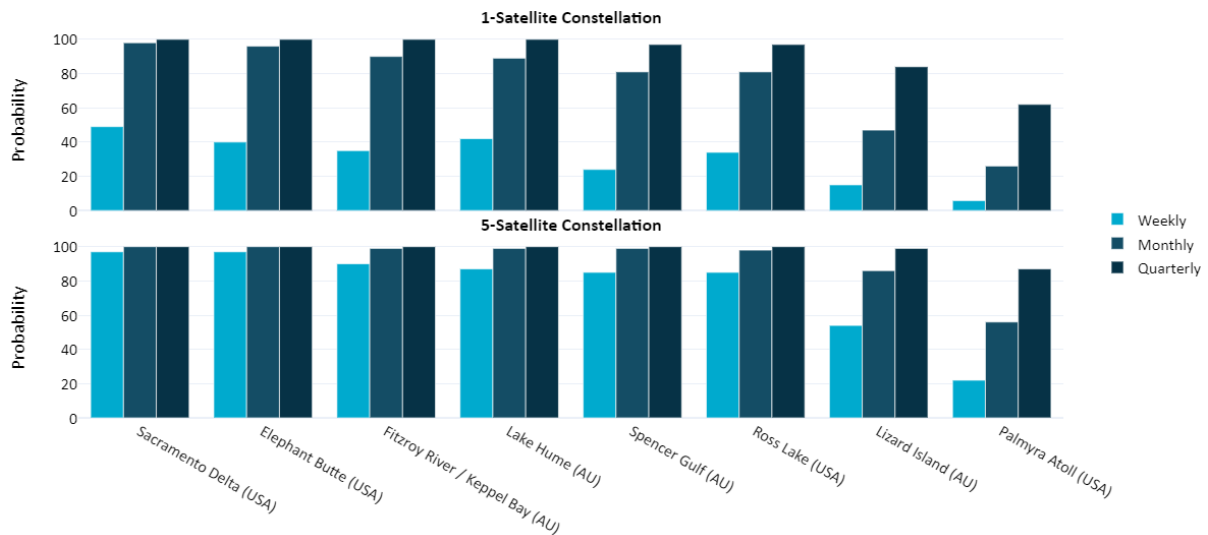


Figure B-2: The probability of a cloud-free image acquisition for weekly, monthly, and quarterly timeframes. 1-satellite (top) and 5-satellites (bottom).

B.3 Hourly distribution of revisits

Figure B-3 is a time-differentiated representation of a 4-satellite constellation imaging opportunities subplot for Sacramento Delta (Lizard Island 5-satellite constellation imaging opportunities subplot is shown in Figure 4-6). The figure provides an example case to illustrate why the mean revisit goes to < 1 day in Table 4-6.

For Sacramento Delta with a 4-satellite constellation, there are multiple satellite passes within quick succession on 13 January 2024, with the third satellite in the constellation (AquaSat-3) having an imaging opportunity at 12:18 and the fourth satellite in the constellation (AquaSat-4) having an imaging opportunity at 12:41. This is because the target site will occasionally fall in a location that is in proximity of two of the satellites in the constellation on the same day.

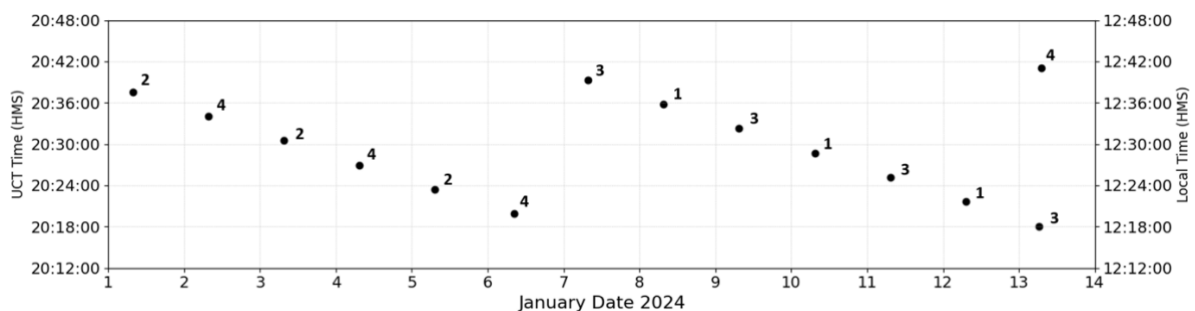


Figure B-3: Time resolved imaging opportunities for Sacramento Delta with a 4-satellite constellation. The left-hand-side vertical axis shows the pass time in Coordinated Universal Time (UTC), and the right-hand-side vertical axis shows the pass time in local time (PST). The numbered labels indicate which satellite in the constellation has the imaging opportunity.

Quick succession passes like those seen in Figure B-3 are observed for constellations of two or more satellites. This is due to the nature of the constellation design, where all the satellites are orbiting in the same orbital plane.

Therefore, the mean revisit shown in Table 4-6 is less than 1 day for a 5-satellite constellation as the number of quick succession revisits increases. It is useful to observe the maximum revisit time as well to understand that daily coverage has been achieved, which is also presented in Table 4-6.

B.4 Clear day definition sensitivity

Increasing the percentage clear threshold from the $\leq 10\%$ total cloud cover used Section 4.3.4 to higher values significantly impacts the results. Figure B-4 illustrates the substantial increase in number of days per year classified as ‘clear’ for each target site as the percentage clear threshold values are raised to $\leq 20\%$, 30% , 40% , 50% , and $> 50\%$.

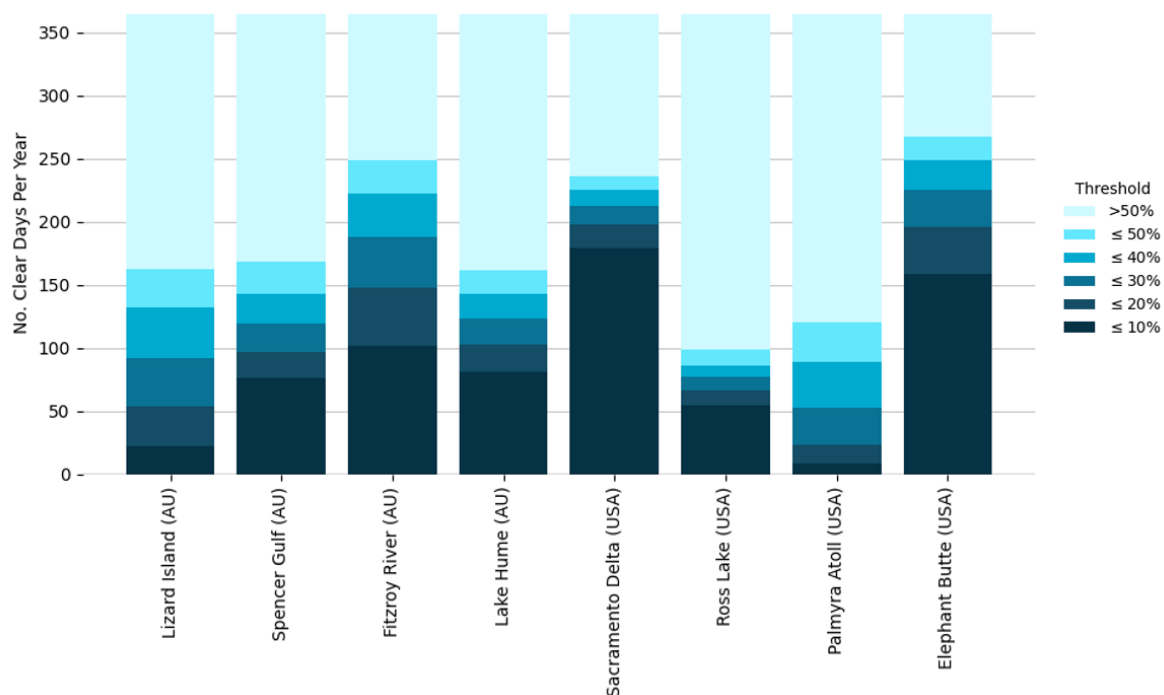
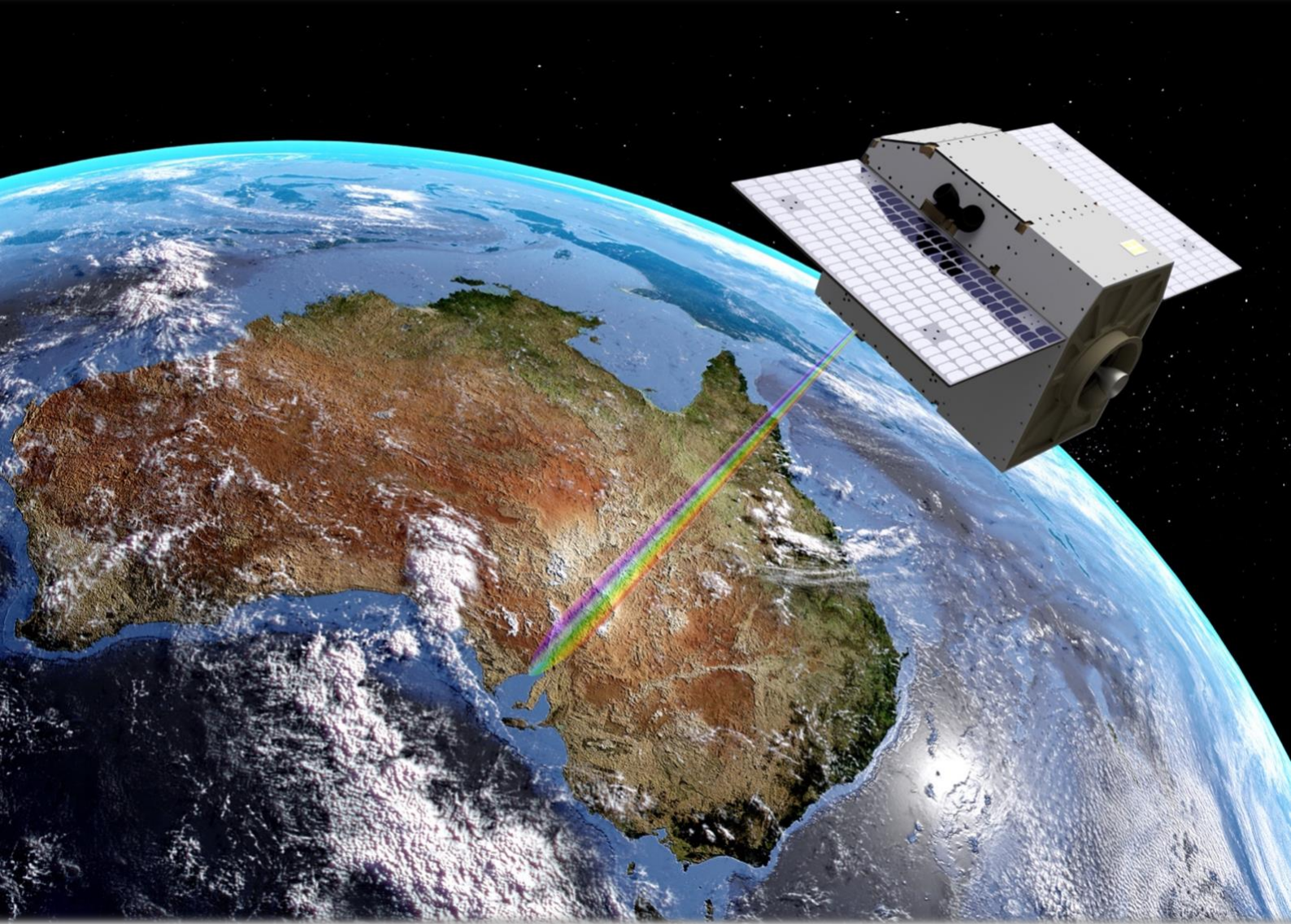


Figure B-4: Number of clear imaging opportunities (days) shown for each target site over one year assuming different ‘clear’ threshold values. The data taken is specific to when the satellite would have passed over the target site.



Contact us

1300 363 400
csiro.au/contact
csiro.au

+1 818 354 4321
4800 Oak Grove Drive
La Cañada Flintridge, CA
91011
jpl.nasa.gov/

For further information

Dr Courtney Bright
+61 460 034 330
courtney.bright@csiro.au

Dr David Ardila
+1 626 658 0693
david.r.ardila@jpl.nasa.gov